NASA TECHNICAL NOTE

NASA TN D-4876

THERMAL ANALYSIS OF SHADOW SHIELDS AND STRUCTURAL MEMBERS IN A VACUUM

by Robert J. Boyle and Richard H. Knoll

Lewis Research Center
Cleveland, Ohio

NATIONAL AERONAUTICS AND SPACE ADMINISTRATION • WASHINGTON, D. C. • NOVEMBER 1968

THERMAL ANALYSIS OF SHADOW SHIELDS AND STRUCTURAL MEMBERS IN A VACUUM

By Robert J. Boyle and Richard H. Knoll

Lewis Research Center
Cleveland, Ohio

NATIONAL AERONAUTICS AND SPACE ADMINISTRATION

For sale by the Clearinghouse for Federal Scientific and Technical Information
Springfield, Virginia 22151 – CFSTI price $3.00

ABSTRACT

An analysis considering nonuniform radiosity and assuming diffusely emitting and reflecting surfaces is presented. The shields are planar and circular, while the sources may be surfaces of revolution. The effects of source geometry, number of shields, spacing, and surface properties are discussed. Shield conductivity and selective coatings are investigated. Specularly and diffusely reflecting surfaces are discussed under the simplifying assumption of uniform radiosity. Also, the effects of thermal radiation on the temperatures of a conducting structural member are analyzed. Results are presented showing the effects of significant parameters on the temperature profiles and heat-transfer rates. The computer program for the shield analysis is listed.

THERMAL ANALYSIS OF SHADOW SHIELDS AND STRUCTURAL MEMBERS IN A VACUUM

by Robert J. Boyle and Richard H. Knoll

Lewis Research Center
Cleveland, Ohio

SUMMARY

An analysis is presented which predicts heat-transfer rates as a function of the number of shadow shields used. The system analyzed consists of two sources and the shields. One of the sources may be solar radiation. It is shown that shields form an effective means of reducing radiant heat transfer. A possible application of these shields is the reduction in the heat transfer to a cryogenic propellant.

The shields are flat disks while the sources may be surfaces of revolution. The sources and shields have a common axis of revolution. The prime analysis used is for diffusely emitting, diffusely reflecting surfaces assuming nonuniform radiosity. The analysis considers thermal radiation and radial shield conduction. The effects of the simplifying assumption of uniform radiosity are considered. It is concluded that for many cases it may be necessary to use the more complicated assumption of nonuniform radiosity in order to have accurate heat-transfer predictions. Specularly reflecting surfaces are examined under the simplifying assumption of uniform radiosity. As the spacing between surfaces increases, the heat transfer for specular surfaces may significantly exceed that for diffusely reflecting surfaces.

In addition to the analysis for the shadow shields, an analysis is presented to predict the temperature distribution along a cylindrical conducting strut. This analysis for the strut considers both internal and external radiation. The struts are needed in order to attach the shields to the rest of the vehicle. The thermal analysis for the strut concludes that increasing the external emissitivity is effective in lowering the conducted heat transfer out of the strut. The interaction of the struts and shields was not considered in the analyses.

For both the shield and strut analyses, predicted temperatures are compared with experimental data. Heat-transfer rates for the shields are also compared with experimental data.

INTRODUCTION

The design of space vehicles for long-term missions often requires thermal protection systems. This is especially true when cryogenic propellants are involved. Shadow shields are a means of reducing the radiant energy absorbed by a propellant tank. This results in reduced boiloff. Shadow shields can also be useful in protecting a relatively warm body, such as a payload, from receiving excessive amounts of solar energy. The primary area of application for shadow shields is in a vacuum. Otherwise, convection may be the dominant mode of heat transfer. The basic purpose of this report is to present an analysis for multishield configurations in a space environment.

Previous studies considered shadow shields for thermal protection of cryogenic propellants on long-term missions, and the protection of payloads passing close to the sun. These studies considered flat disk, spherical, and conical shields (refs. 1 to 5). The analyses in these references were generally for shadow shields of uniform temperature. Reference 3 analyzed flat disks exposed to solar radiation for both zero and infinite radial conductance. Reference 6 determined the local and overall heat-transfer rates for two flat circular sources. In references 3 and 6, the surfaces were treated as having nonuniform radiosity.

In this report, the effects of finite shield conductance and variable surface properties are considered. The analysis presented is applicable for any number of shields, and data are given for up to three shields. Assumptions made concerning the radiosity and reflectivity of the surfaces can affect the predicted heat-transfer rates. The prime analysis assumes diffusely emitting and diffusely reflecting surfaces of nonuniform radiosity. The consequences of making the simplifying assumption of uniform radiosity are examined. Specularly reflecting surfaces are also analyzed under this simplifying assumption.

The shields stand off from the surface which is being protected. It is necessary to support the shields, and an analysis for the appropriate structural members is also presented. However, the interaction between the shields and supports is not analyzed. Therefore, the thermal analysis for the shield support is applicable to cylindrical members in space. The analysis for the support gives the axial temperature distribution along a tube or rod. This analysis considers both conductive and radiant heat transfer.

Comparisons for both the shield and strut analyses are made with experimental data reported in reference 7. A computer code for the shield analysis is listed and discussed. The code is for diffusely emitting and reflecting surfaces of nonuniform radiosity.

METHOD OF ANALYSIS

Shield System

The steady-state temperature distributions in a shield system and consequently the heat-transfer rates are determined by taking heat balances on elemental areas of each shield. These heat balances account for the energy emitted, absorbed and reflected as well as conducted to or from the element under consideration. All of the elements on the shield as well as the surroundings and the elements of the adjacent surfaces enter into the radiant heat terms. Adjacent elements of the same shield also enter the conduction terms of the balance. Appendix A gives the symbol list used in the analyses. Appendix B presents the equations for a system consisting of shields and two sources. One of the sources may be solar radiation. Figure 1 gives a schematic of two possible shadow-shield configurations. From an analytic standpoint, sources are similar to shields except that they have temperature distributions which are known a priori. The sources can be at any temperature; therefore, they may act as sinks.

In order for the analysis to be applicable to a system of shadow shields, the system must satisfy certain requirements. These conditions are:

(1) There can be no more than two sources and these may be surfaces of revolution but they cannot see themselves.

(2) The shields have to be circular and planar.

(3) The shields and the sources have a common axis of revolution.

(4) The size of the shields and sources are such that a surface of either a source or shield sees only one surface. When one of the two sources is solar radiation, the outermost surface, and only this surface, has solar radiation incident upon it.

The derivations of the governing equations in appendix B are made under the following assumptions:

(1) The environment between each pair of surfaces has a single temperature and constant reflectivity. The environment is that space which completes the enclosure between two surfaces.

(2) There is no thermal gradient in a shield in either the circumferential or axial directions.

(3) Heat is transmitted to or from a shield only by radiation. Under this assumption, each shield is isolated from its support structure.

(4) While each shield has a finite thickness, it is assumed that there is no radiation to or from the edge of the shield.

(5) The equations are derived for steady-state conditions.

(6) All surfaces are opaque so that $\alpha + \rho = 1$ at every point on the surfaces.

(7) Emissivity and absorptivity can each be separate functions of radial position and temperature, but are constant in the circumferential direction. These properties are taken to be only a function of the temperature of their surface. Emissivity and absorptivity may be functions of wavelength, but this is not accounted for in the analysis.

(8) Each shield is homogeneous so that the thermal conductivity of the shield is a function only of temperature.

(9) Each of the surfaces is diffusely emitting and diffusely reflecting.

A comparison is made in a later section of the report between the heat-transfer rates for specularly reflecting surfaces and diffusely reflecting surfaces. The equations used for determining the heat-transfer rate between specularly reflecting surfaces of uniform radiosity are presented in appendix C. In the analysis for specular surfaces, it is assumed that the reflectivity is independent of the angle of incidence. Also, polarization effects were neglected.

The equations presented in appendix B for predicting the performance of a shadow-shield system result from each of the surfaces being divided into a series of concentric annuli and heat balances being made on each annulus. Heat enters an element due to solar radiation absorbed on the surface or from thermal energy radiated from an adjacent surface. Energy leaves the annulus due to the emissive power of the element. Additional heat enters or leaves the element due to conduction from the two adjacent elements on the same shield. As the number of annuli increases, each of the annuli approach a differential area in size. When the annuli represent differential areas, the results obtained are for surfaces of nonuniform radiosity. When only a single annulus is used for each surface, the results obtained are those for uniform radiosity surfaces. Unless otherwise noted, the results in this report are for diffusely reflecting surfaces of nonuniform radiosity. In connection with the discussion on specularly reflecting surfaces, a discussion is included on the errors which result from assuming surfaces to have uniform radiosity.

Thermal Distribution Along Structural Member

The analysis in appendix D yields the steady-state, one-dimensional temperature distribution in the axial direction along a structural member which may be either a rod or a tube. Figure 2 gives a representation of a strut. In order for the analysis to predict the temperature distribution for a rod accurately, there should be low thermal resistance in the radial and circumferential directions. The environment is taken to have a uniform temperature and reflective properties. As in the derivation of shadow-shield equations, it is assumed that the surfaces are diffusely emitting and diffusely reflecting. It is necessary to divide the strut into several segments due to the axial temperature variation; and, therefore, the results obtained for the internal radiant heat transfer approach the case of nonuniform radiosity.

The governing equations are determined by taking a heat balance on the elements of the strut. Heat enters an element of the strut by conduction from an adjacent warmer element and may be conducted away to an adjacent colder element. Additional heat enters or leaves the element by thermal radiation from the inside surface of the tube. If the ends of the tube are closed, the end surfaces are taken to be at the same temperature as the ends of the tube. These two end temperatures are the known boundary temperatures. If the ends of the tube are open, the end disks have the properties of the surroundings, which are assumed black, but not necessarily at zero temperature.

The equations presented in appendix B for the shadow shields, and in appendix D for the strut are relatively complex. The solution of these equations is discussed in appendix E, and appendix F presents a computer code for solving the shadow-shield equations of appendix B.

COMPARISON OF RESULTS

This section of the report discusses the comparison of experimental and analytic results. In addition, mention is made of previous analyses with which the work presented herein was compared.

Shadow Shields

The analysis presented in appendix B yields results consistent with the assumptions of uniform radiosity surfaces when each surface is taken to have a single annulus. Under this condition, the results are comparable with those presented in reference 1.

When the analysis is performed using a large number of annuli for each surface, the results obtained approach those for nonuniform radiosity surfaces. In reference 6, analytic results are presented for the heat-transfer rates between two surfaces wherein it is assumed that the surfaces have nonuniform radiosity. Solving the equations of appendix B for the case of nonuniform radiosity gives results which agree with those of reference 6.

Experimental data for shadow-shield systems are given in reference 7 and some of these data are reproduced in the following figures. Figure 3 gives a comparison of analytic and experimental heat-transfer rates as a function of spacing for a one- and three-shield system. The shields were made of copper so that their radial temperature distribution was nearly uniform. The shields were evenly spaced between two plane sources with the warmer source being maintained at 444 K (800° R) and the colder one at 77.8 K (140° R). This figure contains data for both a one- and three-shield system at two different shield emissivities. In one case, the shields were painted to give a nominal

emissivity of 0.94, the same as the sources. While in the other case, the shields were glass blasted to give a nominal emissivity of 0.27. (The surface properties of both the painted surfaces and glass-blasted shields were determined to be a function of temperature so that there was a variation in emissivity from one surface to the next.) As is expected, the heat transfer decreases with the addition of more shields and increases with increasing emissivity.

As the emissivity approaches unity, the difference in the heat-transfer rates between assuming uniform and nonuniform radiosity goes to zero. Therefore, the analytic predictions for the high-emissivity cases are nearly the same using either assumption. Only a single curve is shown for each of these cases. The single glass-blasted shield ($\epsilon \approx 0.27$) was located between two high-emissivity sources. For this case also, both heat-transfer rates are nearly the same. Therefore, only one heat-transfer rate curve is given.

There is a significant difference between the two heat-transfer rates for the three glass-blasted shields ($\epsilon \approx 0.27$). As can be seen, the assumption of nonuniform radiosity gives better agreement with the experimental data.

In figure 4, the experimental and analytic temperatures are plotted as a function of radial position for a three-shield configuration. The shields were made of Mylar which is a very low conducting material; and, consequently, a large radial temperature gradient is present in each of the shields. All of the surfaces were painted with a high-emissivity coating ($\epsilon \approx 0.94$) in order to give a high heat-transfer rate to the colder source. A high heat-transfer rate was desirable in order to improve the accuracy of its measurement. The analytic radial temperature distribution closely follows the experimental one for each of the shields, even to the extent of predicting the temperatures at the outer edge of each of the shields.

In figure 5, the radial temperature distribution is plotted for a two-shield configuration. In the experiment, all surfaces except one were coated with a high-emissivity paint ($\epsilon \approx 0.94$). The side of the warmer shield facing the colder shield was left unpainted except for a rim which covered 0.16 of the radial distance. The purpose of this test was to see if the calculations would accurately predict the behavior of a shadow-shield system when the emissivity of a surface was not constant. The shield with a targeted rim was made of Mylar with a thin layer of aluminum laminated to the Mylar on each side. This resulted in an emissivity of about 0.03 for the unpainted center portion. The colder of the two shields was a plain Mylar shield painted on both sides with a high-emissivity paint. Even though the aluminum increased the conductivity of the warmer shield, the thickness of the aluminum was so small that the overall conductivity was still low. If the rim of the shield were not coated, one would expect a temperature distribution similar to that presented in the previous figure. However, coating the outside surface of the shield causes much more energy to be emitted from the surface. This energy causes a local increase in the temperature of the adjacent colder shield. This effect is illustrated in this

figure. The analytic radial temperature distribution closely follows the experimental distribution for both the warmer and colder shields.

Structural Member

In reference 8, analytic data were presented for the temperature distribution and heat-transfer rates for a pipe penetration with an adiabatic external surface. Setting the external emissivity equal to zero simulated this condition when using the analysis presented herein. For similar cases, results calculated using the equations presented in appendix D, agreed to within the accuracy of the plot reported in reference 8.

In reference 7, experimental temperature distributions were reported for tubes designed as scaled-down representations of support members. Figure 6 gives two of these temperature distributions and an analytic comparison for each distribution. One of the struts was left unpainted while the other was partially painted in the circumferential direction to give an average emissivity of 0.6 in the axial direction. The manner in which the second strut was painted is shown in figure 6. The measured emissivity of the bare metal over the temperature range to which the struts were subjected is closer to 0.25 than the handbook value of 0.3 which was reported in reference 7. The analysis herein uses an emissivity of 0.25 for the bare metal and accounts for internal emissivity. The analytic curves in reference 7 were based on an emissivity of 0.3 and did not account for the effects of internal emissivity. Both struts were made of stainless steel which has a relatively low thermal conductivity. When considering only conduction with a constant thermal conductivity, a straight line would connect the end points in figure 6. It can be seen from this figure that at the higher emissivity the temperature distribution departs more from the straight-line distribution.

One of the possible reasons for the discrepancy between the analytic and experimental results in figure 6 is that the analysis assumes the strut to be a cylinder while the experimental struts formed a cone at each end. Also, the calculations were carried out assuming that the bare metal inside surfaces of the tube were diffusely reflecting. In reference 9, the effects of having specular surfaces on the heat transfer through a nonconducting tube are examined. In this reference, it is shown that for an l/d_t of 20 and an internal emissivity of 0.25, which is representative of the struts reported in reference 7, over four times as much energy can be transported through the tube when the surfaces are specularly reflecting as opposed to when they are diffusely reflecting. Since much of this energy would be reflected at the end of the tube, the temperature profile at the cold end would be altered if the surfaces were specularly reflecting. If, in addition, the energy was polarized so that the component of reflectivity was large in the direction parallel to the axis of the tube, larger heat-transfer rates would result.

Consequences of Assuming Specularly Reflecting Surfaces and Uniform Radiosity

The primary analysis used in this report (appendix B) assumes that all surfaces are diffusely emitting and reflecting and have nonuniform radiosity. In this section of the report, the change in the heat-transfer rate which results from surfaces being diffusely emitting but specularly reflecting is examined. Also, the effects on the heat-transfer rate due to the simplifying assumption that the surfaces have uniform radiosity are discussed. It is simpler to calculate heat-transfer rates assuming surfaces of uniform radiosity. However, this assumption does not yield temperature profiles for each shield and may significantly underestimate the real heat-transfer rates.

Specular surfaces. - In appendix C, the method used to calculate the heat-transfer rates and temperature of each shield for specularly reflecting surfaces is presented. This method is for diffusely emitting surfaces under the assumption of uniform radiosity.

An indication of the effects of assuming specular rather than diffuse reflections is given in figure 7 for various surface emissivities and spacing ratios. The ordinate gives the ratio of the heat-transfer rate to a source at zero temperature for specular surfaces of uniform radiosity to the heat-transfer rate for diffusely reflecting surfaces of uniform radiosity. Both surfaces have the same emissivity and curves of constant emissivity are plotted. It can be seen that as the spacing ratio increases at constant emissivity, the ratio of the heat-transfer rates also increases. In addition, as the emissivity decreases the ratio also increases.

In figure 8, the same parameters as in figure 7 have been plotted except that a shield has been placed midway between the two sources. The surfaces of the shield are specularly reflecting like the sources and have the same emissivity as the sources. The results of placing the shield between the sources is to magnify the ratio of the heat-transfer rates. In figure 8, the shield temperature is uniform due to assuming uniform radiosity and emittance. Because of the assumption of uniform radiosity, these two figures only give an indication of the effects of specular reflectivity. It would be more accurate to consider the effect of nonuniform radiosity on the heat-transfer rates. However, this was beyond the scope of this report.

Comparison of uniform and nonuniform radiosity assumptions. - The two previous figures presented a comparison of the heat-transfer rates for specularly reflecting with diffusely reflecting surfaces under the assumption of uniform radiosity. In figures 9 and 10, comparisons are made in the heat-transfer rates between uniform radiosity and nonuniform radiosity under the assumption of diffusely reflecting surfaces. In figure 9, the ratio of the heat-transfer rates of nonuniform to uniform radiosity is given as a function of spacing ratio for constant emissivity. Both surfaces have the same area; and, again, the ratio is for a cold-source temperature of zero. It can be seen from figure 9

that as the spacing increases, the ratio of the heat-transfer rates reaches a maximum and then decreases. However, the ratio of the heat-transfer rates at any spacing decreases with increasing emissivity.

In figures 10(a) and (b), the same parameters as in figure 9 are plotted except that a shield has been placed midway between the two sources. Figure 10(a) is for a nonconducting shield while figure 10(b) is for a uniform temperature shield. A comparison of these two figures shows that the effects of the shield conductivity assumptions on the heat-transfer ratio are small in relation to the effects of the radiosity assumptions. In each of these figures, the effect of placing a shield between the source is to magnify the ratio of the heat-transfer rates.

In the previous four figures, the heat-transfer ratio was given as the dependent variable. In the next two figures, the actual heat-transfer rate is given as a function of emissivity. In figure 11, the nondimensional heat-transfer rate is plotted as a function of emissivity for two different spacing ratios and the various types of surfaces which have been discussed. In figure 12, the same parameters have been plotted with the addition of a single shield midway between the two sources.

At an L_T/R of 0.1 in either figure 11 or 12, the difference between the heat-transfer rates for diffuse surfaces of uniform radiosity and specular surfaces of uniform radiosity is small. The difference between diffuse surfaces of uniform radiosity and those of nonuniform radiosity is larger. At an L_T/R of 1.0, there is a significant difference in the heat-transfer rates between specular and diffuse surfaces of uniform radiosity. However, an L_T/R of 1.0 represents a relatively large spacing for shadow-shield applications.

By comparing figures 11 and 12, it can be seen that as the number of surfaces involved increases, the differences in the heat-transfer rates caused by the various assumptions generally increase. The curves presented in this report for diffusely reflecting surfaces of nonuniform radiosity might be significantly different from the results obtained for specularly reflecting surfaces of nonuniform radiosity if the number of shields were large and the emissivity low with a large spacing ratio.

In the previous six figures, the cold-source temperature was taken to be zero. When the temperature of the colder source is increased, the change in the heat-transfer rate caused by the different analyses becomes greater. This is illustrated in figure 13 where the increase in the heat-transfer rate is given for various source temperature ratios. The increase in the heat-transfer rate is due to assuming specularly reflecting surfaces over diffusely reflecting surfaces. The increase in the nondimensional heat transfer to the colder source in terms of the warm-source temperature $\left(\Delta\dot{Q}_1 / \sigma A_1 T_2^4\right)$ is plotted as a function of spacing ratio for constant source temperature ratios and a system consisting of two plane sources with no shields. It is necessary to plot the increase in the heat-transfer rate rather than the ratio of the heat-transfer rates because for some cold-source temperature ratios, the heat-transfer rate for diffusely reflecting surfaces goes

to zero. It can be seen from figure 13 that the cold-source temperature has to become a fairly large fraction of the warm-source temperature before the increased heat transfer due to specular reflectivity becomes much greater than the increased value for a cold-source temperature of zero.

It is simpler to calculate heat-transfer relations assuming uniform radiosity surfaces. If one does not require the temperature profile across the shield and the emissivities of the surfaces involved are not too small, the heat-transfer relations presented in reference 1 for diffusely reflecting surfaces of uniform radiosity may suffice. The information presented in the previous figures should aid one in judging whether the assumption of uniform radiosity is satisfactory.

PARAMETRIC DATA

Shadow Shields

The equations used to determine the heat-transfer rates are linear in T^4 when there is no conduction or when the shields have uniform temperatures. An additional requirement for linearity is that surface properties be independent of temperature. In appendix B, it is shown that when the equations are linear, the heat-transfer rate for any pair of source temperatures can be found using only a pair of nondimensional heat-transfer rates. Each of these rates gives the contribution of one of the sources. The equation for the addition of the heat-transfer rates is:

$$\frac{\dot{Q}_1}{A_1} = \sigma\left[\left(\frac{\dot{Q}_1^*}{\sigma A_1 T_2^4}\right)T_2^4 + \left(\frac{\dot{Q}_1'}{\sigma A_1 T_1^4}\right)T_1^4\right] \tag{1}$$

$\dot{Q}_1/A_1$ is the net heat-transfer rate per unit area to source 1. $\dot{Q}_1^*/\sigma A_1 T_2^4$ is the nondimensional heat-transfer rate to source 1 due solely to a temperature on source 2. $\dot{Q}_1'/\sigma A_1 T_1^4$ is the nondimensional heat-transfer rate to 1 resulting from the temperature of source 1. T_1 and T_2 are the source temperatures. The application of this equation is illustrated in a subsequent portion of the report.

One of the applications of shadow shields would be the reduction of the heat transfer to a liquid hydrogen tank. The emissive power of a source at liquid hydrogen temperature is low. Therefore, much of the data in this report is for the heat-transfer rate to a source at 0°. This is done to avoid the necessity of giving two heat-transfer rates for each case. Nonconducting shields yield higher heat-transfer rates than conducting shields. For conservative results, heat-transfer rates are for nonconducting shields un-

less otherwise stated. For simplicity, the data given in this report are for shields of the same size. Planar sources have the same surface area as each side of the shields, and nonplanar sources have the same lateral radius as the shields. Also, for convenience, data are given for black surroundings at zero temperature.

Source geometry. - The heat-transfer rate for two plane sources with and without a single shield placed between them has been given in figures 11 and 12. In figure 14, the heat-transfer rate to a source at zero temperature is given as a function of emissivity for two nonplanar sources and various spacings. Each source is an oblate spheroid whose major radius is $\sqrt{2}$ times the minor radius. It can be seen from this figure that the heat-transfer rate is a strong function of emissivity. As the emissivity decreases, the effects of the spacing ratio become somewhat more pronounced.

In figure 15, the parameters given in figure 14 are plotted for a single planar shield placed midway between the two nonplanar surfaces. With the addition of a single shield, the effects on the heat-transfer rate due to the overall spacing become more pronounced especially at lower emissivities.

Number of shields. - The next two sets of figures are used to determine the net heat-transfer rate to a plane source when both sources have nonzero temperatures. Figures 16(a) to (d) give the heat-transfer rate to a source of zero temperature, and figures 17(a) to (d) give the heat-transfer rate when the other source has a zero temperature.

In figures 16(a) to (d), the heat-transfer rate to source 1 is given as a function of the number of shields placed between the two sources. For each of the figures, the overall spacing ratio (L_T/R) is held constant and curves are given in which all of the surfaces have the same emissivity. It should be noted that figures 16(a) and (b) have one ordinate scale while figures 16(c) and (d) have another scale. Since a fractional number of shields has no physical significance, only integer values of the abscissa have meaning. By comparing particular points on each of these figures, it can be seen that increasing the spacing ratio increases the efficiency of shadow shields.

Figures 17(a) to (d) are the complement of figures 16(a) to (d) in that the heat-transfer rate to source 1 due to the presence of a temperature on source 1 is given. Again, note that there is a scale change in the ordinate of these figures. Figures 17(a) and (b) have one scale while figures 17(c) and (d) have another scale. There is a net heat transfer out of the source for all cases; therefore, the ordinate of figures 17(a) to (d) is negative. It can be seen from these figures that as the spacing between the source and nearest surface becomes large, the heat-transfer rate out of the source approaches the limiting value of $\dot{Q}_1'/\sigma A_1 T_1^4 = \epsilon$. This quantity is the amount of heat which would leave the source if the nearest surface was at an infinite distance from the source.

In order to show how the data in figures 16 and 17 may be used to determine the net heat transfer to a source, an illustrative example is given. The example is for two plane sources with two equally spaced shields. A spacing ratio (L_T/R) of 0.3 is chosen and the emissivity of each surface is 0.1. The warmer source has a temperature of 300 K

(540° R). The colder source has a temperature of 100 K (180° R).

The first nondimensional heat-transfer rate in equation (1) $\left(\dot{Q}_1^*/\sigma A_1 T_1^4\right)$ is found from figure 16(c). The second nondimensional heat-transfer rate $\left(\dot{Q}_1'/\sigma A_1 T_1^4\right)$ is found from figure 17(c). Substituting the appropriate values in equation (1) gives the following result:

$$\frac{\dot{Q}_1}{A_1} = 5.67\times10^{-8}\left[(2.1\times10^{-3})(300)^4 + (-0.065)100^4\right]$$

$$\frac{\dot{Q}_1}{A_1} = 0.595\ \frac{W}{m^2} = \frac{0.189\ Btu}{(hr)(ft^2)}$$

Figure 18 illustrates the effects of varying the temperature of the colder source on the heat-transfer rate. In this figure, the nondimensional heat-transfer rate in terms of the temperature of the warmer source is plotted as a function of emissivity for various temperature ratios. It can be seen from this figure that the colder temperature has to be a fairly large fraction of the warmer temperature before the heat-transfer rate changes a great deal with respect to temperature. It can also be seen from this figure that for some temperature ratios the minimum heat-transfer rate has a negative value. This means that the absolute minimum heat-transfer rate may occur at an emissivity other than zero. When all surfaces have the same emissivity, the minimum heat-transfer rate is not a strong function of emissivity. If the emissivity were allowed to vary from one surface to another, the minimum could be lower. This can be seen from the dashed curve in figure 18. For this curve, the colder source has an emissivity of 0.9 while all other surfaces have the emissivity given by the abscissa of figure 18. The temperature ratio (T_1/T_2) is 0.75.

Up to this point, only heat-transfer rates have been discussed. Shield temperatures are also of interest since the temperature gradients in the shields may affect the design of the shield system. The following figures give temperature profiles for some representative nonconducting shields. Figures 19(a) to (c) present the shield temperature against radial position for a one-, two-, and three-shield case. For each of the three figures, the overall spacing between the sources is held constant. It can be seen that the shield temperatures drop off sharply toward the outer edge of each of the shields. The temperature difference across the shield become slightly greater as the temperature of the shield increases. The short horizontal line crossing each of the curves indicates the temperature of an infinitely conducting shield under the same conditions.

Targeting. - When the emissivity of the surfaces of a shadow-shield system are uniform in the radial direction, reducing the emissivity generally reduces the heat-transfer rate to the colder source. It is sometimes possible to gain a further reduction in the

heat-transfer rate for low-emissivity surfaces by using a high-emissivity coating on the outer edges. Shields for which this is done take on the appearance of targets due to circumferential symmetry. It is generally necessary that there be more than one shield in the system for targeting to produce a reduction in the heat-transfer rate.

Figures 20(a) and (b) illustrate the effects of targeting for uniform temperature shields and nonconducting shields for a system consisting of two plane sources separated by two shields. In order to obtain a decreased heat-transfer rate, it is necessary to target the surface of the warmer shield facing the colder shield. The percentage change in the heat-transfer rate due to targeting is plotted as a function of the percentage area of the shield which is targeted. The results for two overall spacing ratios are shown. From figures 20(a) and (b), it can be seen that for this case there is some decrease in the heat-transfer rate due to targeting uniform temperature shields, but no improvement is noticeable for nonconducting shields. The targeted areas of the uniform temperature shields act like fins in that they are able to take energy from the shield and dissipate it to space. The nonconducting shields are less efficient at doing this. The changing of the shield temperatures due to targeting is illustrated in figures 21(a) to (c) for nonconducting shields. In these figures, the temperature profiles are plotted as a function of radial position for an untargeted system and two combinations of targeted shields. The upper curve gives the temperature of the warmer shield in each figure. In each case, the nondimensional heat-transfer rate is also given. Even if targeting does not provide an improvement in the heat transfer for nonconducting shields, targeting can drastically alter the temperature profile of the shield.

The heat-transfer rate varies little while the temperatures vary substantially in each of the three cases presented. In figure 21(b), the temperature of the outer edge is greatly lowered. This could prove useful in attaching shields to their support members. Shields could be thermally bonded to the support structure. If the rim temperature was lower than that of the adjacent structure, the shields could act as fins to dissipate heat from the strut. In this way, the local temperature of the strut would be lowered and this, in turn, might reduce the conducted heat out of the strut. The interaction of shields and their support structure is not analyzed in this report. In figure 21(c), the radial temperature difference has been lessened for each of the shields by means of targeting.

Shield conductivity. - Figure 22 illustrates the effect of shield conductivity on the heat-transfer rate. As the conductivity of a shield increases, the temperature of the shield becomes more uniform and the heat-transfer rate decreases. Shields which have the same values of the scaling parameter $(kt/\sigma T_2^3 R_1^2$, where T_2 is a reference temperature) have the same radial temperature profiles and heat-transfer rates. In figure 22, heat-transfer ratios for partially conducting shields are given as a function of this parameter. The ordinate of figure 22 is the ratio of the heat-transfer rate to the heat-transfer rate for uniform temperature shields and data are given for one-, two-, and three-shield

configurations. Only when the conductivity parameter has a value of zero or infinity are the equations for the heat-transfer rates linear. It should be noted that at these two extremes the abscissa has been made discontinuous in order to show the effects of the two assumptions which yield linear equations. From this figure, it can be seen that when there are several shields involved, there can be a significant change in the heat-transfer rate due to thermal conductivity. These curves are given for an emissivity of 0.1 and although it is not shown on the figures, the ratio of the heat-transfer rates increases with decreasing emissivity.

When the thermal conductivity has a finite value other than zero, it is necessary to solve nonlinear equations in order to determine the temperature distributions. In appendix B, a solution is given in which the conducted heat transfer is treated as a known quantity during each iteration cycle. As the conductivity of the shields increases, it becomes less desirable to do this. In appendix E, an alternate solution is given in which the radiant heat transfer is treated as a known quantity during each iteration, and the temperature distributions are found by solving the conduction equations.

Shield position. - In the previous figures, the shields were placed so that there were equal spacings between surfaces. Figures 23(a) to (e) illustrate the effects of varying the spacings between surfaces for two emissivities. In each of the figures, the variable giving the relative spacing (L/L_T) is measured from the warmer source.

The ordinate in each figure is the ratio of the heat-transfer rate to the heat-transfer rate for the same number of evenly spaced shields. In figure 23(a), there is a single shield present and in figures 23(b) and (c), there are two and three shields, respectively, with the spacing between shields remaining constant. For these three cases, the spacing for the minimum heat-transfer rate is halfway between the two sources for both emissivities. As the emissivity decreases, the heat-transfer rate is more sensitive to spacing. The heat-transfer rate decreases with increasing number of shields, so that the ordinate is different for each of these figures. The actual heat-transfer rate is lowest for three shields.

Figures 23(d) and (e) are for configurations in which the shields have the same spacing relative to the sources. In figure 23(d), both shields come closer to the center as the abscissa is increased; and in figure 23(e), the center shield remains fixed while the two outer shields approach it for increasing values of the abscissa. In both of these figures, the spacing for minimum heat transfer is a function of emissivity.

Solar radiation. - When one of the sources is solar radiation, this radiation is incident only on the outermost surface. If the equations are linear, the net heat-transfer rate to a source can be found by using two generalized heat-transfer rates. The heat-transfer rate due to solar radiation is proportional to the solar flux (φ) times the solar absorptivity (α_φ). The solar absorptivity is taken to be independent of the emissivity of the surface. In this way, increasing the solar absorptivity is equivalent to increasing the

solar flux. Therefore, these variables can be combined with others to form nondimensional heat-transfer rates.

Figure 24 gives the nondimentional heat-transfer rate due to solar energy as a function of the spacing ratio for two nonconducting shields and a plane source. All surfaces have the same emissivity, and lines of constant emissivity are plotted. It can be seen that as the spacing ratio decreases, the heat-transfer rate increases with the greatest change coming for low-emissivity surfaces. As the spacing ratio reaches a very small value, the heat-transfer rates become less dependent on the emissivity of the surfaces.

In figure 25, the nondimensional heat-transfer rate is plotted as a function of spacing ratio for surfaces of constant emissivity. In this figure, the solar flux is taken to be zero. The inner shield is placed midway between the source and the outer shield. The heat-transfer rate to the plane source is negative since there is no solar flux. From this figure, it can be seen that as the emissivity decreases and spacing ratio increases, the heat-transfer rate approaches the limiting value of $\dot{Q}_1'/\sigma A_1 T_1^4 = \epsilon$.

The information presented in figures 24 and 25 can be utilized in order to determine the net heat-transfer rate into a source when the system is exposed to solar radiation. The solar flux varies with the square of the distance from the sun. At one AU, the solar flux is about 1390 W/m^2 (442 $Btu/(hr)(ft^2)$). If it is desired to approach a one-tenth AU distance from the sun, the solar flux would be 1.390×10^5 W/m^2 (4.42×10^4 $Btu/(hr)(ft^2)$). The sun is not really a point source so that a conical array of shields might be needed. However, at this distance from the sun, the half angle of the cone is less than 3° and this complication is neglected. In order to use figures 24 and 25, a system of two equally spaced nonconducting shields is chosen. The overall spacing is taken to be 0.2 and the source temperature is taken as 300 K (540° R). The emissivity of all of the surface is assumed as 0.1 while the solar absorptivity is taken as 0.02. The net heat-transfer rate to the source can be found from the equation:

$$\frac{\dot{Q}_1}{A_1} = \left(\frac{\dot{Q}_1^*}{A_1 \varphi \alpha_\varphi}\right) \varphi \alpha_\varphi + \left(\frac{\dot{Q}_1'}{\sigma A_1 T_1^4}\right) \sigma T_1^4 \tag{2}$$

The first heat-transfer term is found from figure 24 and the second from figure 25. Substitution of values gives

$$\frac{\dot{Q}_1}{A_1} = (0.0545)1.390\times10^5(0.02) + (-0.064)(5.67\times10^{-8})(300)^4$$

$$\frac{\dot{Q}_1}{A_1} = 122.6 \frac{W}{m^2} = 38.9 \frac{Btu}{(hr)(ft^2)}$$

This value of 122.6 W/m^2 is considerably less than the value of 2734 W/m^2 (867 Btu/(hr)(ft^2)) which would occur if no shields were present.

Structural Member

The structural member which is thermally analyzed in this report could be a support member of a system for shadow shields. It could also be any of several other structural members in an upper stage. The thermal analysis of this member can involve many independent variables. This is especially true when the internal emissivity is not zero. The following figures present datafor a few cases representative of structural members in a space vehicle. In figures 26(a) to (c), the nondimensional total heat-transfer rate is given as a function of emissivity. The solid lines are for closed ends while the dashed line in each figure is for opened ends and an external emissivity of zero. When the ends are closed, the total heat-transfer rate is the conducted heat-transfer rate at the colder end plus the radiant energy absorbed by the end disk. When the ends are open, the total heat-transfer rate is the conducted heat-transfer rate. When the internal emissivity is zero, the internal radiant heat-transfer rate is also zero. For each of these figures, a different l/d_t is given and since the diameter of the tube is held constant, the radiation to conduction parameter $\sigma T_2^3 l^2/kt$ increases with increasing l/d_t. It should be noted that figure 26(c) has a different ordinate scale from figures 26(a) and (b).

From these figures, it can be seen that both the internal and external emissivities can affect the heat-transfer rate. The heat-transfer rate is more sensitive to changes in emissivity at low values of emissivity than at high values. As the external emissivity increases, more energy is radiated to the surroundings. This, in turn, reduces the temperature gradient at the colder end of the strut thereby lowering the conducted heat-transfer rate. In these cases, the surroundings were taken to be at zero temperature. Increasing the internal emissivity causes an increase in the heat-transfer rate at the colder end of the strut in a twofold manner. First, as the internal emissivity increases, the temperatures along the strut increase. This increases the thermal gradient at the colder end which results in an increased conducted heat-transfer rate. Second, for closed ends, increasing the internal emissivity increases the amount of radiant energy which is absorbed by the end of the strut.

In the next series of figures, the temperature profiles are given as a function of external emissivity for constant values of l/d_t. In figures 27(a) to (c), the nondimensional temperature is plotted as a function of axial position. For all of these figures, the internal emissivity is held constant at 0.6 while the l/d_t changes for each figure. By comparing these figures, it can be seen that as the radiation to conduction parameter increases, the temperature profile departs more from the straight line which would occur if conduction were the only mechanism determining the heat-transfer rate. In each of

these figures, increasing the external emissivity causes an increase in the thermal gradient at the warm end of the strut and a decrease in the thermal gradient at the cold end. It should be noted that the thermal conductivity varies greatly between materials. Therefore, the values of the radiation to conduction parameter are strongly dependent on the strut material used. The values of this parameter which are shown on figure 27 were formed using a thermal conductivity representative of fiberglass.

Generally, it is desired to minimize the heat-transfer rate to the colder end of the strut. Returning to figures 26(a) to (c), it can be seen that reducing the internal emissivity of the strut reduces the heat-transfer rate. If the inside of the tube were filled with a very low conductivity material, the effective internal emissivity would be zero and the added heat transfer due to the conduction of the filler would be small. Also, if radiation barriers were placed along the length of the tube, the strut would be divided into a series of nearly isothermal compartments and the effective internal emissivity would be reduced.

In appendix D, it is shown that when the internal emissivity is zero and when emissivity and conductivity are taken to be independent of temperature, the temperature profile, and, consequently, the heat-transfer rate for a thin-walled tube seeing a zero-temperature environment can be expressed by two parameters. One of these parameters is the ratio of the boundary temperatures, and the other contains various specifications of the strut. The second parameter (κ) is $\sigma\epsilon_o T_2^3 l^2 / kt$ and is dimensionless.

Figure 28 presents the ratio of the temperature slope at the colder end of the strut to that obtained by considering conduction only. This is done for an internal emissivity of zero. The data are presented as a function of κ and various temperature ratios. The ordinate of figure 28 can be directly related to the heat transfer out of the tube. The heat-transfer rate out of the tube considering the effects of emissivity is $k\pi d_o t(dT/dx)$ while the heat-transfer rate, when only conduction is considered, is $k\pi d_o t(T_2 - T_1)/l$. Increasing κ decreases the heat-transfer rate. The effects of this parameter become more pronounced as the temperature ratio decreases. When the ordinate of this figure becomes negative, heat is being transferred into the strut from both ends and is dissipated to the surroundings along the length of the tube.

In figures 29(a) to (c), temperature ratio is plotted as a function of axial position for various values of κ. In each of these figures, the temperature ratio is held constant; and it can be seen that as κ increases, the temperature profiles become more distorted. As κ increases, the temperature along the strut becomes lower. If the temperature ratio is sufficiently low and κ is sufficiently high, the temperature along the strut can fall below the colder end temperature. Under this circumstance, heat is transferred into the strut at both ends.

CONCLUSIONS

In this report, the thermal analyses of both a system of shadow shields and a structural member have been carried out. It has been shown that the shadow-shield analysis developed herein is capable of accurately predicting the behavior of shadow-shield systems. The effects of emissivity and spacing ratio on the heat-transfer rates have been shown. This has been done for a system consisting of up to several shadow shields. This report shows that the effectiveness of shadow shields is most pronounced when the emissivity of the surface is low. By targeting shadow shields, large changes in the temperature profile of the shields can be achieved. This can be done with only a moderate change in the heat-transfer rate and may be advantageous in reducing the heat transferred by conduction through the strut if the shields are thermally connected to the support structure. In some cases, the heat-transfer rate will be lowered when targeting is applied.

In addition to protecting a cryogenic propellant, shadow shields may be used to protect a payload or other body from incident solar energy. Here again, shadow shields can be effective in reducing the heat-transfer rate especially when the emissivities of the surfaces are low.

The effects of having specularly reflecting surfaces have been examined for the simplifying case of surfaces with uniform radiosity. It has been shown that with this assumption specularly reflecting surfaces yield a higher heat-transfer rate than diffusely reflecting surfaces. The percentage increase due to specular reflectance increases with increasing shield spacing.

The effects of nonuniform radiosity for diffusely reflecting surfaces have also been examined. It has been shown that for reasonable shield spacings the possible error due to assuming uniform radiosity surfaces can be significant. This error is often greater than the error which would result from treating specularly reflecting surfaces as diffusely reflecting surfaces at the same spacing. For a more complete understanding of the behavior of specular surfaces, an analysis which would account for both specular reflectivity and nonuniform radiosity is necessary.

The ability of the thermal analysis for a structural member to predict the behavior of an actual strut has been examined. By taking advantage of the external emissivity of the strut, the rate of heat transfer through the strut can be greatly affected, even to the point of becoming a negative value. The thermal interaction between the shadow shields and their support members would also be needed for a more complete understanding of the entire system.

Lewis Research Center,
National Aeronautics and Space Administration,
Cleveland, Ohio, July 3, 1968,
124-09-05-12-22.

APPENDIX A

SYMBOLS

A	area of a radiating surface
a	cross-sectional area of an element on the strut
B_{ij}	absorption factor - the fraction of energy which leaves the i^{th} surface and is absorbed by the j^{th} surface
d	diameter of the strut
F	view factor between specular surfaces
f_{ij}	diffuse view factor between the i^{th} and j^{th} surfaces
H	incident energy per unit time and area
h	step size
K	constant used in appendix B
k	thermal conductivity
L	spacing between surfaces in the shield system
l	length of the strut
m	shield number or the number of steps in the solution of the differential equation
n	number of annuli on a shield or the number of elements into which a strut is divided. This symbol is also used as a subscript.
$\dot{Q}$	heat-transfer rate to a whole surface
q	heat-transfer rate to an element
$\mathscr{R}$	thermal resistance between annuli
R	radius of a shield
r	radial distance
T	absolute temperature
t	shield thickness or thickness of a thin-walled tube
W	emissive power per unit area of an element
x	distance along the strut
α	absorptivity
α_{φ}	solar absorptivity

β angle of incidence or reflection

δ_{ij} Kronecker delta; equals 1 when $i = j$; equals 0 if $i \neq j$

ϵ emissivity

ζ number of terms used to approximate the finite series

η number of times energy has been reflected off an adjacent surface

θ nondimensional temperature along the strut

κ radiation to conduction parameter for the strut, $\frac{\epsilon_o T_2^3 \ell^2}{kt}$

ξ transformed independent variable in the strut equation

π a constant

ρ reflectivity, $\rho = 1 - \alpha$

σ Stefan-Boltzmann constant

φ solar flux

The following matrices and vectors are used:

C k-by-k matrix whose elements are the fraction of energy which leaves the q^{th} surface and is reflected by the p^{th} surface $(C)_{qp} = f_{qp}\rho_p - \delta_{pq}$

D n-by-n matrix whose elements are the sum of the entries in Ψ and Ψ^c which refer to the annuli of the shield times the emissivity of the annuli $(D)_{pq} = (\Psi)_{n+p,\,n+q}\epsilon_{n+p} + (\Psi^c)_{pq}\epsilon_p^c$

E column vector of size k whose elements are the emissive power of each surface $(E)_p = W_p A_p = \sigma \epsilon_p T_p^4 A_p$

I identity matrix $(I)_{pq} = \delta_{pq}$

P column vector of size n with entries containing the radiant heat transfer from each element of the shield from known temperature surfaces

Q column vector of size n whose elements contain the heat transfer away from each annulus of the m^{th} shield

U k-by-k matrix whose elements are the absorption factors $(U)_{pi} = B_{pi}$ in the shield system

$\bar{u}$ column vector of U in the shield system $(\bar{u})_p = B_{pj}$ and a vector containing the absorption factors divided by the area of the differential element in the strut system $(\bar{u})_i = \frac{B_{ij}}{A_j}$

V k-by-k matrix whose elements contain the negative of fraction of energy absorbed by a surface $(V)_{pq} = -f_{pq}\alpha_q$

$\bar{v}$ column vector of V in the shadow-shield system $(\bar{v})_q = -f_{qj}\alpha_j$ and a vector containing the negative of the fraction of energy absorbed by a surface in the strut system $(\bar{v})_p = -f_{jp}\frac{\epsilon_j}{A_p}$

Y n-by-n matrix containing the coefficients of the temperatures when the equations are linear in temperature

Z column vector of size n containing $(Z)_j = \sigma A_j T_j^4$

Θ column vector containing the temperatures of the annuli of the shield or the temperatures along the strut

Φ column vector of size k whose entries contain the heat-transfer rate to each annulus in the system

χ m-by-m matrix whose entries contain the temperature coefficients in the solution to the differential equation

Ψ k-by-k matrix defined as $\Psi = U - I$

Ω column vector of size m, the entries of which are the values of the second derivative in the differential equation

Subscripts:

c conductive heat transfer

i any surface in the system

in heat transfer towards the surface

j particular surface under consideration

k total number of elements in a system. Equals $2n + 1$ for a shield system and $n + 2$ for a strut system.

n number of annuli on a shield or segments of a strut

o outside surface of strut

out heat transfer away from the surface

p, q dummy subscripts denoting any element in a matrix or vector

r radiant heat transfer

s shield

sr surroundings

T total heat-transfer rate through the strut or the total spacing between sources

ι inside surface of the strut

1, 2 each of the two sources or each end of the strut

Superscripts:

c complimentary system composed of the m^{th} and $m^{th} + 1$ shields and their surroundings

* source for which the heat-transfer rate is given has a zero temperature

' source for which the heat-transfer rate is given is the only source of thermal energy in the system

+ heat-transfer rate is a ratio to the case of uniform radiosity and diffusely reflecting surfaces

APPENDIX B

DERIVATION OF SHADOW-SHIELD EQUATIONS

The following derivation for determining the temperature distribution for a system of shadow shields follows the work of Gebhart given in reference 10. Heat balances are formulated which consider radiation and radial conduction. The steady-state temperature distribution for each shield is determined from the heat balances, since there is no net heat transfer to the elements of the shield or the shield as a whole. The properties of the shields are allowed to be functions of the shield temperatures. This results in an iterative solution. In order to avoid matrices of cumbersome size, the temperature distribution for each shield is determined assuming that adjacent shields and surroundings have known temperature distributions. As the iterative procedure converges, the assumed and calculated temperature distributions become nearly identical.

Figure 30 gives a schematic of a shield bounded by two other surfaces and the surroundings. In the derivation of the equations for the temperature of the m^{th} shield, it is assumed that the temperatures of the $m^{th} + 1$ and the $m^{th} - 1$ shield are known. Each of the four surfaces (there are two surfaces to consider for the m^{th} shield) are divided into n elements. Because surface properties are assumed constant in the circumferential direction, the elements are a series of concentric annuli. Both surfaces of the j^{th} element of a shield have the same temperature and area, but not necessarily the same surface properties. The temperature of both sides of the shield are the same because it is assumed that there is no axial temperature gradient.

The total rate of heat transfer to the j^{th} element on the m^{th} shield is the sum of the radiant heat transfer occasioned by the shield seeing the $m^{th} + 1$ and $m^{th} - 1$ shields plus the conducted heat transfer from the $j^{th} - 1$ and the $j^{th} + 1$ elements of the m^{th} shield to the j^{th} element. The rate of heat transfer away from the element is the emitted radiation from both surfaces of the element.

The shield temperatures are determined by constructing two closed systems as is illustrated in figure 31. The first system consists of the $m^{th} - 1$ shield, the m^{th} shield, and the surroundings enclosing these two shields. The second system consists of the m^{th} shield, the $m^{th} + 1$ shield, and the surroundings enclosing these two shields. The m^{th} shield forms the common boundary for the two systems. The temperature of the boundary must be the same when viewed from either system. If the enclosures do not represent physical surfaces, they are nonreflective.

There are n elements on each surface of each system. Therefore, there are $2n + 1$ elements in each system. The manner in which elements were assigned subscripts is also illustrated in figure 31. Each element in a system is assigned a unique subscript; therefore, it is not necessary to distinguish elements on the m^{th} shield from

those on the other surface with an additional subscript denoting the particular shield.

The net rate of radiant heat transfer away from the j^{th} element is:

$$q_{r,j} = W_j A_j - B_{1j} W_1 A_1 B_{2j} W_2 A_2 - B_{3j} W_3 A_3 - \ldots - B_{kj} W_k A_k \quad \text{where } k = 2n+1 \qquad \text{(B1)}$$

W_i is the emissive power per unit area of the i^{th} element, and B_{ij} represents the fraction of energy which is emitted from the i^{th} surface and is absorbed by the j^{th} surface. It is assumed that the radiant energy is uniformly distributed over each of the elemental surfaces, and that each of the surfaces emits and reflects energy diffusely. Therefore, B_{ij} can be found in terms of the other B's. The following equations give this relation.

$$B_{1j} = f_{1j}\alpha_j + f_{11}\rho_1 B_{1j} + f_{12}\rho_2 B_{2j} + \ldots + f_{1k}\rho_k B_{kj}$$

$$B_{2j} = f_{2j}\alpha_j + f_{21}\rho_1 B_{1j} + f_{22}\rho_2 B_{2j} + \ldots + f_{2k}\rho_k B_{kj}$$

$$\vdots$$

$$B_{kj} = f_{kj}\alpha_j + f_{k1}\rho_1 B_{1j} + f_{k2}\rho_2 B_{2j} + \ldots + f_{kk}\rho_k B_{kj}$$

This set of linear algebraic equations can be rewritten as:

$$(\rho_1 f_{11} - 1)B_{1j} + \rho_2 f_{12} B_{2j} + \ldots + \rho_k f_{1k} B_{kj} = -f_{1j}\alpha_j$$

$$\rho_1 f_{21} B_{1j} + (\rho_2 f_{22} - 1)B_{2j} + \ldots + \rho_k f_{2k} B_{kj} = -f_{2j}\alpha_j$$

$$\vdots$$

$$\rho_1 f_{k1} B_{1j} + \rho_2 f_{k2} B_{2j} + \ldots + (\rho_k f_{kk} - 1)B_{kj} = -f_{kj}\alpha_j$$

These equations can be rewritten in matrix form for each j. This gives:

$$C\bar{u} = \bar{v} \qquad \text{(B2)}$$

where

$$(C)_{qp} = f_{qp}\rho_p - \delta_{qp}$$

$$(\bar{u})_p = B_{pj}$$

and

$$(\bar{v})_q = -f_{qj}\alpha_j$$

The heat-transfer balance can be taken for each of the other elements in the system. The coefficient matrix C is independent of the surface for which the heat balance is taken. The entire k^2 set of algebraic equations can be represented in terms of k-by-k matrices. The matrix equation for this is:

$$CU = V \tag{B3}$$

Each of the matrices have the following values in their respective elements:

$$(U)_{pq} = B_{pq}$$

$$(V)_{pq} = -f_{pq}\alpha_q$$

and the coefficient matrix C remains the same.

Solving for U yields:

$$U = C^{-1}V \tag{B4}$$

The entire process can be repeated for the other system. And an equation similar to equation (B4) can be written for this system.

$$U^c = \left(C^c\right)^{-1}V^c \tag{B4'}$$

The surface properties and the spacing between surfaces are not necessarily the same in each system. Therefore, there is no necessary correspondence between the systems. In general,

$$C \neq C^c$$

$$U \neq U^c$$

$$V \neq V^c$$

Equation (B1) can be written for each of the elements in each of the systems. For the system containing the m^{th} shield and the $m^{th} - 1$ shield, these equations are:

$$-q_{r,1} = \left(B_{11} - 1\right)W_1A_1 + B_{21}W_2A_2 + \ldots + B_{k1}W_kA_k$$

$$-q_{r,2} = B_{12}W_1A_1 + \left(B_{22} - 1\right)W_2A_2 + \ldots + B_{k2}W_kA_k$$

$$\vdots$$

$$-q_{r,k} = B_{1k}W_1A_1 + B_{2k}W_2A_2 + \ldots + \left(B_{kk} - 1\right)W_kA_k$$

These equations can be written in matrix form giving:

$$\Phi = \Psi^T E \tag{B5}$$

Because the indices are reversed, it is the transpose of the coefficient matrix which is used in the matrix equation. Φ is a column vector whose elements represent the net radiant heat transfer to each of the surfaces in the system. Each of these matrices are made up of the following elements:

$$(\Psi)_{pi} = (U)_{pi} - \delta_{pi} \quad \text{or} \quad \Psi = U - I$$

$$(\Phi)_i = -q_i$$

$$(E)_p = W_pA_p = \sigma\epsilon_pT_p^4A_p$$

For the other system involving the m^{th} and $m^{th} - 1$ shields, it is possible to write the heat-balance equations. These equations in matrix form are:

$$\Phi^c = \left(\Psi^c\right)^T E^c \tag{B5'}$$

The m^{th} shield is common to both systems, and the temperature of each annulus of this shield is the same when viewed from either system ($A_i = A_i^c$ and $T_i = T_i^c$, where i represents any element of the m^{th} shield). However, because the surface properties as well as the spacing between surfaces may be different in each system, there is, in general, no correspondence between equations (B5) and (B5') so that

$$\Phi^c \neq \Phi$$

$$\Psi^c \neq \Psi$$

$$E^c \neq E$$

It is desirable to maintain a system of linear equations. Radiation terms in the heat balances are linear in T^4, while conduction terms are linear in T. In this appendix, equations are given which are linear in T^4. The conduction terms are considered known during an interation and are recalculated after every iteration. When the conduction terms are relatively large compared with the radiation terms, it may be advantageous to solve a system of equations that are linear in T. In appendix E, equations, which are linear in T, are presented for determining the temperatures of partially conducting shields. Either form of the solution should yield the same result since each is iterative in nature so that at the final iteration the terms that were assumed known are truly known. The heat-transfer rate to the j^{th} element by conduction is

$$q_{c,j} = \frac{T_{j+1} - T_j}{\mathscr{R}_{j+1,j}} + \frac{T_{j-1} - T_j}{\mathscr{R}_{j-1,j}} \tag{B6}$$

$\mathscr{R}$ is the thermal resistance between the j^{th} element and an adjacent element

$$\mathscr{R}_{i,j} = \frac{\left|\ln\left(\frac{r_i}{r_j}\right)\right|}{2\pi kt} \qquad \text{where } i = j \pm 1 \tag{B7}$$

In each of the systems considered, only n of the k elements are for the m^{th} shield. It can be seen from figure 31 that for the system containing the m^{th} and $m^{th} - 1$ shields the elements for the m^{th} shield are the $n^{th} + 1$ to the 2n elements. For all of the other 2k - 2n elements in the two systems, temperatures as well as emissivities and, therefore, reflectivities are considered known.

Equations (B5) and (B5') can be added together and rewritten so as to separate the knowns from the unknowns. Our interests are in determining the temperatures of the $2n$ elements common to both systems. The algebraic equations which result from the addition of equations (B5) and (B5') are:

$$\left.\begin{aligned}
(\Phi)_{n+1} + (\Phi^c)_1 &= \sum_{p=1}^{n} (\Psi)_{p,n+1}(E)_p + \sum_{p=n+1}^{k} (\Psi^c)_{p,1}(E^c)_p + (\Psi)_{k,n+1}(E)_k \\
&\quad + \sum_{p=n+1}^{k-1} (\Psi)_{p,n+1}(E)_p + \sum_{p=1}^{n} (\Psi^c)_{p,1}(E^c)_p \\
(\Phi)_{n+2} + (\Phi^c)_2 &= \sum_{p=1}^{n} (\Psi)_{p,n+2}(E)_p + \sum_{p=n+1}^{k} (\Psi^c)_{p,2}(E^c)_p + (\Psi)_{k,n+2}(E)_k \\
&\quad + \sum_{p=n+1}^{k-1} (\Psi)_{p,n+2}(E)_p + \sum_{p=1}^{n} (\Psi^c)_{p,2}(E^c)_p \\
&\vdots \qquad\qquad \vdots \\
(\Phi)_{2n} + (\Phi^c)_n &= \sum_{p=1}^{n} (\Psi)_{p,2n}(E)_p + \sum_{p=n+1}^{k} (\Psi^c)_{p,n}(E^c)_p + (\Psi)_{k,2n}(E)_k \\
&\quad + \sum_{p=n+1}^{k-1} (\Psi)_{p,2n}(E)_p + \sum_{p=1}^{n} (\Psi^c)_{p,n}(E^c)_p
\end{aligned}\right\} \quad (B8)$$

It should be noted that in the equations of (B8), because of the order in which the subscripts were written, the transpose of Ψ or Ψ^c was not used.

For each of the algebraic equations of (B8), the first three terms to the right of the equal sign are for elements with known temperatures. Since there is no net heat transfer to any annulus of the shield, the two terms on the left side of each equation equal the rate of heat transfer away from the annulus by conduction

$$(\Phi)_{n+i} + (\Phi^c)_i = -q_{c,i}$$

If the shield does not have a uniform temperature, it is convenient to write equation (B8) in matrix form. The algebraic equations become:

$$Q = D^T Z \tag{B9}$$

Equation (B9) is composed of an n-by-n matrix D^T and two vectors, each containing n values. $(Q)_i$ represents the heat transfer away from the i^{th} annuli of the m^{th} shield due to conduction less the radiant heat transfer to the annuli from all of the surfaces whose temperatures are known

$$(Q)_i = -q_{c,i} - \sum_{p=1}^{n} (\Psi)_{p,n+i}(E)_p - \sum_{p=n+1}^{k} (\Psi^c)_{p,i}(E^c)_p - (\Psi)_{k,n+i}(E)_k$$

$(Z)_j$ is an entry of a column vector and has the value $\sigma A_j T_j^4$. D is an n-by-n matrix containing the entries:

$$(D)_{j,i} = (\Psi)_{n+j,n+i}\epsilon_{n+j} + (\Psi^c)_{j,i}\epsilon_j^c$$

The transpose of D can be written in terms of the matrices containing the absorption factors. This yields:

$$(D^T)_{i,j} = \left[(U)_{n+j,n+i} - \delta_{j,i}\right]\epsilon_{n+j} + \left[(U^c)_{j,i} - \delta_{j,i}\right]\epsilon_j^c$$

In these equations, ϵ_{n+j} and ϵ_j^c both refer to the j^{th} annulus of the m^{th} shield, but each must be taken from the appropriate system. A_j and T_j are the same in both systems.

When one of the sources is solar radiation, the energy which is absorbed on the outward facing surface of the j^{th} element is $\varphi A_j \alpha_\varphi$ where φ is the incident solar flux, and α_φ is the solar absorptivity. For flat disk shields, A_j equals the area of the annulus. However, if solar energy is incident upon a curved surface A_j, in this instance only, represents the area of the projection of the surface element into a plane perpendicular to the solar flux.

The heat transfer away from the j^{th} annulus when a solar flux is present is:

$$(Q)_i = -q_{c,i} - \varphi A_i \alpha_\varphi - \sum_{p=n+1}^{k} (\Psi^c)_{p,i}(E^c)_p$$

Also, when solar radiation is present, the outer shield is not bounded by either surroundings or another surface. Therefore, none of the energy which leaves the surface in the direction of the solar flux is returned to any annulus of the shield. Under this circumstance, the matrix D has the entries:

$$\left(D\right)_{j,i} = -\delta_{j,i}\epsilon_{n+j} + \left(\Psi^c\right)_{j,i}\epsilon_j^c$$

Equation (B9) can be solved for the vector **Z** to give:

$$Z = \left(D^T\right)^{-1} Q$$

The temperatures of each annulus can be found from the various values of Z

$$T_j = \left[\frac{\left(Z\right)_j}{A_j}\right]^{1/4} \tag{B10}$$

When the temperature of the shield is uniform, equation (B8) can be utilized directly to find the shield temperature. Since there is no net heat transfer to the shield as a whole, the following equation can be written:

$$\sum_{i=1}^{n}\left[\left(\Phi\right)_{n+i} + \left(\Phi^c\right)_i\right] = 0 \tag{B11}$$

The sum of the equations given by equation (B8) can be written as:

$$-\sum_{i=1}^{n}\left[\sum_{p=1}^{n}\left(\Psi\right)_{p,n+i}\left(E\right)_p + \sum_{p=n+1}^{k}\left(\Psi^c\right)_{p,i}\left(E^c\right)_p + \left(\Psi\right)_{k,n+i}\left(E\right)_k\right]$$

$$= \sum_{i=1}^{n}\left[\sum_{j=n+1}^{k-1}\left(\Psi\right)_{j,n+i}\left(E\right)_j + \sum_{j=1}^{n}\left(\Psi^c\right)_{j,i}\left(E^c\right)_j\right] \tag{B12}$$

All of the quantities on the left side of this equation are known. The shield temperature can be factored out of the right side of the equation. This yields:

$$T_m^4 = \frac{-\sum_{i=1}^{n}\left[\sum_{p=1}^{n}(\Psi)_{p,n+i}(E)_p + \sum_{p=n+1}^{\kappa}(\Psi^c)_{p,i}(E^c)_p + (\Psi)_{k,n+i}(E)_k\right]}{\sigma\sum_{i=1}^{n}\left\{\sum_{j=1}^{n}A_j\left[(\Psi)_{n+j,n+i}\epsilon_{n+j} + (\Psi^c)_{j,i}\epsilon_j^c\right]\right\}} \tag{B13}$$

When there is solar radiation present, the temperature of an infinitely conducting shield can be found from the amount of solar radiation absorbed by the shield as a whole. The shield temperature is found from the following equation:

$$T_m^4 = \frac{-\sum_{i=1}^{n}\left[\varphi A_i\alpha_\varphi + \sum_{p=n+1}^{k}(\Psi^c)_{p,i}(E^c)_p\right]}{\sigma\sum_{i=1}^{n}\left\{\sum_{j=1}^{n}A_j\left[(\Psi^c)_{j,i}\epsilon_j^c - \delta_{i,j}\epsilon_{n+j}\right]\right\}} \tag{B14}$$

When the conducted heat transfer to an element ($q_{c,j}$) is zero so that the shield is either nonconducting or the shield has a uniform temperature, and all properties are independent of temperature, the equations for determining the temperature are linear in T^4. When the equations are linear, the shield temperature and heat-transfer rates can be found by summing up the contributions of each source separately.

If there is no heat transfer between the elements of the shields, entries of the vector Q in equation (B9) can be portioned into two parts with each part being the negative of the heat transfer to the element due to one of the sources. Since the matrix D is a function only of the surface properties of the sources and not their temperatures, the values in the vector Z are proportional to the magnitude of the entries of Q. The entries of Z are $\sigma A_i T_i^4$. T^4 for every element can be found by summing the contribution due to each source.

Similarly, the heat-transfer rates due to each of the sources appears in the numerator of equation (B13) in a linear combination. Therefore, if the shield has a uniform temperature, this temperature can be found by summing up the contributions due to each source taken separately.

When the equations are linear and there is only one source with a finite temperature, the shield temperatures are porportional to this temperature. The heat-transfer rates are proportional to this temperature raised to the fourth power. In this way, if the source

temperature is doubled, the shield temperature will also double while the heat-transfer rate will increase by a factor of 16. The additive procedure, when the case resolved itself into a linear problem for a single shield between two sources, is illustrated as follows:

$T = 0$	$T = T_2$	$T = T_2$
$T_s^4 = T_{s1}^4$	$+ \quad T_s^4 = T_{s2}^4$	$= \quad T_s = \sqrt[4]{T_{s1}^4 + T_{s2}^4}$
$\dot{Q} = \dot{Q}'$	$\dot{Q} = \dot{Q}^*$	$\dot{Q} = \dot{Q}' + \dot{Q}^*$
$T = T_1$	$T = 0$	$T = T_1$

The procedure can be extended to the situation in which more than one shield is present.

The heat-transfer rate into the j^{th} element is the sum of conduction and radiation heat-transfer rates and equals zero

$$q_{c,j} + q_{r,j+n} + q_{r,j}^{c} = 0$$

Substituting values from equations (B1) and (B6) gives:

$$\frac{\left(T_{j+1} - T_j\right)}{\mathscr{R}_{j+1,j}} + \frac{\left(T_{j-1} - T_j\right)}{\mathscr{R}_{j-1,j}} = \sum_{p=1}^{k} \left[\left(\Psi\right)_{p,n+j} \left(E\right)_p + \left(\Psi^c\right)_{p,j} \left(E^c\right)_p \right] \tag{B15}$$

So long as the ratio of the radii (r_i/r_j where $i = j \pm 1$) stays constant, the thermal resistances are not a function of the radiating area. Each term on the right side of equation (B15) is proportional to the radiating area. However, for a linearly scaled system in which the spacing ratio (L/R) between surfaces remains constant, a reference area A_1 may be factored out. Since it is assumed that the projection of all surfaces is circular, this reference area is proportional to its lateral radius squared ($A_1 \propto R_1^2$). When all properties are independent of temperature, it is convenient to express temperatures as a ratio to a reference value T_2. Physically, A_1 could be the area of a cold source, while T_2 could be the temperature of a warm source. Equation (B15) can be nondimensionalized to give:

$$\frac{kt}{T_2^3 R_1^2}\left[\ln\left(\frac{r_j}{r_{j-1}}\right)\left(\frac{T_{j+1}-T_j}{T_2}\right)+\ln\left(\frac{r_{j+1}}{r_j}\right)\left(\frac{T_{j-1}-T_j}{T_2}\right)\right]=K\sum_{p=1}^{k}\left[\left(\Psi\right)_{p,\,n+j}\epsilon_p\frac{A_p}{A_1}\left(\frac{T_p}{T_2}\right)^4\right.$$

$$\left.+\left(\Psi^c\right)_{p,\,j}\epsilon_p^c\frac{A_p^c}{A_1}\left(\frac{T_p^c}{T_2}\right)^4\right] \qquad \text{(B16)}$$

K is a nondimensional constant determined by the shape of the reference area A_1. For a plane source

$$K = 0.5\ln\left(\frac{r_{j+1}}{r_j}\right)\ln\left(\frac{r_j}{r_{j-1}}\right)$$

APPENDIX C

HEAT TRANSFER BETWEEN SPECULARLY REFLECTING SURFACES

The purpose of this section of the report is to present the relations used to determine the shield temperature and heat-transfer rates for diffusely emitting, specularly reflecting surfaces of uniform radiosity. Because of the assumptions of uniform radiosity and uniform emittance, there is no thermal gradient in the shields.

The equations for the heat-transfer rate between two plane specular surfaces having uniform radiosity (diffuse emissivity) are given in reference 11. The sources appear mirror-like so that the view factor between surfaces is a function of the number of reflections encountered by the bundle of energy. Figure 32 gives an illustration of the way the apparent spacing increases due to each reflection for the specular surfaces. The surfaces numbered 1 and 3 are specularly reflecting, while the other two surfaces are simply windows to let the radiant energy escape. The apparent spacing for the direct view factor from 1 to 3 is the actual spacing between 1 and 3. The apparent spacing for the view factor from 1 to 1 after being reflected off 3 is twice the actual spacing. Thus, the energy appears to be coming from the dashed surface immediately to the left of surface 3. Figure 33 is a schematic of a shield and two sources. The surfaces are specular so that the angle of incidence equals the angle of reflection ($\beta = \beta'$).

The net heat transfer away from a surface is:

$$\frac{\dot{Q}}{A} = \sigma \epsilon T^4 - \alpha H \tag{C1}$$

where H, the incident energy per unit time and area, is composed of two parts. The first part is the energy from the other surface, and the second is the energy from the surface under consideration which is incident on itself after it has been reflected off the other surface. For surface 1:

$$H_1 = \sigma \epsilon_3 T_3^4 \left[F_{1,3} + F_{1,3(1,3)} \rho_1 \rho_3 + F_{1,3(1,3,1,3)} \rho_1^2 \rho_3^2 + \cdots \right] + \sigma \epsilon_1 T_1^4 \left[F_{1,1(3)} \rho_3 + F_{1,1(3,1,3)} \rho_3^2 \rho_1 + F_{1,1(3,1,3,1,3)} \rho_3^3 \rho_1^2 + \cdots \right] \tag{C2}$$

The view factor from surface 1 to surface 3 is used so as to have only one area (A_1) in the equation. This is done by the use of the reciprocity theorem which states that:

$$F_{1,3} A_1 = F_{3,1} A_3$$

Rewriting equation (C2) in terms of an infinite series gives:

$$H_1 = \sigma \epsilon_3 T_3^4 \sum_{\eta=0}^{\infty} F_{1,3(1^{\eta},3^{\eta})} \rho_1^{\eta} \rho_3^{\eta} + \sigma \epsilon_1 T_1^4 \sum_{\eta=1}^{\infty} F_{1,1(3^{\eta},1^{\eta-1})} \rho_3^{\eta} \rho_1^{\eta-1} \qquad \text{(C3)}$$

The view factor between two disks is given in reference 1 and the view factor is a function of the spacing ratio $F = g(L/R)$. As the apparent distance between the shields increases due to an increasing number of reflections, the view factors decrease due to the widening distances between images. Returning to figure 32 shows that the direct view factor between a pair of surfaces ($F_{1,3}$) is a function of the actual spacing between surfaces $F_{1,3} = g(L/R)$. The view factor from a surface to itself as seen in the other surface ($F_{1,1(3)}$) is a function of twice the actual spacing between the surfaces $F_{1,1(3)} = g(2L/R)$. The view factor after two reflections from the opposite surface is a function of three times the actual spacing $F_{1,3(1,3)} = g(3L/R)$. In general

$$F_{1,3(1^{\eta},3^{\eta})} = g((2^{\eta} + 1)L/R)$$

and

$$F_{1,1(3^{\eta},1^{\eta-1})} = g(2^{\eta}L/R) \qquad \text{for } \eta > 0 \qquad \text{(C4)}$$

Equation (C3) is evaluated by taking a large number of terms in each of the series and estimating the remainder. The terms in the remainder are estimated by assuming the remainder forms a geometric series. For a constant view factor, the remainder would be exactly a geometric series. The value of the parameter in the geometric series is the ratio of the two final terms. Equation (C3) is approximated as:

$$H_1 \cong \sigma \epsilon_3 T_3^4 \left[\sum_{\eta=0}^{\zeta} \left(F_{1,3(1^{\eta},3^{\eta})} \rho_1^{\eta} \rho_3^{\eta} \right) + \frac{F_{1,3\left(1^{\zeta+1},3^{\zeta+1}\right)} \rho_1^{\zeta+1} \rho_3^{\zeta+1}}{1 - \frac{F_{1,3\left(1^{\zeta+2},3^{\zeta+2}\right)} \rho_1 \rho_3}{F_{1,3\left(1^{\zeta+1},3^{\zeta+1}\right)}}} \right]$$

$$+ \sigma \epsilon_1 T_1^4 \left[\sum_{\eta=1}^{\zeta} \left(F_{1,1(3^{\eta},1^{\eta-1})} \rho_3^{\eta} \rho_1^{\eta-1} \right) + \frac{F_{1,1\left(3^{\zeta+1},1^{\zeta}\right)} \rho_3^{\zeta+1} \rho_1^{\zeta}}{1 - \frac{F_{1,1\left(3^{\zeta+2},1^{\zeta+1}\right)} \rho_1 \rho_3}{F_{1,1\left(3^{\zeta+1},1^{\zeta}\right)}}} \right] \qquad \text{(C5)}$$

The value of ζ was chosen so that the remainders (the last term in each bracket) were less than 0.1 percent of the first term in the bracket which is the value found by summing over ζ.

A shield placed between two sources has no net heat transfer to it in steady-state conditions. This fact can be utilized to determine the shield temperature. Figure 33 gives an illustration of a single shield placed between two plane sources. The four-surface system is divided into two two-surface systems, and the heat-transfer rate to the surfaces of the shield can be found in terms of the source temperature for each system. The sum of the heat transfer to the shield from both systems is zero and the shield temperature is determined.

APPENDIX D

DERIVATION OF THE DIFFERENTIAL EQUATION FOR A STRUCTURAL MEMBER

The equation giving the temperature distribution along the strut is derived by considering the heat balance on an element of the structural member. Figure 34 gives a schematic of a strut. Heat enters the element by conduction from the warmer adjacent element and leaves by means of conduction to the colder adjacent element. Heat is transmitted to or from the element by radiation on both the inside and outside surfaces of the element.

The rate at which heat enters the element due to conduction at the position x on the strut is given by:

$$q_{in,c} = -ka\left.\frac{dT}{dx}\right|_x = -\frac{k\pi}{4}\left(d_o^2 - d_\iota^2\right)\left.\frac{dT}{dx}\right|_x \tag{D1}$$

The rate at which heat leaves the element due to conduction at $x + \Delta x$ is given by:

$$q_{out,c} = -ka\left.\frac{dT}{dx}\right|_{x+\Delta x} = -\frac{k\pi}{4}\left(d_o^2 - d_\iota^2\right)\left.\frac{dT}{dx}\right|_{x+\Delta x} \tag{D2}$$

Since the environment is assumed black ($\epsilon_{sr} = 1$), energy which is emitted or reflected from the outside surface of the strut is absorbed by the surroundings and cannot return to any part of the strut. The rate at which heat is absorbed by the element due to the surroundings is given by:

$$q_{in,sr} = \sigma\epsilon_{sr}A_{sr}f_{sr-x}T_{sr}^4\alpha_o = \sigma A_{sr}f_{sr-x}T_{sr}^4\alpha_o$$

The reciprocity theorm for view factors yields the relation:

$$A_{sr}f_{sr-x} = A_x f_{x-sr} = \pi d_o\,\Delta x\, f_{x-sr}$$

The view factor from the element to the surroundings (f_{x-sr}) is unity.

The rate at which heat is radiated from the outside surface toward the surroundings is $\sigma\pi\epsilon_o d_o\,\Delta x\,T^4$. It is assumed that the surfaces are gray; therefore, $\epsilon_o = \alpha_o$. The net rate of radiant heat transfer from the outside surface of the element is therefore:

$$q_{out,r} = \sigma \pi d_o \epsilon_o \Delta x \left(T^4 - T_{sr}^4\right) \tag{D3}$$

The net rate at which heat is absorbed on the internal surface due to radiation from the rest of the strut is found by Gebhart's solution for problems of radiant interchange in an enclosure. This method has been described in appendix B.

In attempting to determine the temperature distribution along the strut, a differential equation is derived. In deriving the equation, the limit is taken as the area for radiant interchange approaches zero. The view factor to an infinitesimal area from another surface approaches zero, though the view factor from the infinitesimal area to the surface is not necessarily zero. It is desirable, therefore, to express view factors as going from the infinitesimal element to the other surface rather than going from the other surface to the infinitesimal area.

The net radiant heat-transfer rate for the internal surface is found by dividing the strut into $n + 1$ sections. One of these sections is the element under consideration and the size of this element approaches zero. Physically, this represents the division of the strut into n sections. The amount of radiant energy which leaves the element and is later absorbed by the element goes to zero as the size of the element decreases. If j represents the element under consideration, this last statement is equivalent to saying that B_{jj} approaches zero in the heat-transfer balances. (The mathematical justification for this is shown at a later stage in the development of the equations.) In addition to the n physical sections of the strut, there are two additional sections necessary to complete the enclosure. These two sections are the end disks of the strut.

The set of algebraic equations for the $n + 2$ nonzero values of B_{ij} for the heat-transfer rate to the j^{th} element are:

$$\left.\begin{aligned}
B_{1j} &= \epsilon_j f_{1j} + \rho_1 f_{11} B_{1j} + \rho_2 f_{12} B_{2j} + \cdots + \rho_k f_{1k} B_{kj} \\
B_{2j} &= \epsilon_j f_{2j} + \rho_1 f_{21} B_{1j} + \rho_2 f_{22} B_{2j} + \cdots + \rho_k f_{2k} B_{kj} \\
&\vdots \qquad\qquad \vdots \\
B_{kj} &= \epsilon_j f_{kj} + \rho_1 f_{k1} B_{1j} + \rho_2 f_{k2} B_{2j} + \cdots + \rho_k f_{kk} B_{kj}
\end{aligned}\right\} \tag{D4}$$

where $k = n + 2$.

These equations can be rewritten as:

$$\left(\rho_1 f_{11} - 1\right) B_{1j} + \rho_2 f_{12} B_{2j} + \ldots + \rho_k f_{1k} B_{kj} = -\epsilon_j f_{1j}$$

$$\rho_1 f_{21} B_{1j} + \left(\rho_2 f_{22} - 1\right) B_{2j} + \ldots + \rho_k f_{2k} B_{kj} = -\epsilon_j f_{2j}$$

$$\vdots \qquad\qquad \vdots$$

$$\rho_1 f_{k1} B_{1j} + \rho_2 f_{k2} B_{2j} + \ldots + \left(\rho_k f_{kk} - 1\right) B_{kj} = -\epsilon_j f_{kj}$$

The reciprocity theorem for view factors gives:

$$A_i f_{ij} = A_j f_{ji}$$

If each side of every equation is divided by A_j and the view factors on the right side are transformed so that they are from the j^{th} element to another source, one obtains:

$$\left.\begin{aligned}
&\left(\rho_1 f_{11} - 1\right) \frac{B_{1j}}{A_j} + \rho_2 f_{12} \frac{B_{2j}}{A_j} + \ldots + \rho_k f_{1k} \frac{B_{kj}}{A_j} = -\frac{\epsilon_j f_{j1}}{A_1} \\
&\rho_1 f_{21} \frac{B_{1j}}{A_j} + \left(\rho_2 f_{22} - 1\right) \frac{B_{2j}}{A_j} + \ldots + \rho_k f_{2k} \frac{B_{kj}}{A_j} = -\frac{\epsilon_j f_{j2}}{A_2} \\
&\vdots \qquad\qquad\qquad\qquad\qquad\qquad \vdots \\
&\rho_1 f_{k1} \frac{B_{1j}}{A_j} + \rho_2 f_{k2} \frac{B_{2j}}{A_j} + \ldots + \left(\rho_k f_{kk} - 1\right) \frac{B_{kk}}{A_j} = -\frac{\epsilon_j f_{jk}}{A_k}
\end{aligned}\right\} \qquad \text{(D5)}$$

These equations can be placed in matrix form

$$C\bar{u} = \bar{v} \qquad \text{(D6)}$$

where C is a coefficient matrix and is independent of j. The entries of C are:

$$(C)_{pi} = \rho_i f_{pi} - \delta_{pi}$$

$\bar{v}$ is a column vector with the entries $(\bar{v})_p = -(\epsilon_j f_{jp})/A_p$. $\bar{u}$ is a column vector which contains the values of B_{ij}/A_j. $\bar{u}$ is found from equation (D6) by taking the inverse of C

$$\bar{u} = C^{-1}\bar{v} \tag{D7}$$

The net heat-transfer rate to the j^{th} element due to internal radiation is:

$$q_{in,r} = \sum_{i=1}^{k} B_{ij}(E)_i - \left(1 - B_{jj}\right)\sigma A_j T_j^4 \epsilon_j \tag{D8}$$

It should be noted that E contains only entries for the finite area elements, and therefore the emissive power of the element under consideration (j) is not an entry in E. Equation (D8) can be expressed in terms of the column vector $\bar{u}$ to give:

$$q_{in,r} = A_j\left[\sum_{i=1}^{k} (\bar{u})_i(E)_i\right] - (1 - B_{jj})\sigma A_j T_j^4 \epsilon_j$$

If B_{jj} had been included as the $k + 1$ equation of (D4), the above equation would be:

$$q_{in,r} = A_j\left[\sum_{i=1}^{k} (\bar{u})_i(E)_i - \sigma T_j^4 \epsilon_j\right] + \sigma T_j^4 \epsilon_j A_j^2 (\bar{u})_{k+1} \tag{D9}$$

A_j is the internal surface area of the element under consideration ($\pi d_\iota \Delta x$). In subsequently forming the differential equation, the right side of equation (D9) is divided by Δx and the limit is taken as Δx approaches zero. When this is done, the last term in equation (D9) goes to zero. Therefore, the net radiant heat transfer into the internal surface of the element is:

$$q_{in,r} = \pi d_\iota \Delta x\left[\sum_{i=1}^{k} (\bar{u})_i(E)_i - \sigma T_j^4 \epsilon_j\right] \tag{D10}$$

Equating the rate at which heat enters the element with the rate at which it leaves gives:

$$q_{in,c} - q_{out,c} = q_{out,r} - q_{in,r} \tag{D11}$$

Expanding each term and collecting common factors gives:

$$-\frac{k\pi}{4}\left(d_o^2 - d_\ell^2\right)\left(\left.\frac{dT}{dx}\right|_x - \left.\frac{dT}{dx}\right|_{x+\Delta x}\right) = \pi\sigma\,\Delta x\left\{T_j^4\left(\epsilon_j d_\ell + \epsilon_o d_o\right) - \epsilon_o d_o T_{sr}^4 - d_\ell\left[\sum_{i=1}^{k}(\bar{u})_i A_i \epsilon_i T_i^4\right]\right\}$$

Taking the limit as $\Delta x \to 0$ for both sides of the equation yields:

$$\frac{k\left(d_o^2 - d_\ell^2\right)}{4\sigma}\frac{d^2T}{dx^2} = T^4\left(\epsilon_\ell d_\ell + \epsilon_o d_o\right) - \epsilon_o d_o T_{sr}^4 - d_\ell\left[\sum_{i=1}^{k}(\bar{u})_i A_i \epsilon_i T_i^4\right] \qquad \text{(D12)}$$

In equation (D12), the subscript j has been dropped. However, the entries in $\bar{u}$ do depend on the relative position of the differential element and the finite area sections.

The differential equation is integrated from zero to ℓ where ℓ is the length of the strut. By letting $\xi = x/\ell$, the range of the independent variable is from zero to one. Since $dx = \ell d\xi$, equation (D12) becomes:

$$\frac{k\left(d_o^2 - d_\ell^2\right)}{4\sigma\ell^2}\frac{d^2T}{d\xi^2} = T^4\left(\epsilon_\ell d_\ell + \epsilon_o d_o\right) - \epsilon_o d_o T_{sr}^4 - d_\ell\left[\sum_{i=1}^{k}(\bar{u})_i A_i \epsilon_i T_i^4\right] \qquad \text{(D13)}$$

When the thermal conductivity and emissivity are independent of temperature, non-dimensional temperature profiles can be obtained. Since both end temperatures (T_1 and T_2) are known, the differential equation has known boundary values. Dividing each side of the equation by T_2^4 yields:

$$\frac{k\left(d_o^2 - d_\ell^2\right)}{4\sigma\ell^2 T_2^3}\frac{d^2\left(\frac{T}{T_2}\right)}{d\xi^2} = \left(\frac{T}{T_2}\right)^4\left(\epsilon_\ell d_\ell + \epsilon_o d_o\right) - \epsilon_o d_o\left(\frac{T_{sr}}{T_2}\right)^4 - d_\ell\left[\sum_{i=1}^{k}(\bar{u})_i A_i \epsilon_i\left(\frac{T_i}{T_2}\right)^4\right]$$

Letting $\theta = T/T_2$ one obtains:

$$\frac{k\left(d_o^2 - d_\ell^2\right)}{4\sigma\ell^2 T_2^3}\frac{d^2\theta}{d\xi^2} = \theta^4\left(\epsilon_\ell d_\ell + \epsilon_o d_o\right) - \epsilon_o d_o \theta_{sr}^4 - d_\ell\left[\sum_{i=1}^{k}(\bar{u})_i A_i \epsilon_i \theta_i^4\right] \qquad \text{(D14)}$$

The boundary conditions are $\theta_2 = 1$ and $\theta_1 = T_1/T_2$. Since the values of θ_i are functions of the temperature distribution along the strut, they are determined by θ.

When the strut is a thin-walled tube, the cross-sectional area is approximately πdt where t is the thickness of the tube and d represents either the inside or outside diam-

eter. For a thin-walled tube equation (D14) becomes:

$$\frac{kt}{\sigma l^2 T_2^3}\frac{d^2\theta}{d\xi^2} = \theta^4\left(\epsilon_i + \epsilon_o\right) - \epsilon_o\theta_{sr}^4 - \sum_{i=1}^{k}(\bar{u})_i A_i \epsilon_i \theta_i^4 \tag{D15}$$

When the temperature of the surroundings goes to zero and the internal emissivity is reduced to zero, equation (D15) becomes:

$$\frac{d^2\theta}{d\xi^2} = \frac{\sigma l^2 T_2^3 \epsilon_o \theta^4}{kt} \tag{D16}$$

The total heat-transfer rate out of the cold end of the strut is the sum of the conducted heat transfer out and the radiant energy absorbed by the end disk. For illustration, consider the end at which x equals zero. From figure 34 it is seen that the end disk is the k^{th} element in the system. The temperature of the strut at this end is T_1 and for closed disks T_k would probably equal T_1. The total heat-transfer rate is:

$$\dot{Q}_T = \dot{Q}_c + \dot{Q}_r = ka\left.\frac{dT}{dx}\right|_{x=0} + \sum_{i=1}^{k}\left(B_{ik} - \delta_{ik}\right)(E)_i \tag{D17}$$

Note that since the end disk is a finite area element, B_{kk} is not zero. In reference 10, it is shown that $\epsilon_k B_{ki} A_k = \epsilon_i B_{ik} A_i$ for gray surfaces. Equation (D17) can be rewritten as:

$$\dot{Q}_T = k\frac{\pi}{4}\left(d_o^2 - d_l^2\right)\left.\frac{dT}{dx}\right|_{x=0} + \sigma\epsilon_k\frac{\pi d_l^2}{4}\left[\sum_{i=1}^{k}\left(B_{ki} - \delta_{ik}\right)T_i^4\right]$$

Introducing nondimensional parameters gives:

$$\frac{4\dot{Q}_T}{\pi\sigma T_2^4 d_l^2} = \frac{k\left(d_o^2 - d_l^2\right)}{\sigma T_2^3 l d_l^2}\left.\frac{d\theta}{d\xi}\right|_{\xi=0} + \epsilon_k\sum_{i=1}^{k}\left(B_{ki} - \delta_{ik}\right)\theta_i^4 \tag{D18}$$

For a constant internal emissivity $\epsilon_k = \epsilon_i$. The absorption factors B_{ki} depend only on the internal emissivities and l/d_l of the tube.

APPENDIX E

SOLUTION OF EQUATIONS

The purpose of this appendix is to discuss the solution of the equations presented in appendix B for the shadow-shield system and the equations presented in appendix D for the thermal analysis of a structural member.

Shadow-Shield Equations

In appendix B, equations are given for the shield temperature and concomitant heat-transfer rates when the equations are linear in T^4. As the conducted heat transfer increases relative to the radiant heat transfer, it becomes more advantageous to solve the equations for the shield temperatures assuming that the equations are linear in T. The various terms contributing to the heat balance for an element are shown in figure 30. The conduction heat-transfer rate into the j^{th} element is given by equation (B6). The equations of (B8) give the radiant heat-transfer rate into each element of the shield. In steady state, the net heat-transfer rate into each element is zero. Adding equations (B6) and (B8) for the j^{th} element gives:

$$q_{c,j} + (\Phi)_{n+j} + (\Phi^c)_j = 0 \tag{E1}$$

Expanding this equation and placing terms involving known temperature sources on the right side yields for the j^{th} element:

$$\left(\frac{T_{j-1} - T_j}{\mathscr{R}_{j-1,j}}\right) + \left(\frac{T_{j+1} - T_j}{\mathscr{R}_{j+1,j}}\right) + \sum_{i=1}^{n} (\Psi)_{n+i,\,n+j}(E)_{n+i} + \sum_{i=1}^{n} (\Psi^c)_{i,j}(E^c)_i$$

$$= -\left[\sum_{p=1}^{n} (\Psi)_{p,\,n+j}(E)_p + (\Psi)_{k,\,n+j}(E)_k + \sum_{p=n+1}^{k} (\Psi^c)_{p,i}(E^c)_p\right]$$

Factoring out the temperature of each element of the shield gives:

$$\left(\frac{T_{j-1} - T_j}{\mathscr{R}_{j-1,j}}\right) + \left(\frac{T_{j+1} - T_j}{\mathscr{R}_{j+1,j}}\right) + \sum_{i=1}^{n}\left[\left(\Psi\right)_{n+i,\,n+j}\epsilon_{n+i} + \left(\Psi^c\right)_{i,\,j}\epsilon_i^c\right]\sigma A_i T_i^3 T_i$$

$$= -\left[\sum_{p=1}^{n}\left(\Psi\right)_{p,\,n+j}\left(E\right)_p + \left(\Psi\right)_{k,\,n+j}\left(E\right)_k + \sum_{p=n+1}^{k}\left(\Psi^c\right)_{p,\,i}\left(E^c\right)_p\right]$$

An equation can be written for each of the n elements of the shield. This results in the matrix equation:

$$Y\Theta = P \tag{E2}$$

Y is an n-by-n matrix containing the entries:

$$\left(Y\right)_{i,\,j} = \left[\left(\Psi\right)_{n+j,\,n+i}\epsilon_{n+j} + \left(\Psi^c\right)_{j,\,i}\epsilon_j^c\right]\sigma A_j T_j^3 - \delta_{i,\,j}\left(\frac{1}{\mathscr{R}_{j-1,j}} + \frac{1}{\mathscr{R}_{j+1,j}}\right) + \frac{\delta_{i,\,j+1}}{\mathscr{R}_{i-1,i}} + \frac{\delta_{i,\,j-1}}{\mathscr{R}_{i+1,i}}$$

Θ is a column vector containing the temperature for each annulus

$$\left(\Theta\right)_j = T_j$$

P is a column vector containing the negative of the radiant heat transfer to each annulus from the sources with known temperatures.

$$\left(P\right)_i = -\left[\sum_{p=1}^{n}\left(\Psi\right)_{p,\,n+i}\left(E\right)_p + \left(\Psi\right)_{k,\,n+i}\left(E\right)_k + \sum_{p=n+1}^{k}\left(\Psi^c\right)_{p,\,i}\left(E^c\right)_p\right]$$

The temperatures are found by taking the inverse of Y in equation (E2). This gives:

$$\Theta = Y^{-1}P \tag{E3}$$

The equation for the matrix Y can be expanded to give:

$$(Y)_{i,j} = \left\{\left[(U)_{n+j,n+1} - \delta_{i,j}\right]\epsilon_{n+j} + \left[(U^c)_{j,i} - \delta_{i,j}\right]\epsilon_j^c\right\}\sigma A_j T_j^3$$

$$- \delta_{i,j}\left(\frac{1}{\mathscr{R}_{j-1,j}} + \frac{1}{\mathscr{R}_{j+1,j}}\right) + \frac{\delta_{i,j+1}}{\mathscr{R}_{i-1,i}} + \frac{\delta_{i,j-1}}{\mathscr{R}_{i+1,i}}$$

When one of the sources is solar radiation, the matrix Y and the vector P become:

$$(Y)_{i,j} = \left\{-\delta_{i,j}\epsilon_{n+j} + \left[(U^c)_{j,i} - \delta_{j,i}\right]\epsilon_j^c\right\}\sigma A_j T_j^3 - \delta_{i,j}\left(\frac{1}{\mathscr{R}_{j-1,j}} + \frac{1}{\mathscr{R}_{j+1,j}}\right) + \frac{\delta_{i,j+1}}{\mathscr{R}_{i-1,i}} + \frac{\delta_{i,j-1}}{\mathscr{R}_{i+1,i}}$$

$$(P)_i = -\varphi A_i \alpha_\varphi - \sum_{p=n+1}^{k} (\Psi^c)_{p,i}(E^c)_p$$

From the equations presented above and those of appendix B, it can be seen that when the equations are linear and only one shield present, the shield temperatures are determined explicitly. The equations can be nonlinear due to a finite shield conductivity or temperature-dependent surface properties. When the equations are nonlinear or there is more than a single shield, an iterative procedure is used. This iterative procedure simply sets a new trial value for each annulus of each shield at a value lying between the old estimate and the latest calculated value. When the shields are conducting, the new estimate lies close to the old estimate. The computer program chooses this degree of closeness so as to minimize computer time, but also insuring that the system of equations remains stable. The tolerance used to determine when the iteration has converged is 0.0055 K (0.01° R). The difference between the calculated and estimated temperatures is less than this value for each annulus of each shield at convergence. To insure that the tolerance is sufficiently fine, the first case in each run is automatically rerun with the tolerance halved.

When the conduction term does not enter into the equations, convergence is fairly rapid. With a two-shield system and no conduction, about five iterations are required to obtain a solution. The number of iterations increases with the number of shields involved going to about 20 iterations for a four-shield system with no conduction. The number of iterations required when the shields have a uniform temperature is about the same as when there is no conduction between annuli. If there is conduction between annuli, the number of iterations increases drastically so that a factor of 10 in the number of iterations required would not be unexpected.

The execution time for the program is proportional to the number of iterations and the number of shields involved. It is proportional to the square of the number of annuli

into which each shield is divided. A two-shield configuration with conduction and 14 annuli per surface would take about 2 minutes to execute on an IBM 7094 mod II digital computer. If conduction were neglected, the execution time would be less than half a minute.

In order to obtain heat-transfer rates for surfaces of nonuniform radiosity, each of the annuli should represent a differential area. To closely approximate this directly using a computer would result in an exceedingly large amount of running time. The results for nonuniform radiosity surfaces, which constitute the bulk of the data in this report, are obtained by graphing the heat-transfer rate as a function of the reciprocal of the number of annuli. This procedure is illustrated in figure 35. In this figure, the ratio of the heat-transfer rate to the heat-transfer rate for uniform radiosity surfaces (a single annulus per surface) is given as a function of the reciprocal of the number of annuli per surface. The ratio refers to the heat-transfer rate to the colder source, and is given for two emissivities and two spacing ratios. The single shield was spaced evenly between the two sources and all surfaces had the same emissivity. The point on the graph corresponding to an infinite number of annuli ($1/n = 0$) corresponds to the heat-transfer rate for surfaces of nonuniform radiosity. The solid line represents points for which data were actually generated, and the dashed line represents an extrapolation. It can be seen from this figure that the accuracy of the extrapolation decreases with decreasing emissivity. Also, it can be seen from this figure that increasing the number of annuli (this results in increased computer time) reduces the uncertainty in the extrapolation.

Thermal Equations for Struts

The differential equation presented in appendix D for the thermal analysis of a structural member is a second-order nonlinear equation with known boundary values. A finite difference scheme is used to solve the differential equation. In this technique, the length of the strut is taken as unity. The strut is divided into several equally spaced intervals, each with an axial length h. The second derivative expressed in terms of the dependent variable and the step size is

$$\frac{d^2T_i}{d\xi^2} = \frac{T_{i-1} - 2T_i + T_{i+1}}{h^2} \tag{E4}$$

Here i represents the particular point along the strut for which the differential equation is being approximated. Because the range of the independent variable is from zero to one, $h = 1/(m + 1)$. Where m is the number of interior points on the strut at which the differential equation is evaluated. The first point along the strut at which the differential equation is evaluated is a distance h from the end. Since this is a boundary value prob-

lem, the end temperatures (T_o and T_{m+1}) are known a priori. There are m equations of the same form as equation (E4) and these can be written in matrix form as:

$$\Omega = \chi\Theta \tag{E5}$$

Ω is a column vector of size m containing the evaluations of the second derivatives.

$$(\Omega)_p = h^2 \frac{d^2T_p}{d\xi^2} - \left(\delta_{1,p}T_o + \delta_{m,p}T_{m+1}\right) \tag{E6}$$

χ is an m-by-m coefficient matrix containing the coefficients of the temperatures. The entries of this matrix are clustered along the diagonal and have the values:

$$(\chi)_{p,q} = -2\delta_{p,q} + \delta_{p,q+1} + \delta_{p,q-1} \tag{E7}$$

Θ is a column vector containing the temperatures at each node point

$$(\Theta)_q = T_q \tag{E8}$$

Equation (E5) can be solved to yield the temperature distribution along the strut. This yields the equation:

$$\Theta = \chi^{-1}\Omega \tag{E9}$$

Since the second derivative is dependent upon the temperature distribution along the strut, an iterative procedure is used to determine the correct temperature distribution. This iterative procedure is much like the one employed in the solution of the equations for the shadow shield.

APPENDIX F

COMPUTER CODE FOR SHADOW-SHIELD CALCULATIONS

The purpose of this section of the report is to discuss the computer code used to solve the shadow-shield equations. The procedure for reading in the necessary data and the resulting output are discussed. Following this are general descriptions of the various routines used to make up the code. Flowcharts are given for these routines. This appendix concludes with a listing of the program and a sample output.

Description of Input

All of the necessary data enter the program through READ statements in the routine INPUT. For every case in a run this routine is called by SHIELD. Whenever view factor data for nonplanar sources are read in INPUT is called by TBVUF. All data enter the program through the use of NAMELIST statements. NAMELIST is an input/output feature of the FORTRAN IV language in which this code was written. The use of this feature is described in FORTRAN IV manuals such as reference 12.

The NAMELIST input/output feature uses names in place of Format numbers in the read and write statements. There are two names used in the reading statements of the INPUT routine. These two names are INPUT1 and INPUT2. The first of these is used to read in all of the data when there is only planar sources or solar radiation. When there is one or more nonplanar sources present data are read in for view factors through the use of the name INPUT2.

The necessary data are described in the listing of the routine INPUT. At the beginning of a run, prior to reading any data, many input variables are assigned certain values. This is done to reduce the amount of data which are read in. NAMELIST provides a flexible means of entering data into core. It is not necessary to specify all of the variables which are associated with a NAMELIST name, therefore, only those data necessary to execute a case need be provided. There is no provision for storing data for more than one case, so that at least one variable must be read in for each case in a multiple case run. However, only the data which change need be specified for each case. The program continues to search for new data until all of the input has been processed. (This programming results in a warning diagnostic for the routine SHIELD at compilation.) Because of the flexibility of NAMELIST, it is possible to inadvertently omit some of the data necessary to run a case. This will result in either error messages during execution or erroneous results. The latter situation is the more troublesome of the two. In order to be able to check the data, a listing of the input is provided at the beginning of each case.

This listing may be more extensive than the input because it consists of all of the data which have a bearing on the results. The sample case given at the end of the listing is for two nonconducting shields and a planar tank. The outermost shield is exposed to solar radiation. The variables required are determined from the listing of the routine INPUT. The values used for each variable are found in the output.

Description of Output

The output from a successfully executed case is written by the routine SHIELD. A description of the variables printed out can be found by consulting the listing of this routine. In addition to the expected output there may be additional output. Faulty data may result in an illegal operation such as division by zero. The execution monitor will then print out its own message. Faulty data may also result in the routine FACTOR encountering a singular matrix. If this occurs, an error message is printed and the run is terminated.

As mentioned previously, a large number of iterations is required when the shields are partially conducting. If the number of iterations exceeds the value of the variable ITMAX, a message is printed along with the last estimates of the shield temperatures. When the shields are partially conducting, a solution may become divergent from a given starting condition, or may become divergent due to the means used to calculate the solution. There are two starting conditions for partially conducting shields and these are specificed by the variable IVCOND. These starting conditions are either uniform temperature shields or nonconducting shields. The solution for partially conducting shields can be found by assuming that the equations are linear in T or linear in T^4. The initial assumption concerning the linearity of the equations is governed by the value of the variable NCALCR. If, starting with the specified values for IVCOND and NCALCR, the solution appears to be diverging, one of the variables is changed, and the case is restarted. If, after the four possible combinations have been tried, the solution still appears to be diverging, the case is abandoned. Each time a change is made a message is printed. The current values of IVCOND and NCALCR are stored in ICOND and NCALC, respectively, and these values are printed as part of the message. All of these messages occur from the routine SHIELD.

Whenever a case is run involving one or two nonplanar surfaces, a check is made to insure that the necessary view factor data have been read in. This check is for the spacing ratio between surfaces, the type of surfaces, the ratio of the axial radius to the lateral radius for the nonplanar surfaces, and the number of annuli used. If the check fails, an error message is printed from the routine TBVUF and the run is terminated.

Description of Computer Code

This section of the appendix discusses the computer program which performs the calculations of the shadow-shield equations. This program is composed of several routines each of which performs a specific function. In the program, one of the sources is referred to as a heater and the other source is referred to as a tank. It is convenient to describe the computer program using these terms for the sources. The following is a brief description of each of the routines used in the program. Most of the routines have an accompanying flowchart and following some of the routines is a list of the FORTRAN symbols which correspond to symbols used in appendix B. The FORTRAN variables which are needed as input are described in the listing of the program and are not repeated here. Some variables are used throughout the program while others are limited to one or two routines. The FORTRAN symbols which are used throughout the program are given after the routine SHIELD and the others are given after the first routine in which they appear. The list of FORTRAN symbols is not exhaustive but is limited to the major variables. Accompanying the description of the FORTRAN variables is a key. This key describes the subscripting of variables and is explained after the discussion of the routines FACTOR and INVERT.

INPUT. - This subroutine reads in the necessary data. All of the input to the program enters through this routine. Figure 36 is a flowchart of this routine. The listing of the routine contains a description of the input.

SHIELD. - This is the main program. One of the functions of this routine is to provide a means of controlling the calling sequence to the subroutines which perform the actual calculations. Also, the iterative procedure for calculating the shield temperatures is done by this routine. With the exception of error messages, all output is generated in this routine. Figure 37 is a flowchart of this program. The numbers in connectors or to the left of a function block represent statement numbers in the program.

FORTRAN name	Variable in appendix B	Description	Key
AREA	A	The area of each annulus of each surface	1
AB	α	The absorptivity of each annulus of each surface	2
EMS	ϵ	The emissivity of each annulus of each surface	2
REF	ρ	The reflectivity of each annulus of each surface	2
COND	k	The thermal conductivity between annuli of a shield	1

FORTRAN name	Variable in appendix B	Description	Key
RES	$\mathscr{R}$	The thermal resistance between annuli of a shield	1
T	T	The temperature of each annulus of each surface	1
FNNHTT	f	The view factor from the surface of an annulus facing towards the tank to an annulus on a surface facing towards the heater. If there are no shields present, this is the view factor from an annulus on the heater to an annulus on the tank	3
FNNTTH	f	The complement of FNNHTT except that this is the view factor from an annulus towards the tank to an annulus towards the heater	3

TBVUF. - This routine calls INPUT to read view-factor data when nonplanar sources are present. These view factors were obtained using the computer program given in reference 13. This routine is set up so that all the data which are generated for nonplanar surfaces may be kept together and read in as a unit. Figure 38 is a flowchart of this subroutine.

VUFAC1. - This routine calculates the radii and areas for planar surfaces and sets up the call to the routines TBVUF and SUBVF in order to generate the view factors between annuli. VUFAC1 calculates the view factors between whole surfaces by summing up view factors. Figure 39 is a flowchart of this routine.

SUBVF. - This subroutine calculates the view factors between planar surfaces. The view-factor relations that are given in reference 1 are used in this routine. Figure 40 is a flowchart of this routine.

SCHLC. - This routine calculates the temperatures of the shields assuming that the temperatures of adjacent surfaces are known for each shield. Figure 41 is a flowchart of this routine.

FORTRAN name	Variable in appendix B	Description
PHI	φ	The solar flux
Q	Q	The rate of heat transfer to an annulus from known temperature sources
D	D^T	The matrix containing the absorption factors times emissivity

COEF. - This routine determines the absorption factors for each system consisting of two surfaces and the surroundings. Figure 42 is a flowchart of this subroutine.

FORTRAN name	Variable in appendix B	Description	Key
A	C	The coefficient matrix in the solution of the absorption factors	4
Y	V	The matrix containing the negative of the view factors times absorptivity	4
AI	C^{-1}	The inverse of A	4
B	U	The matrix containing the absorption factors	4

QDOT. - This routine calculates the heat-transfer rates to the tank as well as both the adjacent surface and the surroundings between these two surfaces. Figure 43 is a flowchart of this routine.

FACTOR and INVERT. - These two routines are used to invert a matrix. The method used is given in reference 14. As a consequence of the way these two routines are programmed, four warning diagnostics result at compilation.

Explanation of keys. -

Key

1 These variables are doubly subscripted. The first subscript refers to an annulus of a surface. The first element is the innermost annulus. The second subscript refers to the particular surface beginning with the heater. Thus AREA (5, 2) is the area of the fifth annulus of the first shield.

2 These variables are triply subscripted. The first two subscripts have the same meaning as the two subscripts for variables with a key 1. The third subscript denotes the particular side of the shields. The side designated a 1 faces the heater while side 2 faces the tank. Thus AB (5, 2, 2) is the absorptivity of the fifth annulus of the first shield on the side facing towards the tank.

3 These variables are triply subscripted. The first two subscripts refer to annuli on the originating and receiving surfaces, respectively. The third subscript refers to the pair of surfaces involved. These subscripts are arranged in the same fashion as the two previous keys. Thus, FNNTTH (1, 10, 1) refers to the view factor from the innermost annulus to the tenth annulus and is from an annulus of a shield or source adjacent to the heater to an annulus on the heater itself.

4 These variables are doubly subscripted and represent matrices. The two subscripts refer to the rows and columns of each matrix, respectively.

```
$IBFTC INPUT   DECK

      SUBROUTINE INPUT(JR)
C
C     THE PURPOSE OF THIS ROUTINE IS TO READ IN ALL OF THE DATA TO THE
C     PROGRAM
C
      EQUIVALENCE
     1(NE(1)  ,NE1B) , (NE(21) ,NE1T) , (NE(41) ,NE2B) , (NE(61) ,NE2T),
     2(NE(81) ,NE3B) , (NE(101),NE3T) , (NE(121),NE4B) , (NE(141),NE4T),
     3(NE(161),NE5B) , (NE(181),NE5T) , (NA(1)  ,NA1B) , (NA(21) ,NA1T),
     4(NA(41) ,NA2B) , (NA(61) ,NA2T) , (NA(81) ,NA3B) , (NA(101),NA3T),
     5(NA(121),NA4B) , (NA(141),NA4T) , (NA(161),NA5B) , (NA(181),NA5T)
      EQUIVALENCE
     1(CVABS(1) ,TBABS1) , (CVABS(5) ,TBABS2) , (CVABS(9) ,TBABS3) ,
     2(CVABS(13),TBABS4) , (CVABS(17),TBABS5) , (CVABS(21),TBABS6) ,
     3(CVABS(25),TBABS7) , (CVABS(29),TBABS8) , (CVABS(33),TBABS9) ,
     4(CVABS(37),TBABSL) , (CVEMS(1) ,TBEMS1) , (CVEMS(5) , TBEMS2) ,
     5(CVEMS(9) ,TBEMS3) , (CVEMS(13),TBEMS4) , (CVEMS(17),TBEMS5) ,
     6(CVEMS(21),TBEMS6) , (CVEMS(25),TBEMS7) , (CVEMS(29),TBEMS8) ,
     7(CVEMS(33),TBEMS9) , (CVEMS(37),TBEMSL)
      EQUIVALENCE
     1(CVCOND(1) ,TBCON1) , (CVCOND(5),TBCON2) , (CVCOND(9),TBCON3) ,
     2(CVCOND(13),TBCON4) , (CVCOND(17),TBCON5)
      DATA ( ID(I),I=1,10) /1H1,1H2,1H3,1H4,1H5,1H6,1H7,1H8,1H9,1HL /
      DATA(DNE(I),I=1,12) /72H NEH =NE1B =NE1T =NE2B =NE2T =NE3B =NE3T =
     1NE4B =NE4T =NE5B =NE5T = NET =  /
      DATA(DNA(I),I=1,12) /72H NAH =NA1B =NA1T =NA2B =NA2T =NA3B =NA3T =
     1NA4B =NA4T =NA5B =NA5T = NAT =   /
      DATA (DTEM(I),I=1,2) /6H  TH =,6H  TT =  /
      DATA DAHS , DATS / 6H AHS = , 6H ATS = /
      COMMON C(1000)
      EQUIVALENCE
     1(C(1)  ,ABSR  ) , (C(11) ,ARES  ) , (C(21) ,D     ) ,
     2(C(31) ,ES    ) , (C(41) ,IVCOND) , (C(42) ,ICONDR) ,
     3(C(43) ,ITMAX ) , (C(51) ,NAH   ) , (C(71) ,NAT   ) ,
     4(C(91) ,NA    ) , (C(291),NEH   ) , (C(311),NET   ) ,
     5(C(331),NE    ) , (C(531),NCOND ) , (C(541),NCASE ) ,
     6(C(542),NELIPS) , (C(543),NRADS ) , (C(544),NRNGS ) ,
     7(C(545),NSHLDS) , (C(546),NCALCR) , (C(547),NVUFH ) ,
     8(C(548),NVUFT ) , (C(549),PHI   ) , (C(550),PI    ) ,
     9(C(551),RS    ) , (C(561),RSH   ) , (C(562),RST   ) ,
     A(C(563),RH    ) , (C(564),RT    ) , (C(565),SOLAR ) ,
     B(C(566),SIGMA ) , (C(567),TOL   ) , (C(568),WI    ) ,
     C(C(571),SOLABS) , (C(591),STHICK) , (C(601),CVABS ) ,
     D(C(641),CVCOND) , (C(681),CVEMS ) , (C(721),TH    ) ,
     E(C(741),TS    ) , (C(751),TT    ) , (C(771),REFS  )
      COMMON / ELIP2 / EN , EL , RMHD , RMTD , XLOR , MXS , ATS(10) ,
     1                 AHS(10) , F(100) , LIST , NR1
```

```
      INPUT      -  EFN   SOURCE STATEMENT  -  IFN(S)  -

      DIMENSION DNE(12) , DNA(12) , DTEM(2) , NF(10) ,ID(10)
      DIMENSION CVABS(4,10) , CVEMS(4,10) , CVCOND(4,5) , NEH(20) ,
     1          NAH(20) , NET(20) , NAT(20) , NE(20,10) , NA(20,10) ,
     2          TT(20) , TH(20) , ABSR(10) , ES(10) , ARES(10) , TS(10),
     3          D(10)
      DIMENSION   TBEMS1(4) , TBEMS2(4) , TBEMS3(4) , TBEMS4(4) ,
     1            TBEMS5(4) , TBEMS6(4) , TBEMS7(4) , TBEMS8(4) ,
     2            TBEMS9(4) , TBEMSL(4) , TBABS1(4) , TBABS2(4) ,
     3            TBABS3(4) , TBABS4(4) , TBABS5(4) , TBABS6(4) ,
     4            TBABS7(4) , TBABS8(4) , TBABS9(4) , TBABSL(4) ,
     5            TBCON1(4) , TBCON2(4) , TBCON3(4) , TBCCN4(4) ,
     6            TBCON5(4)
      DIMENSION NE1B(20) , NE1T(20) , NE2B(20) , NE2T(20) , NE3B(20) ,
     1          NE3T(20) , NE4B(20) , NE4T(20) , NE5B(20) , NE5T(20) ,
     2          NA1B(20) , NA1T(20) , NA2B(20) , NA2T(20) , NA3B(20) ,
     3          NA3T(20) , NA4B(20) , NA4T(20) , NA5B(20) , NA5T(20) ,
     4          RS(5) , STHICK(5) , NCOND(5)
      NAMELIST / INPUT1 /
     1   ABSR    ,  ARES    ,  D       ,  ES      ,  ICONDR  ,
     2   ITMAX   ,  IVCOND  ,  NAH     ,  NAT     ,  NA1B    ,
     3   NA2B    ,  NA3B    ,  NA4B    ,  NA5B    ,  NA1T    ,
     4   NA2T    ,  NA3T    ,  NA4T    ,  NA5T    ,  NCALCR  ,
     5   NEH     ,  NET     ,  NE1B    ,  NE2B    ,  NE3B    ,
     6   NE4B    ,  NE5B    ,  NE1T    ,  NE2T    ,  NE3T    ,
     7   NE4T    ,  NE5T    ,  NCOND   ,  NCASE   ,  NELIPS  ,
     8   NRADS   ,  NRNGS   ,  NSHLDS  ,  NVUFH   ,  NVUFT   ,
     9   PHI     ,  RH      ,  RS      ,  RSH     ,  RST     ,
     A   RT      ,  SIGMA   ,  SOLABS  ,  SOLAR   ,  STHICK  ,
     B   TBABS1  ,  TBABS2  ,  TBABS2  ,  TBABS3  ,  TBABS4  ,
     C   TBABS5  ,  TBABS6  ,  TBABS7  ,  TBABS8  ,  TBABS9  ,
     D   TBABSL  ,  TBCON1  ,  TBCON2  ,  TBCON3  ,  TBCON4  ,
     E   TBCON5  ,  TBEMS1  ,  TBEMS2  ,  TBEMS3  ,  TBEMS4  ,
     F   TBEMS5  ,  TBEMS6  ,  TBEMS7  ,  TBEMS8  ,  TBEMS9  ,
     G   TBEMSL  ,  TH      ,  TOL     ,  TS      ,  TT      ,
      NAMELIST/OUTPU1/
     1   ICONDR  ,  ITMAX   ,  IVCOND  ,  NCALCR  ,  NCASE   ,
     2   NELIPS  ,  NRADS   ,  NRNGS   ,  NSHLDS  ,  NVUFH   ,
     3   NVUFT   ,  PHI     ,  RH      ,  RSH     ,  RST     ,
     4   RT      ,  SIGMA   ,  SOLABS  ,  SOLAR   ,  TOL
      NAMELIST / INPUT2 / AHS , ATS , F , FL , FN , LIST , MXS , NR1 ,
     2                    RMHD , RMTD , XLOR
      NAMELIST / OUTPU2 / FL , FN , LIST , MXS , NR1 , RMHD , RMTD ,XLOR
C
C     LIST OF INPUT FOR SHADOW SHIELD PROGRAM
C
C
C     VARIABLES READ IN THROUGH THE USE OF THE NAMELIST NAME INPUT1
C
C     NAME              DESIGNATION                          QUANTITY    CODES
C
C     ABSR      ABSORPTIVITY OF THE SURROUNDINGS.            NSHLDS+1    A
C               UNLESS INPUT THESE VARIABLES HAVE
C               A VALUE OF 1.0
C     ARES      AREA OF THE SURROUNDINGS. UNLESS             NSHLDS+1    A
C               INPUT THESE VARIABLES HAVE A VALUE
C               OF 1.0
C     D         DISTANCE BETWEEN SURFACES.                   NSHLDS+1    A
C     ES        EMISSIVITY OF THE SURROUNDINGS.              NSHLDS+1    A
```

```
C                INPUT      -  EFN   SOURCE STATEMENT  -  IFN(S)  -
C                     UNLESS INPUT THESE VARIABLES HAVE
C                     A VALUE OF 1.0
C       ICONDR        INDICATES THE TYPE OF SHIELDS USED.     1
C                     0 WHEN THE SHIELDS ARE PARTIALLY
C                     CONDUCTING. 1 WHEN THE SHIELDS ARE
C                     NON-CONDUCTING. 2 WHEN THE SHIELDS
C                     HAVE A UNIFORM TEMPERATURE. ICONDR
C                     IS INITIALLY ASSIGNED A VALUE OF 1.
C                     THIS VARIABLE HAS SIGNIFICANCE ONLY
C                     IF NRNGS IS GREATER THAN 1, AND
C                     CANNOT BE ZERO WHEN NRNGS IS 1.
C       ITMAX         THE MAXIMUM NUMBER OF ITERATIONS        1
C                     BEFORE THE SOLUTION OF THE
C                     IS ABANDONED. UNLESS SPECIFIED
C                     THIS VARIABLE IS ASSIGNED THE
C                     VALUE 200
C       IVCOND        1 WHEN THE SOLUTION FOR PARTIALLY
C                     CONDUCTING SHIELDS IS STARTED
C                     FROM A NON CONDUCTING SOLUTION.
C                     2 IF THE STARTING POINT IS FROM
C                     THE UNIFORM TEMPERATURE SOLUTION.
C       NAH           KEY USED TO SPECIFY ABSORPTIVITY        NRNGS       B,C
C                     OF ELEMENTS OF HEATER.
C       NAT           THE EQUIVALENT OF NAH EXCEPT FOR        NRNGS       B,C
C                     THE TANK.
C       NA1B          KEY USED TO SPECIFY ABSORPTIVITY        NRNGS       B,C
C                     OF ELEMENTS ON SIDE OF SHIELD
C                     CLOSEST TO HEATER FACING THE
C                     HEATER.
C       NA1T          THE EQUIVALENT OF NA1B EXCEPT           NRNGS       B,C
C                     FOR SIDE FACING AWAY FROM HEATER.
C       NA2B          THE EQUIVALENT OF NA1B OR NA1T          NRNGS       B,C
C       NA3B          EXCEPT THAT THESE VARIABLES
C       NA4B          REFER TO THE SECOND THROUGH THE
C       NA5B          FIFTH SHIELDS RESPECTIVELY.
C       NA2T
C       NA3T
C       NA4T
C       NA5T
C       NCALCR        0 WHEN THE SOLUTION IS FOUND WITH       1
C                     THE EQUATIONS LINEAR IN T**4.
C                     1 WHEN THE EQUATIONS ARE LINEAR IN T.
C       NCASE         1 IF THE LAST CASE IS TO BE RERUN       1
C                     WITH THE TOLERANCE ON THE
C                     TEMPERATURE DISTRIBUTION HALVED.
C                     A VALUE OF 1 IS ASSIGNED FOR THE
C                     FIRST CASE AND UNLESS A VALUE IS
C                     INPUT A VALUE OF 2 IS ASSIGNED
C                     EACH SUCEEDING CASE.
C       NCOND         KEY DENOTING THE THERMAL CONDUC-        NSHLDS      C
C                     TIVITY OF EACH OF THE SHIELDS.
C       NEH           KEY USED TO SPECIFY EMISSIVITY OF       NRNGS       B,C
C                     ELEMENTS OF HEATER.
C       NET           THE EQUIVALENT OF NEH EXCEPT FOR        NRNGS       B,C
C                     THE TANK.
C       NELIPS        THIS VARIABLE HAS MEANING ONLY IF       1
```

```
C               VIEW FACTOR DATA FOR A NONPLANAR
C               HEATER OR TANK IS READ IN FOR A CASE
C               OTHER THAN THE FIRST CASE IN A RUN.
C               SET EQUAL TO 0 FOR EACH CASE IN WHICH
C               VIEW FACTOR DATA ARE READ IN. CARE
C               SHOULD BE TAKEN IF VIEW FACTOR DATA
C               ARE READ IN MORE THAN ONCE, SINCE
C               SUCEEDING DATA OVERWRITE PRECEEDING
C               DATA.
C     NE1B      KEY USED TO SPECIFY EMISSIVITY OF      NRNGS        B,C
C               ELEMENTS ON SIDE OF SHIELD CLOSEST
C               TO HEATER FACING THE HEATER.
C     NE1T      THE EQUIVALENT OF NE1B EXCEPT FOR      NRNGS        B,C
C               SIDE FACING AWAY FROM HEATER.
C     NE2B      THE EQUIVALENT OF NE1B OR NE1T         NRNGS        B,C
C     NE3B      EXCEPT THAT THESE VARIABLES REFER
C     NE4B      TO THE SECOND THROUGH THE FIFTH
C     NE5B      SHIELD RESPECTIVELY.
C     NE2T
C     NE3T
C     NE4T
C     NE5T
C     NRADS     1 WHEN EQUAL AREA ANNULI ARE CHOSEN    1
C               FOR EACH SURFACE. 0 WHEN EQUAL
C               RADII ANNULI ARE CHOSEN FOR EACH
C               SURFACE. UNLESS A VALUE IS
C               SPECIFIED A VALUE OF 1 IS ASSIGNED.
C               THIS VARIABLE IS IGNORED FOR SURFACES
C               OPPOSITE NON PLANAR SOURCES.
C     NRNGS     THE NUMBER OF ANNULI ON EACH SURFACE.  1
C               NRNGS NORMALLY CANNOT EXCEED 20, BUT
C               IT CANNOT EXCEED 10 IF NON PLANAR
C               SURFACES ARE INVOLVED.
C     NSHLDS    THE NUMBER OF SHIELDS. THERE MAY BE    1
C               UP TO 5 SHIELDS IN THE SYSTEM.
C     NVUFH     1 WHEN THE HEATER SURFACE IS NON       1
C               PLANAR. OTHERWISE 0. A VALUE OF
C               0 IS ASSIGNED INITIALLY.
C     NVUFT     THE EQUIVALENT OF NVUFH EXCEPT         1
C               FOR THE TANK SURFACE.
C     PHI       SOLAR FLUX PER UNIT TIME AND AREA.     1
C     RH        THE RADIUS OF THE HEATER IN THE
C               LATERAL DIRECTION.
C     RS        THE RADIUS OF THE SHIELDS.             NSHLDS
C     RSH       THE RATIO OF THE RADIUS IN THE AXIAL   1
C               DIRECTION TO THE RADIUS IN THE
C               LATERAL DIRECTION FOR A NONPLANAR HEATER.
C               NEED NOT BE SPECIFIED IF THE HEATER
C               IS PLANAR ( NVUFH=0 ).
C     RST       THE EQUIVALENT OF RSH EXCEPT           1
C               FOR THE TANK.
C     RT        THE RADIUS OF THE TANK IN THE          1
C               LATERAL DIRECTION.
C     SIGMA     STEFAN-BOLTZMAN CONSTANT. THE UNITS    1
C               OF THIS CONSTANT DETERMINE THE
C               UNITS OF ALL OTHER DIMENSIONED
```

```
      INPUT      -  EFN   SOURCE STATEMENT  -  IFN(S)  -

C                VARIABLES. UNLESS SPECIFIED
C                SIGMA IS IN ENGLISH UNITS AND HAS
C                THE VALUE 1.713E-09 BTU/HR/FT**2/R**4
C     SOLABS     SOLAR ABSORPTIVITY                    1
C     SOLAR      0.0 WHEN NEITHER SOURCE REPRESENTS
C                SOLAR RADIATION. 1.0 IF ONE SOURCE
C                IS SOLAR RADIATION. INITALLY ASSIGNED
C                A VALUE OF 0.0
C     STHICK     THE THICKNESS OF EACH SHIELD          NSHLDS
C     TBABS1     THE CONSTANTS FOR THE POLYNOMIAL      1-4          D
C                GIVING ABSORPTIVITY AS A FUNCTION
C                OF TEMPERATURE. THIS SET OF ONE
C                TO FOUR CONSTANTS IS USED WHEN AN
C                ABSORPTIVITY KEY IS DESIGNATED AS 1
C     TBABS2     THE CONSTANTS FOR THE ABSORPTIVITY    1-4          D
C     THROUGH    POLYNOMIAL WHEN THE KEYS ARE          EACH
C     TBABSL     DESIGNATED AS 2 THROUGH 10
C     TBCON1     THE CONSTANTS FOR THE POLYNOMIAL      1-4          D
C     THROUGH    GIVING THE THERMAL CONDUCTIVITY AS A  EACH
C     TBCON5     FUNCTION OF TEMPERATURE. EACH SET
C                OF FROM 1 TO 4 CONSTANTS IS USED
C                DEPENDING ON THE VALUE OF NCOND
C                FOR THE SHIELD.
C     TBEMS1     THE EQUIVALENT OF TBABS1 THROUGH      1-4          D
C     THROUGH    TBABSL EXCEPT THAT THESE CURVES       EACH
C     TBEMSL     ARE FOR EMISSIVITIES.
C     TOL        THE MAXIMUM ALLOWABLE DIFFERENCE
C                BETWEEN EACH TRIAL AND CALCULATED
C                TEMPERATURE OF THE SHIELDS AT THE
C                TIME OF CONVERGENCE. ASSIGNED A
C                VALUE OF 0.01
C     TH         THE TEMPERATURE FOR EACH ANNULUS      NRNGS        B
C                OF THE HEATER.
C     TT         THE TEMPERATURE FOR EACH ANNULUS      NRNGS        B
C                OF THE TANK.
C     TS         THE TEMPERATURES FOR EACH OF THE      NSHLDS+1     A
C                SURROUNDINGS. UNLESS SPECIFIED
C                THESE VARIABLES ARE ASSIGNED A
C                VALUE OF 0.
C
C     VARIABLES READ IN THROUGH THE USE OF NAMELIST NAME INPUT2
C
C     NAME              DESIGNATION                QUANTITY     CODE
C
C     AHS        THE AREA OF EACH ANNULUS ON THE       NR1          E
C                HEATER OR THE SURFACE OPPOSITE THE TANK.
C     ATS        THE AREA OF EACH ANNULUS ON THE TANK  NR1          E
C                OR SURFACE OPPOSITE THE HEATER.
C     LIST       1 IF ALL THE DATA FOR NONPLANAR       1
C                SOURCES ARE TO BE LISTED. 0 IF THIS
C                DATA ARE NOT LISTED. INITIALLY
C                ASSIGNED A VALUE OF 0
C     MX1        DESIGNATION FOR TYPE OF SURFACES      1            E
C                INVOLVED. 1 IF A NONPLANAR HEATER
C                SEES A PLANAR TANK OR SHIELD.
C                2 IF A NONPLANAR TANK SEES A PLANAR
```

```
                INPUT      -  EFN   SOURCE STATEMENT  -  IFN(S)  -

C                    SHIELD OR HEATER. 3 IF A NONPLANAR
C                    TANK SEES A NONPLANAR HEATER.
C       NR1          THE NUMBER OF ANNULI ON EACH SURFACE.   1
C       F            VIEW FACTORS FROM ANNULI ON THE         NR1**2        E,F
C                    TANK TO ANNULI ON THE HEATER.
C       FN           THE SET OF DATA FOR A GIVEN CONFIG-     1             G
C                    URATION WHICH IS STORED ON TAPE 1
C                    CAN BE FOR SEVERAL DIFFERENT NUMBERS
C                    OF ANNULI. AT THE END OF EACH SET OF
C                    DATA FN IS SET EQUAL TO 1
C       FL           SET EQUAL TO 1 AT THE END OF THE        1
C                    LAST SET OF DATA. THERE IS A MAXIMUM
C                    OF 30 SETS OF DATA. IF IT IS DESIRED
C                    TO READ IN ADDITIONAL DATA FOR NONPLANAR
C                    SOURCES, FL IS SET EQUAL TO 1.0 JUST
C                    PRIOR TO EACH RETURN TO TBVUF.
C       RMHD         THE RATIO OF THE RADIUS IN THE AXIAL    1             E,H
C                    DIRECTION TO THE RADIUS IN THE LATERAL
C                    DIRECTION FOR THE NONPLANAR HEATER.
C       RMTD         THE EQUIVALENT OF RMHD EXCEPT FOR       1             E,H
C                    THE TANK.
C       XLOR         THE SPACING RATIO (L/R) BETWEEN THE     1
C                    NONPLANAR SURFACE AND THE SURFACE NEXT
C                    TO IT.
C
C              EXPLAINATION OF CODES
C
C       CODE
C       A      WHEN THERE IS SOLAR RADIATION PRESENT ONLY NSHLDS VALUES OF
C              THESE VARIABLES NEED BE READ IN. HOWEVER, SINCE THE
C              NUMBERING BEGINS WITH THE HEATER, THE VALUE STORED IN THE
C              SECOND LOCATION REPRESENTS THE PROPERTY BETWEEN THE FIRST
C              AND SECOND SHIELDS.
C       B      IF THE VALUES FOR THESE VARIABLES ARE THE SAME ACROSS A
C              SURFACE, THEN DENOTING THE SECOND VALUE AS ZERO CAUSES
C              THE PROGRAM TO ASSIGN THE FIRST VALUE TO ALL OF THE VALUES
C              FOR THE VARIABLE
C       C      KEYS RELATE THE PROPERTIES OF AN ELEMENT OR SHIELD TO THE
C              CONSTANTS GIVING THAT PROPERTY. THUS THE ENTRY NET(3)=4
C              INDICATES THAT THE EMISSIVITY OF THE THIRD ANNULUS OF THE
C              TANK IS DETERMINED BY THE VALUES IN TBEMS4. IF ALL OF THE
C              ANNULI ON A SURFACE HAVE THE SAME KEY FOR A VARIABLE,
C              ASSIGNING A VALUE OF 0 TO THE SECOND ANNULUS CAUSES THE
C              PROGRAM TO ASSIGN THE VALUE FOR THE FIRST ANNULUS TO ALL OF
C              ANNULI ON THE SURFACE.
C       D      THE POLYNOMIALS ARE IN ASCENDING ORDER SO THAT THE FIRST
C              COEFFICIENT IS A CONSTANT WHILE THE FOURTH COEFFICIENT IS
C              MULTIPLIED BY THE TEMPERATURE CUBED.
C       E       THE VIEW FACTOR DATA CONSISTS OF BETWEEN 1 AND 30 SETS OF
C               DATA. EACH SET IS FOR A DIFFERENT SPACING RATIO OR SHAPE
C               OF THE NONPLANAR HEATER OF TANK. WITHIN A SET OF DATA
C               INFORMATION CAN BE PROVIDED FOR DIFFERING NUMBERS OF ANNULI
C               FOR EACH SET OF DATA THERE IS A SUBSET FOR EACH NUMBER OF
C               ANNULI. EACH SUBSET CONTAINS THE AREAS OF EACH ANNULUS ON
C               THE NONPLANAR SURFACE AND THE SURFACE ADJACENT TO IT, AS
C               WELL AS THE VIEW FACTORS BETWEEN ANNULI.
```

```
      INPUT      -  EFN   SOURCE STATEMENT  -  IFN(S)  -

C     F       THE VIEW FACTORS ARE READ IN THROUGH A ONE DIMENSIONAL
C             VECTOR(F). THE VIEW FACTORS ARE STORED SERIALLY. THE VIEW
C             FACTORS ARE FROM THE TANK SIDE TO THE HEATER SIDE. THUS
C             FOR MX1=3 THE VALUES OF F ARE VIEW FACTORS FROM ANNULI ON
C             THE TANK TO ANNULI ON THE HEATER. THE FIRST VIEW FACTOR IS
C             FROM THE INNERMOST ANNULUS ON THE TANK TO THE INNERMOST
C             ANNULUS ON THE HEATER. THE SECOND VIEW FACTOR IS FROM THE
C             INNERMOST ANNULUS ON THE TANK TO THE SECOND ANNLUUS ON THE
C             HEATER.
C     G       ALL OF THE DATA FOR A CONFIGURATION SHOULD BE READ IN AS
C             A BLOCK OF DATA. EACH BLOCK CAN CONTAIN DATA FOR SEVERAL
C             DIFFERENT NUMBER OF ANNULI. THUS THE VIEW FACTORS ARE
C             STORED IN A TRIPLY SUBSCRIPTED ARRAY WITH THE THIRD INDEX
C             GIVING THE NUMBER OF ANNULI ON EACH SURFACE.
C     H       THESE VARIABLES ARE READ IN SO AS TO DISTINGUISH DIFFERENT
C             TYPES OF SURFACES. FOR A HEMISPHERE THEY WOULD HAVE A VALUE
C             OF 1.0, AND FOR AN OBLATE SPHEROID THEY WOULD BE LESS THAN
C             1.0
C
C
      GO TO (1,2),JR
C
C     READ IN ALL DATA OTHER THAN THAT FOR THE VIEW FACTORS BETWEEN
C     NONPLANAR SURFACES.
C
    1 READ(5,INPUT1)
      WRITE(6,10)
   10 FORMAT(42X,18HLISTING OF INPUT    )
      WRITE(6,OUTPU1)
      DO 11 I=1,10
      SUM1=0.0
      SUM2=0.0
      DO 12 J=1,4
      SUM1= SUM1 + CVABS(J,I)
      SUM2=SUM2 + CVEMS(J,I)
   12 CONTINUE
      IF ( SUM1 .EQ. 0.0 ) GO TO 14
      WRITE(6,13) ID(I) , (CVABS(J,I),J=1,4)
   13 FORMAT(3X,5HTBABS,A1,4E12.4)
   14 IF ( SUM2 .EQ. 0.0 ) GO TO 11
      WRITE(6,15) ID(I) , (CVEMS(J,I),J=1,4)
   15 FORMAT(1H+,66X,5HTBEMS,A1,4E12.4)
   11 CONTINUE
      IF( ICONDR .NE. 0 .OR. NSHLDS .EQ. 0 ) GO TO 16
      DO 17 I=1,5
      SUM1=0.0
      DO 18 J=1,4
      SUM1=SUM1 + CVCOND(J,I)
   18 CONTINUE
      IF ( SUM1 .EQ. 0.0 ) GO TO 17
      WRITE(6,19) ID(I) , ( CVCOND(J,I),J=1,4)
   19 FORMAT(3X,5HTBCON,A1,4E12.4)
   17 CONTINUE
      WRITE(6,3) ( STHICK(I),I=1,NSHLDS)
    3 FORMAT(18H SHIELD THICKNESS= ,5E12.4)
      WRITE(6,6) ( NCOND(I),I=1,NSHLDS)
```

```
     6 FORMAT( 19H CONDUCTIVITY KEYS=,5I5)
    16 WRITE(6,4) ( RS(I),I=1,NSHLDS)
     4 FORMAT(16H SHIELD RADIUS =,5E12.4)
       NX=NSHLDS+1
       NS=1
       IF ( SOLAR .NE. 0.0 ) NS=2
       IF ( NS .GT. NX ) GO TO 21
       WRITE(6,22) ( I , D(I) , ARES(I) , ABSR(I) , ES(I) , TS(I) ,
      1              I=NS,NX)
    22 FORMAT(//36X,44HPROPERTIES OF SURROUNDINGS BETWEEN SURFACES  /76H
      1 SPACING  DISTANCE       AREA    ABSORPTIVITY    EMISSIVITY   TEMP
      2ERATURE    /(I6,3F13.3,F15.3,F13.3))
    21 DO 23 K=1,6
       NF(K)=NRNGS
       IF ( K .LE. 3 .AND. SOLAR .NE. 0.0 ) GO TO 23
       GO TO ( 31,32,33,34,35,36),K
    31 IF ( NEH(2) .EQ. 0 ) NF(1)=1
       GO TO 23
    32 IF ( NAH(2) .EQ. 0 ) NF(2)=1
       GO TO 23
    33 IF ( TH(2) .EQ. 0.0 ) NF(3)=1
       GO TO 23
    34 IF ( NET(2) .EQ. 0 ) NF(4)=1
       GO TO 23
    35 IF ( NAT(2) .EQ. 0 ) NF(5)=1
       GO TO 23
    36 IF ( TT(2) .EQ. 0.0 ) NF(6)=1
    23 CONTINUE
       IF ( SOLAR .NE. 0.0 ) GO TO 27
       N1=NF(1)
       WRITE(6,24) DNE(1) , ( NEH(I),I=1,N1)
       N1=NF(2)
    24 FORMAT(12X,A6,20I3)
       WRITE(6,24) DNA(1) , ( NAH(I),I=1,N1)
       N1=NF(3)
       WRITE(6,25) DTEM(1) , ( TH(I),I=1,N1)
    25 FORMAT ( 12X,A6,10F11.3/18X,10F11.3)
    27 NX=NSHLDS*2
       IF ( NX .EQ. 0 ) GO TO 28
       DO 26 N=1,NX
       N1=NRNGS
       IF ( NE(2,N) .EQ. 0 ) N1=1
       WRITE(6,24) DNE(N+1) , (NE(I,N),I=1,N1)
       N1=NRNGS
       IF ( NA(2,N) .EQ. 0 ) N1=1
       WRITE(6,24) DNA(N+1) , ( NA(I,N) , I=1,N1)
    26 CONTINUE
    28 N1=NF(4)
       WRITE(6,24) DNE(12) , ( NET(I),I=1,N1)
       N1=NF(5)
       WRITE(6,24) DNA(12) , ( NAT(I),I=1,N1)
       N1=NF(6)
       WRITE(6,25) DTEM(2) , ( TT(I),I=1,N1)
       RETURN
C
C      READ IN VIEW FACTORS AND AREAS FOR NONPLANAR SURFACES
```

```
          INPUT      -   EFN    SOURCE STATEMENT  -   IFN(S)  -

C
     2 READ(5,INPUT2)
       IF ( LIST .EQ. 0 ) RETURN
       WRITE(6,5)
     5 FORMAT(1H1,42X,30HLISTING OF VIEW FACTOR DATA          )
       WRITE(6,OUTPU2)
       WRITE(6,50) DAHS , ( AHS(J),J=1,NR1)
    50 FORMAT(6X,A6,10F11.4)
       WRITE(6,50) DATS , ( ATS(J),J=1,NR1)
       WRITE(6,53)
    53 FORMAT(12X,30H VIEW FACTORS BETWEEN ANNULI     )
       NR2=NR1**2
       WRITE(6,51) ( F(N),N=1,NR2)
    51 FORMAT(10E12.4)
       RETURN
       END
```

```
$IBFTC SHIELD  DECK

      DIMENSION ES(10) , ABSR(10) , REFS(10) , TS(10) , ARES(10)
      EQUIVALENCE
     1     (CVCOND,CVK) , (CVEMS , CVX) , (CVABS , CVY)
      DIMENSION RS(9) , STHICK(7) , NCOND(7) , D(8) ,
     1            TH(20) , TT(20) , CVCOND(4,10) , CVABS(4,10) ,
     2            CVEMS(4,10) , NEH(20) , NET(20) , NAH(20) , NAT(20) ,
     3            CVX(40) , CVY(40) , CVK(20) , NE(20,10) , NA(20,10)
      DIMENSION NE1(200) , NA1(200)
      EQUIVALENCE ( NE1 , NE ) , ( NA1 , NA )
      COMMON / BULL/ EMS(20,9,2) , AB(20,9,2) , REF(20,9,2)
      COMMON/NEW/ FSSHTT(6) , FSSTTH(6) , FSNHTT(20,6) , FSNTTH(20,6) ,
     1            FNNHTT(20,20,6) , FNNTTH(20,20,6) , AREA(20,7) ,
     2            FNSHTT(20,6) , FNSTTH(20,6) , R(20,7) , AREAT(7) ,
     3          FNHTSR(20,6) , FNTTSR(20,6) , FSRTNH(20,6) ,
     4            FSRTNT(20,6) , FSRSR(6)
      COMMON / EAS / AT , AH , QOA , T(20,10) , F13 , F14 , F23 , F24
      COMMON /CONDT/ COND(20,10) , RES(20,10)
      COMMON / KSLV / TO(20,10) , LOOK , LCOND , ICOND , NCALC , TMAX
      COMMON /T3/ QOA2 , QSUR , QOAS
      DIMENSION RORS(20)
      COMMON C(1000)
      EQUIVALENCE
     1(C(1)  ,ABSR  ) , (C(11) ,ARES  ) , (C(21) ,D     ) ,
     2(C(31) ,ES    ) , (C(41) ,IVCOND) , (C(42) ,ICONDR) ,
     3(C(43) ,ITMAX ) , (C(51) ,NAH   ) , (C(71) ,NAT   ) ,
     4(C(91) ,NA    ) , (C(291),NEH   ) , (C(311),NET   ) ,
     5(C(331),NE    ) , (C(531),NCOND ) , (C(541),NCASE ) ,
     6(C(542),NELIPS) , (C(543),NRADS ) , (C(544),NRNGS ) ,
     7(C(545),NSHLDS) , (C(546),NCALCR) , (C(547),NVUFH ) ,
     8(C(548),NVUFT ) , (C(549),PHI   ) , (C(550),PI    ) ,
     9(C(551),RS    ) , (C(561),RSH   ) , (C(562),RST   ) ,
     A(C(563),RH    ) , (C(564),RT    ) , (C(565),SOLAR ) ,
     B(C(566),SIGMA ) , (C(567),TOL   ) , (C(568),WI    ) ,
     C(C(571),SOLABS) , (C(591),STHICK) , (C(601),CVABS ) ,
     D(C(641),CVCOND) , (C(681),CVEMS ) , (C(721),TH    ) ,
     E(C(741),TS    ) , (C(751),TT    ) , (C(771),REFS  )
      COMMON / ELIP2 / FN , FL , RMHD , RHTD , XLOR , MXS , ATS(10) ,
     1                 AHS(10) , F(10,10), LIST
      LOGICAL PASS
C
C
C     INITIALIZE DATA AND GIVE INPUT VARIABLES THEIR ASSIGNED VALUES
C
      DO 510 I=1,200
      NE1(I)=0
      NA1(I)=0
      IF ( I .GT. 40 ) GO TO 510
      CVX(I) = 0.0
      CVY(I) = 0.0
      IF ( I .GT. 20 ) GO TO 510
```

```
      CVK(I) = 0.0
      NET(I)=0
      NEH(I)=0
      NAT(I)=0
      NAH(I)=0
      TH(I)=0.0
      TT(I)=0.0
      IF( I .GT. 10 ) GO TO 510
      D(I) =0.0
      TS(I)=0.0
      ARES(I)=1.0
      ES(I)=1.0
      ABSR(I)=1.0
  510 CONTINUE
      TOL = 0.01
      NI =0
      NRADS = 1
      NVUFT =0
      NVUFH =0
      SOLAR =0.0
      IVCOND=1
      ICCNCR=1
      NCASE=1
      WI=0.4
      NELIPS=0
      LIST=0
      ITMAX=200
      NCALCR=1
      PI = 3.14159
      SIGMA= 0.1713E-08
 1000 WRITE (6,100)
  100 FORMAT (1H1)
C
C     READ INPUT DATA
C
  106 CALL INPUT (1)
      IF ( NELIPS .EQ. 0 .AND. ( NVUFT .NE. 0 .OR. NVUFH .NE. 0 ) )
     1           CALL TBVUF(0)
      WRITE(6,107)
  107 FORMAT(42X,18HLISTING OF OUTPUT         )
      NELIPS=1
      TOLX = TOL
      IF( ICONDR .NE. 0 ) ICOND=ICONDR
      IF ( IVCOND .EQ. 0 ) IVCOND=1
      IF ( ICONDR .EQ. 0 ) ICOND=IVCOND
      NCALC=NCALCR
      ICASE=0
      SDT=1.0E10
      ITCOND=1
      W=1.0
      LW=0
      LOCK=1
      WX=WI
      TEMPH=TH(1)
      TEMPT=TT(1)
      IF (NI.EQ.0) WRITE (6,100)
```

```
  506 NI = 1
      DO 501 L=1,2
C
C     STORE DATA FOR EMISSIVITY KEYS AND TEMPERATURES
C
      DO 501 M=1,5
      JJ=2*M +L-2
      DO 501 K=1,8
      IF ( JJ .EQ. 1 ) GO TO 520
      IF ( K-7 ) 502 , 517 , 518
  520 GO TO ( 511 , 512 , 513 , 514 , 515 , 516 , 517 , 518 ) , K
  511 NS=TH(2)
      GO TO 519
  512 NS=TT(2)
      GO TO 519
  513 NS=NET(2)
      GO TO 519
  514 NS=NEH(2)
      GO TO 519
  515 NS=NAT(2)
      GO TO 519
  516 NS=NAH(2)
      GO TO 519
  517 NS=NE(2,JJ)
      GO TO 519
  518 NS=NA(2,JJ)
  519 DO 521 N=2,20
      IF ( NS .NE. 0 ) GO TO 502
      GO TO ( 531 , 532 , 533 , 534 , 535 , 536 , 537 , 538 ) , K
  531 TH(N)=TH(1)
      GO TO 521
  532 TT(N)=TT(1)
      GO TO 521
  533 NET(N)=NET(1)
      GO TO 521
  534 NEH(N)=NEH(1)
      GO TO 521
  535 NAT(N)=NAT(1)
      GO TO 521
  536 NAH(N)=NAH(1)
      GO TO 521
  537 NE(N,JJ)=NE(1,JJ)
      GO TO 521
  538 NA(N,JJ)=NA(1,JJ)
  521 CONTINUE
  502 CONTINUE
  501 CONTINUE
      DO 540 N=1,NRNGS
      T(N,1)=TH(N)
      T(N,NSHLDS+2)=TT(N)
  540 CONTINUE
C
C     DETERMINE SURFACE PROPERTIES OF HEATER AND TANK
C
      DO 503 N=1,NRNGS
      J=NEH(N)
```

```
      EMS(N,1,2) = CVEMS(1,J) + ( CVEMS(2,J) + TH(N)* ( CVEMS(3,J) +
     1             CVEMS(4,J)*TH(N) ))*TH(N)
      J=NAH(N)
      AB(N,1,2)= CVABS(1,J) + ( CVABS(2,J) + TH(N)*( CVABS(3,J) +
     1             CVABS(4,J)*TH(N) ) )*TH(N)
      REF(N,1,2) = 1.0 -AB(N,1,2)
      J=NET(N)
      EMS(N,NSHLDS+2,1) = CVEMS(1,J) + ( CVEMS(2,J) + TT(N)*( CVEMS(3,J)
     1           + CVEMS(4,J)*TT(N) ) )*TT(N)
      J=NAT(N)
      AB(N,NSHLDS+2,1)= CVABS(1,J) + ( CVABS(2,J) + TT(N)*( CVABS(3,J)+
     1             CVABS(4,J)*TT(N) ) )*TT(N)
      REF(N,NSHLDS+2,1)=1.0-AB(N,NSHLDS+2,1)
  503 CONTINUE
      DO 541 M=1,10
      REFS(M)=1.0-ABSR(M)
  541 CONTINUE
C
C     CALCULATE VIEW FACTORS BETWEEN PAIRS OF SURFACES
C
      CALL VUFAC1
      IF ( NSHLDS .EQ. 0 ) GO TO 10
      IF ( ICONDR .NE. 0 ) GO TO 400
C
C     CALCULATE THERMAL RESISTANCE BETWEEN ANNULI
C
      NF = NRNGS - 1
      DO 600 M = 1,NSHLDS
      RESK=SIGMA/STHICK(M)/2.0/PI
      DO 601 N = 1,NF
      IF(N.EQ.1) RES(N,M)=RESK*ALOG((R(2,M+1)+R(1,M+1))/R(1,M+1))
      IF(N.GT.1) RES(N,M)=RESK*ALOG((R(N+1,M+1)+R(N,M+1))/
     1                              (R(N,M+1)+R(N-1,M+1)))
  601 CONTINUE
  600 CONTINUE
C
C     MAKE INITIAL ESTIMATES OF TEMPERATURE DISTRIBUTIONS
C
  400 IF ( ICASE .GT. C ) GO TO 20
      IF ( SOLAR .EQ. 0.0) TEMPX = TEMPH
      IF ( SOLAR .NE. 0.0) TEMPX = 500.0
      T(1,2) =  TEMPX -(TEMPX-TEMPT)/FLOAT(NSHLDS+1)
      IF ( NSHLDS .EQ. 1 ) GO TO 20
      NSF=NSHLDS+1
      DO 15 M=3,NSF
      T(1,M) = T(1,M-1) - (TEMPX -T(1,2))
   15 CONTINUE
C
C     CALCULATE SURFACE PROPERTIES AND THERMAL CONDUCTIVITIES FOR
C     SHIELDS
C
   20 DO 21 M = 1,NSHLDS
      JK = NCOND(M)
      K=M+1
      DO 21 L = 1,2
      JJ = 2*M + L - 2
```

```
      DO 21 N=1,20
      IF ( LOOK .NE. 1 .AND. ICASE .NE. 0 ) GO TO 17
      T(N,K)=T(1,K)
      TO(N,K)=T(N,K)
   17 IF ( N .GT. NRNGS ) GO TO 21
      J=NE(N,JJ)
      EMS(N,K,L)=CVEMS(1,J)+CVEMS(2,J)*T(N,K)+CVEMS(3,J)*T(N,K)**2
     1           +CVEMS(4,J)*T(N,K)**3
      J = NA(N,JJ)
      AB(N,K,L) =CVABS(1,J)+CVABS(2,J)*T(N,K)+CVABS(3,J)*T(N,K)**2
     1           +CVABS(4,J)*T(N,K)**3
      REF(N,K,L) = 1.0 - AB(N,K,L)
      IF(N.EQ.NRNGS.OR.ICOND.NE.0) GO TO 21
      TMS= ( T(N,K) + T(N+1,K) )/2.0
      COND(N,M) = CVCOND(1,JK)+CVCOND(2,JK)*TMS+CVCOND(3,JK)*TMS**2+
     1            CVCOND(4,JK)*TMS**3
   21 CONTINUE
      TMAX=0.0
C
C     CALCULATE SHIELD TEMPERATURES
C
  201 CALL SHCLC
      IF ( TMAX .NE. 0.0 ) GO TO 7
  202 DO 210 M = 1,NSHLDS
      K=M+1
      DO 210 N = 1,NRNGS
      IF ( ICOND .EQ. 2 ) T(N,K) = T(1,K)
  210 CONTINUE
C
C     TEST TO SEE IF TEMPERATURES HAVE CONVERGED
C
      SDTX=0.0
      PASS=.TRUE.
      DO 6 M = 1,NSHLDS
      K=M+1
      NF = NRNGS
      IF( ICOND .EQ. 2 ) NF = 1
      DO 6 N = 1,NF
      TEST = ABS(TO(N,K) - T(N,K) )
      IF ( TEST .GT. TOLX ) PASS=.FALSE.
      SDTX=SDTX+TEST
    6 CONTINUE
      IF ( PASS .AND. .TRUE. ) GO TO 9
      ICASE=1
      LOOK=LOOK+1
      IF ( LOOK .GT. ITMAX ) GO TO 14
      IF ( ICOND .NE. 0 ) GO TO 8
      IF ( SDTX .GT. SDT ) GO TO 13
      SDT=SDTX
      GO TO 8
   13 SDT=1.0E10
      LW=LW+1
      IF ( LW .EQ. 8 ) GO TO 7
      ICOND=ICONDL
      W=1.0
      ICASE=0
```

```
      GO TO 400
    8 DO 1 M=1,NSHLDS
      K=M+1
      DO 2 N=1,NRNGS
      IF ( ICOND .EQ. 2 .AND. N .GT. 1 ) GO TO 2
      T(N,K)=TO(N,K) -W*(TO(N,K)-T(N,K) )
      TO(N,K)=T(N,K)
    2 CONTINUE
    1 CONTINUE
      GO TO 20
    7 GO TO ( 22,23,24,25),ITCOND
   22 ICOND=IVCOND
      GO TO 11
   23 ICOND=3-IVCOND
      GO TO 11
   24 ICOND=3-IVCOND
      GO TO 11
   25 WRITE(6,101) NCALC ,ICOND
  101 FORMAT(28H  CASE ABANDONED WITH NCALC=,I3,6X,6HICOND=,I3)
   19 M=NSHLDS+1
      WRITE(6,109) (( TO(N,K),N=1,NRNGS),K=2,M)
  109 FORMAT(30H  PREVIOUS TEMPERATURE VALUES    /(10F12.3)  )
      NCASE=2
      ICASE=0
      GO TO 10
   11 ITCOND=ITCOND+1
      ICASE=0
      W=1.0
      NCALC=1-NCALC
      LW=0
      WRITE(6,12) NCALC , ICOND
   12 FORMAT(44H  CASE DIVERGING, CHANGING NCALC AND ICOND  ,12X,
     1        6HNCALC=,I1,12X,6HICOND=,I1)
      GO TO 400
   14 WRITE(6,18)
   18 FORMAT(36H  EXCESSIVE NUMBER OF ITERATIONS      )
      GO TO 19
    9 IF ( ICOND .EQ. ICONDR ) GO TO 10
      IF ( LW .EQ. 0 ) GO TO 26
      W=WX/2.0
      ICASE=1
      ICOND=ICONDR
      GO TO 20
   26 ICONDL=ICOND
      ICOND=ICONDR
      W=WI
      ICASE=1
      GO TO 20
C
C     DETERMINE HEAT TRANSFER RATE FOR TANK
C
   10 CALL QDOT
C
C     WRITE OUTPUT
C
      IF ( NSHLDS .NE. 0 ) GO TO 105
```

```
      WRITE(6,108) SOLAR , QOA , QOA2 , QOAS
C
C                              LISTING OF OUTPUT VARIABLES
C
C     SOLAR    SAME VARIABLE AS IN INPUT LIST
C     QOA      HEAT TRANSFER RATE PER UNIT AREA TO SOURCE DESIGNATED AS
C              THE TANK.
C     QOA2     HEAT TRANSFER RATE PER UNIT AREA TO SURFACE OPPOSITE TO
C              THE TANK.
C     QOAS     HEAT TRANSFER RATE PER UNIT AREA TO THE SURROUNDINGS
C              BETWEEN THE TANK AND THE OPPOSITE SURFACE.
C     LOOK     THE NUMBER OF ITERATIONS
C     TOLX     THE MAXIMUM DIFFERENCE BETWEEN EACH ESTIMATED AND
C              CALCULATED TEMPERATURE FOR THE SHIELDS.
C     M        THE SHIELD NUMBER.
C     T        THE TEMPERATURE OF EACH ANNULUS OF EACH SHIELD.
C     R(N)     THE RADIAL DISTANCE TO THE OUTER EDGE OF THE NTH ANNULUS.
C     RORS     R(N) DIVIDED BY THE RADIUS OF THE SHIELD ( RS ).
C
  108 FORMAT(1H  /12H      SOLAR =,F3.1,6X,6H QOA =,E12.4,6X,6HQOA2 =,
     1E12.4,6X,6HQOAS =,E12.4)
  110 FORMAT(1HL)
      GO TO 106
  105 WRITE(6,102) LOOK , SOLAR , QOA , TOLX
  102 FORMAT(///17H NO. ITERATIONS =,I4,6X,8H SOLAR =,F3.0,10X,
     1           7H QOAT =,E12.4,10X,6H TOLX=,F7.5)
      WRITE(6,110)
      DO 16 M=1,NSHLDS
      K=M+1
      DO 204 N =1,NRNGS
      RORS(N) = R(N,M+1)/R(NRNGS,M+1)
  204 CONTINUE
      WRITE(6,103) M , T(1,K) , R(1,K) , RORS(1)
  103 FORMAT(//48H      M          TEMP          R(N)      R(N)/RS          /
     1 I6,3F12.3)
      IF ( NRNGS .EQ. 1 ) GO TO 16
      WRITE(6,104) ( T(N,K) , R(N,K) , RORS(N) , N=2,NRNGS )
  104 FORMAT(F18.3,2F12.3)
   16 CONTINUE
      IF(NCASE .NE. 1 ) GO TO 1000
      NCASE = 2
      TOLX = TOLX/2.0
      ICASE = 1
      LOOK=2
      ITCOND=1
      WRITE (6,100)
      GO TO 20
      STOP

ERROR MESSAGE NUMBER     1
      END
```

```
$IBFTC TBVUF   DECK

      SUBROUTINE TBVUF ( JR)
C
C     THIS ROUTINE READS IN AND STORES DATA FOR VIEW FACTORS AND AREAS
C     OF NONPLANAR SURFACES.
C
C     A MAXIMUM OF 10 ANNULI CAN BE USED WHEN THERE ARE NONPLANAR
C     SURFACES, AND THE NUMBER OF ANNULI USED SHOULD CORRESPOND TO THE
C     NUMBER OF ANNULI FOR WHICH DATA HAS BEEN STORED.
C
      COMMON / ELIPT / M , XOR , MX1
      COMMON/NEW/ FSSHTT(6) , FSSTTH(6) , FSNHTT(20,6) , FSNTTH(20,6) ,
     1            FNNHTT(20,20,6) , FNNTTH(20,20,6) , AREA(20,7) ,
     2            FNSHTT(20,6) , FNSTTH(20,6) , R(20,7) , AREAT(7) ,
     3          FNHTSR(20,6) , FNTTSR(20,6) , FSRTNH(20,6) ,
     4            FSRTNT(20,6) , FSRSR(6)
      DIMENSION XT(30) , MX(30) , RMHS(30) , RMTS(30) , NRG(10,30)
      DIMENSION FT(1000) , FX(10,10,10)
      DIMENSION ASTORE(10,10,2) , ASY(200)
      EQUIVALENCE ( FT , FX )
      EQUIVALENCE ( ASY , ASTORE )
      LOGICAL PASS
      COMMON C(1000)
      EQUIVALENCE
     1(C(1)  ,ABSR  ) , (C(11) ,ARES  ) , (C(21) ,D     ) ,
     2(C(31) ,ES    ) , (C(41) ,IVCOND) , (C(42) ,ICONDR) ,
     3(C(43) ,ITMAX ) , (C(51) ,NAH   ) , (C(71) ,NAT   ) ,
     4(C(91) ,NA    ) , (C(291),NEH   ) , (C(311),NET   ) ,
     5(C(331),NE    ) , (C(531),NCOND ) , (C(541),NCASE ) ,
     6(C(542),NELIPS) , (C(543),NRADS ) , (C(544),NRNGS ) ,
     7(C(545),NSHLDS) , (C(546),NCALCR) , (C(547),NVUFH ) ,
     8(C(548),NVUFT ) , (C(549),PHI   ) , (C(550),PI    ) ,
     9(C(551),RS    ) , (C(561),RSH   ) , (C(562),RST   ) ,
     A(C(563),RH    ) , (C(564),RT    ) , (C(565),SOLAR ) ,
     B(C(566),SIGMA ) , (C(567),TOL   ) , (C(568),WI    ) ,
     C(C(571),SOLABS) , (C(591),STHICK) , (C(601),CVABS ) ,
     D(C(641),CVCOND) , (C(681),CVEMS ) , (C(721),TH    ) ,
     E(C(741),TS    ) , (C(751),TT    ) , (C(771),REFS  )
      COMMON / ELIP2 / FN , FL , RMHD , RMTD , XLOR , MXS , ATS(10) ,
     1                 AHS(10) , F(100) , LIST , NR1
      IF ( JR .NE. 0 ) GO TO 10
      REWIND 1
      I=1
   12 FN=0.0
      FL=0.0
C
C     READ VIEW FACTOR DATA.
C
      CALL INPUT (2)
C
C     CONVERT THE VIEW FACTORS WHICH ARE STORED SERIALLY INTO THE PROPER
```

```
C     ARRAY FORM. THE FIRST VIEW FACTOR IS THE ONE BETWEEN THE INNERMOST
C     ANNULUS ON THE SURFACE CLOSER TO THE TANK TO THE INNERMOST ANNULUS
C     ON THE SURFACES CLOSER TO THE HEATER. THE NEXT VIEW FACTOR IS FROM
C     THE INNERMOST ANNULUS ON THE TANK SIDE TO THE SECOND ANNULUS ON
C     THE HEATER SIDE. AFTER NRNGS VIEW FACTORS HAVE BEEN READ IN, THE
C     VIEW FACTOR FROM THE SECOND ANNULUS ON THE TANK SIDE TO THE
C     INNERMOST ANNULUS ON THE HEATER SIDE IS READ IN. THE PROCESS IS
C     REPEATED UNTIL ALL THE VIEW FACTORS BETWEEN A PAIR OF SURFACES ARE
C     DETERMINED.
C
      NT=NR1**2
      DO 21 N=1,NT
      J= 1 + ( N-1)/NR1
      K=N-(J-1)*NR1
      FX(K,J,NR1)=F(N)
   21 CONTINUE
      DO 23 N=1,NR1
      ASTORE(N,NR1,1)=AHS(N)
      ASTORE(N,NR1,2)=ATS(N)
   23 CONTINUE
      NRG(NR1,I)=NR1
      IF ( FN .NE. 0.0 ) GO TO 22
      GO TO 12
   22 XT(I)=XLOR
      MX(I)=MXS
      RMHS(I)=RMHD
      RMTS(I)=RMTD
C
C     STORE VIEW FACTORS AND AREAS ON TAPE.
C
      WRITE(1)   XLOR , MXS , ( FT(J),J=1,1000) , ( ASY(J),J=1,200)
      IF ( FL .NE. 0.0 ) RETURN
      I=I+1
      GO TO 12
C
C     CHECK TO SEE IF SPACING AND SURFACES ARE IN TABLES
C
   10 L=0
      DO 13 K=1,I
      PASS = .TRUE.
      IF ( ( MX1 .EQ. 1 .OR. MX1 .EQ. 3 ) .AND.
     1 ABS(RSH-RMHS(K) ) .GT. 0.05*RSH ) PASS=.FALSE.
      IF ( ( MX1 .EQ. 2 .OR. MX1 .EQ. 3 ) .AND.
     1 ABS(RST-RMTS(K) ) .GT. 0.05*RST ) PASS=.FALSE.
      IF ( ABS(XOR-XT(K)) .GT. 0.05*XOR ) PASS=.FALSE.
      IF ( NRNGS .NE. NRG(NRNGS,K) ) PASS=.FALSE.
      IF ( PASS .AND. .TRUE. ) L=K
   13 CONTINUE
      IF ( L .EQ. 0 .OR. NRNGS .GT. 10 ) GO TO 14
      REWIND 1
C
C     READ VIEW FACTORS FROM TAPE
C
      DO 15 K=1,L
      READ(1) XLOR , MXS , ( FT(J),J=1,1000) , ( ASY(J),J=1,200)
   15 CONTINUE
```

```
          TBVUF      -  EFN   SOURCE STATEMENT  -  IFN(S)  -

C
C     STORE VIEW FACTORS AND AREAS IN CORE
C
      AREAT(M)=0.0
      AREAT(M+1)=0.0
      DO 17 N=1,NRNGS
      DO 16 NN=1,NRNGS
      FNNTTH(NN,N,M)=FX(NN,N,NRNGS)
   16 CONTINUE
      AREA(N,M)=ASTORE(N,NRNGS,1)
      AREA(N,M+1)=ASTORE(N,NRNGS,2)
      AREAT(M)=AREAT(M) + AREA(N,M)
      AREAT(M+1)= AREAT(M+1) + AREA(N,M+1)
   17 CONTINUE
C
C     READJUST RADII OF PLANAR SURFACES TO AGREE WITH INPUT DATA
C
      IF( NSHLDS .EQ. 0 ) GO TO 18
      IF ( M .EQ. 1 ) R(N,2)=SQRT(AREA(N,2)/PI)
      IF ( M.EQ. NSHLDS+1 ) R(N,M)=SQRT(AREA(N,M)/PI)
   18 RETURN
   14 WRITE(6,20)
   20 FORMAT(42H    NO SPACING ENTRY IN TABLE                    )
      ASTOP=SQRT(-2.0)
      RETURN
      END
```

```
$IBFTC VUFAC1  DECK

      SUBROUTINE VUFAC1
C
C     THIS ROUTINE DETERMINES VIEW FACTORS BETWEEN ANNULI AND BETWEN
C     WHOLE SURFACES.
C
      DIMENSION ES(10) , ABSR(10) , REFS(10) , TS(10) , ARES(10)
      COMMON / ELIPT / M , XOR , MX1
      DIMENSION RS(10) , D(11)
      COMMON/NEW/ FSSHTT(6) , FSSTTH(6) , FSNHTT(20,6) , FSNTTH(20,6) ,
     1            FNNHTT(20,20,6) , FNNTTH(20,20,6) , AREA(20,7) ,
     2            FNSHTT(20,6) , FNSTTH(20,6) , R(20,7) , AREAT(7) ,
     3          FNHTSR(20,6) , FNTTSR(20,6) , FSRTNH(20,6) ,
     4            FSRTNT(20,6) , FSRSR(6)
      COMMON / EAS / AT , AH , QOA , T(20,10) , F13 , F14 , F23 , F24
      COMMON C(1000)
      EQUIVALENCE
     1(C(1)  ,ABSR  ) , (C(11) ,ARES  ) , (C(21) ,D     ) ,
     2(C(31) ,ES    ) , (C(41) ,IVCOND) , (C(42) ,ICONDR) ,
     3(C(43) ,ITMAX ) , (C(51) ,NAH   ) , (C(71) ,NAT   ) ,
     4(C(91) ,NA    ) , (C(291),NEH   ) , (C(311),NET   ) ,
     5(C(331),NE    ) , (C(531),NCOND ) , (C(541),NCASE ) ,
     6(C(542),NELIPS) , (C(543),NRADS ) , (C(544),NRNGS ) ,
     7(C(545),NSHLDS) , (C(546),NCALCR) , (C(547),NVUFH ) ,
     8(C(548),NVUFT ) , (C(549),PHI   ) , (C(550),PI    ) ,
     9(C(551),RS    ) , (C(561),RSH   ) , (C(562),RST   ) ,
     A(C(563),RH    ) , (C(564),RT    ) , (C(565),SOLAR ) ,
     B(C(566),SIGMA ) , (C(567),TOL   ) , (C(568),WI    ) ,
     C(C(571),SOLABS) , (C(591),STHICK) , (C(601),CVABS ) ,
     D(C(641),CVCOND) , (C(681),CVEMS ) , (C(721),TH    ) ,
     E(C(741),TS    ) , (C(751),TT    ) , (C(771),REFS  )
C
C     DETERMINE THE RADII OF EACH ANNULI OF EACH SURFACE
C
      FN=NRNGS
      IF ( NRADS .NE. 0 ) FN=SQRT(FN)
      NSP=NSHLDS+2
      DO 101 J=1,NSP
      SUMA=0.0
      DO 102 N=1,NRNGS
      FNI=N
      IF ( NRADS .NE. 0 ) FNI=SQRT(FNI)
      IF ( J .NE. 1 ) GO TO 120
      IF ( SOLAR .NE. 0.0 ) GO TO 101
      R(N,J)=RH*FNI/FN
      IF ( NVUFH .EQ. 0 ) GO TO 121
      GO TO 130
  120 IF ( J .EQ. NSP ) GO TO 122
      R(N,J)=RS(J-1)*FNI/FN
      IF ( J .NE.NSP-1 .OR. J .NE. 2 ) GO TO 121
      IF ( J .EQ. NSP-1 .AND. NVUFT .EQ. 0 ) GO TO 121
```

```
      IF ( J .EQ.2 .AND. NVUFH .EQ.0 ) GO TO 121
      GO TO 130
  121 IF ( N .EQ. 1 ) AREA(1,J)=PI*R(1,J)**2
      IF ( N .NE. 1 ) AREA(N,J)=PI*( R(N,J)**2 - R(N-1,J)**2 )
      GO TO 130
  122 R(N,J)=RT*FNI/FN
      IF ( NVUFT .EQ. C ) GO TO 121
  130 SUMA=SUMA + AREA(N,J)
  102 CONTINUE
C
C     CALCULATE THE AREA OF THE PLANAR SURFACES
C
      IF ( SOLAR .NE. 0.0 .OR. J .NE. 1 ) GO TO 131
      AH=SUMA
      AREAT(1)=AH
      GO TO 101
  131 AREAT(J)=SUMA
      IF ( J .EQ. NSP ) AT=AREAT(J)
  101 CONTINUE
      MF=NSHLDS+1
      DO 103 M=1,MF
      IF ( M .EQ. 1 .AND. SOLAR .NE. 0.0 ) GO TO 103
C
C     DETERMINE IF NON PLANAR SURFACES ARE INVOLVED.
C
      IF ( M .NE. 1 .AND . M .NE. MF ) GO TO 300
      IF ( NSHLDS .NE. 0 ) GO TO 301
      IF ( NVUFT .EQ. C .AND. NVUFH .EQ. 0 ) GO TO 300
      IF ( NVUFT .NE. C .AND. NVUFH .NE. 0 ) MX1=3
      IF ( NVUFH .NE. C .AND. NVUFT .EQ. 0 ) MX1=1
      IF ( NVUFT .NE. C .AND. NVUFH .EQ. 0 ) MX1=2
      GO TO 302
  301 IF ( M .NE. 1 ) GO TO 303
      IF ( NVUFH .EQ. C ) GO TO 300
      MX1=1
      GO TO 302
  303 IF ( NVUFT .EQ. C ) GO TO 300
      MX1=2
C
C     EXTRACT DATA FOR VIEW FACTORS FROM STORAGE.
C
  302 IF ( M .EQ. 1 ) MT=1
      IF ( M .EQ. MF) MT=MF
      XOR=C(MT)/R(NRNGS,MT+1)
      CALL TBVUF(1)
      DO 105 N=1,NRNGS
      SUMH1=0.0
      DO 132 NN=1,NRNGS
      FNNHTT(N,NN,M)=FNNTTH(NN,N,M)*AREA(NN,M+1)/AREA(N,M)
      SUMH1= SUMH1 + FNNHTT(N,NN,M)
  132 CONTINUE
      FNSHTT(N,M)=SUMH1
      FSNTTH(N,M)=FNSHTT(N,M)*AREA(N,M)/AREAT(M+1)
      FNHTSR(N,M)= 1.0-FNSHTT(N,M)
      FSRTNH(N,M)=FNHTSR(N,M)*AREA(N,M)/ARES(M)
  105 CONTINUE
```

```
C
C     CALCULATE THE VIEW FACTORS FROM AN ANNULUS TO A WHOLE SHIELD.
C
  112 DO 133 N=1,NRNGS
      SUMT1=0.0
      DO 134 NN=1,NRNGS
      SUMT1=SUMT1 + FNNTTH(N,NN,M)
  134 CONTINUE
      FNSTTH(N,M)=SUMT1
      FSNHTT(N,M)=FNSTTH(N,M)*AREA(N,M+1)/AREAT(M)
      FNTTSR(N,M) = 1.0 - FNSTTH(N,M)
      FSRTNT(N,M) = FNTTSR(N,M)*AREA(N,M+1)/ARES(M)
  133 CONTINUE
      GO TO 304
C
C     CALCULATE THE VIEW FACTORS BETWEEN PLANAR ANNULI.
C
  300 DO 106 N=1,NRNGS
      IF ( N .EQ. 1 ) GO TO 107
      CALL SUBVF ( 2 , R(NRNGS,M+1), 0.0, R(N-1,M), R(N,M), D(M) )
      FSNTTH(N,M)=F14
      FNSHTT(N,M)=FSNTTH(N,M)*AREAT(M+1)/AREA(N,M)
      GO TO 108
  107 CALL SUBVF ( 1 , R(NRNGS,M+1) , 0.0 , R(1,M) , 0.0 , D(M) )
      FSNTTH(1,M)=F13
      FNSHTT(1,M)=FSNTTH(1,M)*AREAT(M+1)/AREA(1,M)
  108 FNHTSR(N,M)=1.0 - FNSHTT(N,M)
      FSRTNH(N,M) = FNHTSR(N,M)*AREA(N,M)/ARES(M)
      DO 109 NN=1,NRNGS
        IF ( N .EQ. 1 ) GO TO 110
      IF ( NN .EQ. 1 ) GO TO 111
      CALL SUBVF ( 4,R(NN-1,M+1) , R(NN,M+1) , R(N-1,M) , R(N,M) , D(M))
      FNNTTH(NN,N,M)=F24
      FNNHTT(N,NN,M)=FNNTTH(NN,N,M)*AREA(NN,M+1)/AREA(N,M)
      GO TO 109
  111 CALL SUBVF ( 2 , R(1,M+1) , 0.0 , R(N-1,M) , R(N,M) , D(M) )
      FNNTTH(1,N,M)=F14
      FNNHTT(N,1,M)=FNNTTH(1,N,M)*AREA(1,M+1)/AREA(N,M)
      GO TO 109
  110 IF ( NN .EQ. 1 ) GO TO 113
      CALL SUBVF ( 3 , R(NN-1,M+1) , R(NN,M+1) , R(1,M) , 0.0 , D(M) )
      FNNTTH(NN,1,M) = F23
      FNNHTT(1,NN,M)=FNNTTH(NN,1,M)*AREA(NN,M+1)/AREA(1,M)
      GO TO 109
  113 CALL SUBVF ( 1 , R(1,M+1) , 0.0 , R(1,M) , 0.0 , D(M) )
      FNNTTH(1,1,M)=F13
      FNNHTT(1,1,M)=FNNTTH(1,1,M)*AREA(1,M+1)/AREA(1,M)
  109 CONTINUE
  106 CONTINUE
      GO TO 112
C
C     CALCULATE VIEW FACTORS BETWEEN WHOLE SURFACES.
C
  304 SUMSR1=0.0
      SUMSR2=0.0
      SUMT3=0.0
```

```
      SUMH3=0.0
      DO 114 N=1,NRNGS
      SUMSR1= SUMSR1 + FSRTNH(N,M)
      SUMSR2=SUMSR2 + FSRTNT(N,M)
      SUMT3=SUMT3 + FSNTTH(N,M)
      SUMH3=SUMH3 + FSNHTT(N,M)
  114 CONTINUE
      FSRSR(M) = 1.0-SUMSR1-SUMSR2
      FSSTTH(M)=SUMT3
      FSSHTT(M)=SUMH3
  103 CONTINUE
      RETURN
      END
```

```
$IBFTC SUBVF   DECK

      SUBROUTINE SUBVF(IJ,R1A,R2A,R3A,R4A,ALA)
      COMMON / EAS / AT , AH , QOA , T(20,10) , F13 , F14 , F23 , F24
      DOUBLE PRECISION R1,R2,R3,R4,AL,C1,C2,C3,C4,C5,C6,C7,C8,C9
      R1=R1A
      R2=R2A
      R3=R3A
      R4=R4A
      AL=ALA
      GO TO (1,2,3,4),IJ
C
C     CALCULATE THE VIEW FACTOR BETWEEN TWO DISKS
C
    1 C1 = (1.+(R3**2+AL**2)/R1**2)**2-4.*(R3**2)/R1**2
      F13 = .5*(1.+(R3**2+AL**2)/R1**2-SQRT(C1))
      RETURN
C
C     CALCULATE THE VIEW FACTOR BETWEEN A DISK AND AN ANNULUS
C
    2 C2 = (1.+(R4**2+AL**2)/R1**2)**2-4.*(R4**2)/R1**2
      C3 = (1.+(R3**2+AL**2)/R1**2)**2-4.*(R3**2)/R1**2
      F14 = .5*((R4**2-R3**2)/R1**2-SQRT(C2)+SQRT(C3))
      RETURN
C
C     CALCULATE THE VIEW FACTOR BETWEEN AN ANNULUS AND A DISK
C
    3 C4=(R2**2+R3**2+AL**2)**2-(2.*R2*R3)**2
      C5 = (R1**2+R3**2+AL**2)**2-(2.*R1*R3)**2
      F23 = (.5/(R2**2-R1**2))*(R2**2-SQRT(C4)+SQRT(C5)-R1**2)
      RETURN
C
C     CALCULATE THE VIEW FACTOR BETWEEN TWO ANNULI
C
    4 C6 = (R2**2+R3**2+AL**2)**2-(2.*R2*R3)**2
      C7 = (R2**2+R4**2+AL**2)**2-(2.*R2*R4)**2
      C8 = (R1**2+R4**2+AL**2)**2-(2.*R1*R4)**2
      C9 = (R1**2+R3**2+AL**2)**2-(2.*R1*R3)**2
      F24 = (.5/(R2**2-R1**2))*(SQRT(C6)-SQRT(C7)+SQRT(C8)-SQRT(C9))
      RETURN
      END
```

```
$IBFTC SHCLC   DECK

      SUBROUTINE SHCLC
C
C     THIS ROUTINE CALCULATES THE RADIAL TEMPERATURE DISTRIBUTION OF A
C     SHIELD ASSUMING THAT THE TEMPERATURES OF THE ADJACENT SURFACES ARE
C     KNOWN
C
      DIMENSION ES(10) , ABSR(10) , REFS(10) , TS(10) , ARES(10)
      COMMON / T2 / A(41,41) , Q(41)
      EQUIVALENCE ( A(1),B )
      DIMENSION B(41,41)
      DIMENSION D(20,20) , DI(20,20) , DUMMY(20)
      COMMON / CONDT/ COND(20,10) , RES(20,10)
      COMMON/NEW/ FSSHTT(6) , FSSTTH(6) , FSNHTT(20,6) , FSNTTH(20,6) ,
     1            FNNHTT(20,20,6) , FNNTTH(20,20,6) , AREA(20,7) ,
     2            FNSHTT(20,6) , FNSTTH(20,6) , R(20,7) , AREAT(7) ,
     3         FNHTSR(20,6) , FNTTSR(20,6) , FSRTNH(20,6) ,
     4            FSRTNT(20,6) , FSRSR(6)
      COMMON / BULL/ EMS(20,9,2) , AB(20,9,2) , REF(20,9,2)
      COMMON / EAS / AT , AH , QOA , T(20,10) , F13 , F14 , F23 , F24
      COMMON / KSLV / TO(20,10) , LOOK , LCOND , ICOND , NCALC , TMAX
      COMMON C(1000)
      EQUIVALENCE
     1(C(1)  ,ABSR  ) , (C(11) ,ARES  ) , (C(21) ,DIS   ) ,
     2(C(31) ,ES    ) , (C(41) ,IVCOND) , (C(42) ,ICONDR) ,
     3(C(43) ,ITMAX ) , (C(51) ,NAH   ) , (C(71) ,NAT   ) ,
     4(C(91) ,NA    ) , (C(291),NEH   ) , (C(311),NET   ) ,
     5(C(331),NE    ) , (C(531),NCOND ) , (C(541),NCASE ) ,
     6(C(542),NELIPS) , (C(543),NRADS ) , (C(544),NRNGS ) ,
     7(C(545),NSHLDS) , (C(546),NCALCR) , (C(547),NVUFH ) ,
     8(C(548),NVUFT ) , (C(549),PHI   ) , (C(550),PI    ) ,
     9(C(551),RS    ) , (C(561),RSH   ) , (C(562),RST   ) ,
     A(C(563),RH    ) , (C(564),RT    ) , (C(565),SOLAR ) ,
     B(C(566),SIGMA ) , (C(567),TOL   ) , (C(568),WI    ) ,
     C(C(571),SOLABS) , (C(591),STHICK) , (C(601),CVABS ) ,
     D(C(641),CVCOND) , (C(681),CVEMS ) , (C(721),TH    ) ,
     E(C(741),TS    ) , (C(751),TT    ) , (C(771),REFS  )
      DO 1 M=1,NSHLDS
      SUMQT=0.0
      SUMQX=0.0
      IF ( M .NE. 1 .OR. SOLAR .EQ. 0.0 ) GO TO 15
C
C     CALCULATE HEAT TRANSFER DUE TO SOLAR FLUX.
C
      DO 17 N=1,NRNGS
      IF ( N .EQ. 1 ) Q(1)=PHI*PI*R(1,2)**2*SOLABS/SIGMA
      IF ( N .NE. 1 ) Q(N)=PHI*PI*(R(N,2)**2-R(N-1,2)**2)*SOLABS/SIGMA
      IF ( ICOND .EQ. 2 ) GO TO 7
      DO 18 NN=1,NRNGS
      D(N,NN)=0.0
      IF ( N.EQ. NN ) D(N,NN) =-EMS(NN,2,1)
```

```
   18 CONTINUE
      GO TO 17
    7 SUMQX=SUMQX-EMS(NN,2,1)*AREA(NN,2)
   17 CONTINUE
      GO TO 16
C
C     CALCULATE HEAT TRANSFER FROM SURFACE CLOSER TO HEATER.
C
   15 CALL COEF(M,B)
      IF ( ICOND .EQ. 2 ) GO TO 11
      DO 30 N=1,NRNGS
      SUMQ=0.0
      L=N+NRNGS
      DO 21 NN=1,NRNGS
      SUMQ= SUMQ + B(NN,L)*T(NN,M)**4*EMS(NN,M,2)*AREA(NN,M)
      K=NN+NRNGS
      DK=0.0
      IF ( N .EQ. NN ) DK=1.0
      D(N,NN)=( B(K,L)-DK)*EMS(NN,M+1,1)
   21 CONTINUE
      Q(N)=SUMQ + B(2*NRNGS+1,L)*TS(M)**4*ES(M)*ARES(M)
   30 CONTINUE
      GO TO 16
   11 SUMQT=0.0
      SUMQX=0.0
      DO 12 N=1,NRNGS
      L=N+NRNGS
      SUMQ=0.0
      SUM1=0.0
      DO 13 NN=1,NRNGS
      K=NN+NRNGS
      SUM1 = SUM1 + B(K,L)*EMS(NN,M+1,1)*AREA(NN,M+1)
      SUMQ = SUMQ + B(NN,L)*EMS(NN,M,2)*AREA(NN,M)*T(NN,M)**4
   13 CONTINUE
      SUMQX=SUMQX+SUM1
      Q(N) = SUMQ + B(2*NRNGS+1,L)*TS(M)**4*ES(M)*ARES(M)
      SUMQT=SUMQT-Q(N)
   12 CONTINUE
C
C     CALCULATE HEAT TRANSFER FROM SURFACES CLOSER TO TANK.
C
   16 CALL COEF( M+1 , A )
      IF ( ICOND .EQ. 2 ) GO TO 2
      IF ( NCALC .EQ. 0 .OR. ICOND .NE. 0 ) GO TO 3
      DO 4 N=1,NRNGS
      SUMQ=0.0
      DO 5 NN=1,NRNGS
      K=NN+NRNGS
      SUMQ = SUMQ + A(K,N)*EMS(NN,M+2,1)*T(NN,M+2)**4*AREA(NN,M+2)
      DK=0.0
      IF ( N .EQ. NN ) DK=1.0
      D(N,NN) = ( ( A(NN,N) - DK )*EMS(NN,M+1,2) + D(N,NN) )*
     1          AREA(NN,M+1)*T(NN,M+1)**3
      IF ( N .NE. NN ) GO TO 6
      IF ( N.NE. 1 ) D(N,NN)=D(N,NN) - COND(N-1,M)/RES(N-1,M)
      IF ( N .NE. NRNGS ) D(N,NN) = D(N,NN) - COND(N,M)/RES(N,M)
```

```
      GO TO 5
    6 IF ( N.EQ. NN+1 ) D(N,NN) = D(N,NN) + COND(N-1,M)/RES(N-1,M)
      IF ( N .EQ. NN-1 ) D(N,NN)=D(N,NN) + COND(N,M)/RES(N,M)
    5 CONTINUE
      Q(N) = - Q(N) - SUMQ - A(2*NRNGS+1,N)*TS(M+1)**4*ES(M+1)*ARES(M+1)
    4 CONTINUE
      GO TO 9
    3 DO 8 N=1,NRNGS
      SUMQ=0.0
      DO 10 NN=1,NRNGS
      K=NN+NRNGS
      SUMQ = SUMQ + A(K,N)*T(NN,M+2)**4*EMS(NN,M+2,1)*AREA(NN,M+2)
      DK=0.0
      IF ( N .EQ. NN ) DK=1.0
      D(N,NN) = ( A(NN,N) - DK )*EMS(NN,M+1,2) + D(N,NN)
      IF ( ICOND .NE. 0 ) GO TO 10
      IF ( N .NE. NN ) GO TO 28
      IF ( N .NE. 1 ) D(N,NN)=D(N,NN)-COND(N-1,M)/T(N,M+1)**3/RES(N-1,M)
      IF( N .NE. NRNGS) D(N,NN)=D(N,NN)-COND(N,M)/T(N,M+1)**3/RES(N,M)
      GO TO 10
   28 IF(N .EQ. NN+1)D(N,NN)=D(N,NN)+COND(N-1,M)/T(NN,M+1)**3/RES(N-1,M)
      IF(N .EQ. NN-1) D(N,NN)=D(N,NN)+COND(N,M)/T(NN,M+1)**3/RES(N,M)
   10 CONTINUE
      Q(N) = -Q(N) - SUMQ - A(2*NRNGS+1,N)*TS(M+1)**4*ES(M+1)*ARES(M+1)
    8 CONTINUE
    9 IF ( NRNGS .NE. 1 ) GO TO 14
      DI(1,1)=1.0/D(1,1)
      GO TO 19
   14 CALL FACTOR( D , DUMMY , NRNGS , 20 )
      CALL INVERT( D , DUMMY , NRNGS , 20 , DI )
   19 DO 22 N=1,NRNGS
      SUM=0.0
      DO 23 NN=1,NRNGS
      SUM = SUM + DI(N,NN)*Q(NN)
   23 CONTINUE
      IF ( NCALC .EQ. 0 .OR. ICOND .NE. 0 ) GO TO 24
      IF ( ABS(SUM) .GT. 1.0E04 ) TMAX=1.0
      IF ( TMAX .NE. 0.0 ) RETURN
      IF ( SUM .LT. 0.0 ) SUM=0.8*T(N,M+1)
      T(N,M+1)=SUM
      GO TO 22
   24 IF ( SUM .GT. 1.0E15 .OR. SUM .LT. 0.0 ) TMAX=1.0
      IF ( TMAX .NE. 0.0 ) RETURN
      T(N,M+1) = ( SUM/AREA(N,M+1) )**0.25
   22 CONTINUE
      GO TO 1
C
C     CALCULATE SHIELD TEMPERATURE FOR INFINITELY CONDUCTING SHIELD.
C
    2 DO 25 N=1,NRNGS
      SUM2=0.0
      SUMQ=0.0
      DO 26 NN=1,NRNGS
      K=NN+NRNGS
      SUM2 = SUM2 + A(NN,N)*EMS(NN,M+1,2)*AREA(NN,M+1)
      SUMQ= SUMQ + A(K,N)*T(NN,M+2)**4*EMS(NN,M+2,1)*AREA(NN,M+2)
```

```
26 CONTINUE
   Q(N) = SUMQ + A(2*NRNGS+1,N)*TS(M+1)**4*ES(M+1)*ARES(M+1)
   SUMQX = SUMQX + SUM2 - ( EMS(N,M+1,1) + EMS(N,M+1,2) )*AREA(N,M+1)
   SUMQT = SUMQT -Q(N)
25 CONTINUE
   T(1,M+1) = (SUMQT/SUMQX)**0.25
   DO 27 N=1,NRNGS
   T(N,M+1)=T(1,M+1)
27 CONTINUE
 1 CONTINUE
   RETURN
   END
```

```
$IBFTC COEF    DECK

      SUBROUTINE COEF ( MM , B )
C
C     THIS SUBROUTINE DETERMINES THE VALUE OF THE COEFFICIENTS ( B )
C     USED TO FIND THE HEAT TRANSFER.
C
      DIMENSION ES(10) , ABSR(10) , REFS(10) , TS(10) , ARES(10)
      COMMON/NEW/ FSSHTT(6) , FSSTTH(6) , FSNHTT(20,6) , FSNTTH(20,6) ,
     1            FNNHTT(20,20,6) , FNNTTH(20,20,6) , AREA(20,7) ,
     2            FNSHTT(20,6) , FNSTTH(20,6) , R(20,7) , AREAT(7) ,
     3         FNHTSR(20,6) , FNTTSR(20,6) , FSRTNH(20,6) ,
     4            FSRTNT(20,6) , FSRSR(6)
      COMMON / BULL/ EMS(20,9,2) , AB(20,9,2) , REF(20,9,2)
      DIMENSION A(41,41) , Y(41,41) , AI(41,41) , DUMMY(41)
      DIMENSION B(41,41)
      COMMON C(1000)
      EQUIVALENCE
     1(C(1)   ,ABSR   ) , (C(11) ,ARES   ) , (C(21) ,D      ) ,
     2(C(31) ,ES     ) , (C(41) ,IVCOND) , (C(42) ,ICONDR) ,
     3(C(43) ,ITMAX  ) , (C(51) ,NAH    ) , (C(71) ,NAT    ) ,
     4(C(91) ,NA     ) , (C(291),NEH    ) , (C(311),NET    ) ,
     5(C(331),NE     ) , (C(531),NCOND  ) , (C(541),NCASE  ) ,
     6(C(542),NELIPS) , (C(543),NRADS  ) , (C(544),NRNGS  ) ,
     7(C(545),NSHLDS) , (C(546),NCALCR) , (C(547),NVUFH  ) ,
     8(C(548),NVUFT  ) , (C(549),PHI    ) , (C(550),PI     ) ,
     9(C(551),RS     ) , (C(561),RSH    ) , (C(562),RST    ) ,
     A(C(563),RH     ) , (C(564),RT     ) , (C(565),SOLAR  ) ,
     B(C(566),SIGMA  ) , (C(567),TOL    ) , (C(568),WI     ) ,
     C(C(571),SOLABS) , (C(591),STHICK) , (C(601),CVABS  ) ,
     D(C(641),CVCOND) , (C(681),CVEMS  ) , (C(721),TH     ) ,
     E(C(741),TS     ) , (C(751),TT     ) , (C(771),REFS   )
      M=MM
      NDIM=41
      NS=NRNGS+1
      NF=2*NRNGS
      DO 4 N=1,NRNGS
C
C     CALCULATE THE VALUES OF THE MATRICES A AND Y BETWEEN ONE SURFACE
C     AND ITSELF
C
      DO 1 NN=1,NRNGS
      Y(N,NN)=0.0
      IF ( N .EQ. NN ) GO TO 2
      A(N,NN)=0.0
      GO TO 1
    2 A(N,NN)=-1.0
    1 CONTINUE
C
C     CALCULATE THE VALUES OF THE MATRICES A AND Y BETWEEN ONE SURFACE
C     AND THE OTHER SURFACE
C
```

```
      DO 3 NN=NS,NF
      N1=NN-NRNGS
      A(N,NN)=REF(N1,M+1,1)*FNNHTT(N,N1,M)
      Y(N,NN)= -AB(N1,M+1,1)*FNNHTT(N,N1,M)
    3 CONTINUE
    4 CONTINUE
      DO 5 N=NS,NF
C
C     CALCULATE THE VALUES OF THE MATRICES A AND Y BETWEEN THE OTHER
C     SURFACE AND THE CRIGINAL SURFACE
C
      N1=N-NRNGS
      DO 6 NN=1,NRNGS
      A(N,NN)=REF(NN,M,2)*FNNTTH(N1,NN,M)
      Y(N,NN)= -AB(NN,M,2)*FNNTTH(N1,NN,M)
    6 CONTINUE
C
C     CALCULATE THE VALUES OF THE MATRICES A AND Y BETWEEN THE OTHER
C     SURFACE AND ITSELF
C
      DO 7 NN=NS,NF
      Y(N,NN)=0.0
      IF( N .EQ. NN ) GO TO 8
      A(N,NN)=0.0
      GO TO 7
    8 A(N,NN)=-1.0
    7 CONTINUE
    5 CONTINUE
C
C     CALCULATE THE VALUES OF THE MATRICES A AND Y BETWEEN THE SURFFACES
C     AND THE SURROUNDINGS.
C
      DO 9 N=1,NF
      IF ( N .GT. NRNGS) GO TO 10
      A(NF+1,N) = REF(N,M,2)*FSRTNH(N,M)
      Y(NF+1,N) =  -AB(N,M,2)*FSRTNH(N,M)
      GO TO 9
   10 N1=N-NRNGS
      A(NF+1,N)=REF(N1,M+1,1)*FSRTNT(N1,M)
      Y(NF+1,N)= -AB(N1,M+1,1)*FSRTNT(N1,M)
    9 CONTINUE
      DO 11 N=1,NF
      IF ( N .GT. NRNGS ) GO TO 12
      A(N,NF+1)=REFS(M)*FNHTSR(N,M)
      Y(N,NF+1) = - ABSR(M)*FNHTSR(N,M)
      GO TO 11
   12 N1=N-NRNGS
      A(N,NF+1)=REFS(M)*FNTTSR(N1,M)
      Y(N,NF+1)= - ABSR(M)*FNTTSR(N1,M)
   11 CONTINUE
      A(NF+1,NF+1)= REFS(M)*FSRSR(M) - 1.0
      Y(NF+1,NF+1) = -ABSR(M)*FSRSR(M)
      NFZ=NF+1
C
C     DETERMINE THE INVERSE OF THE MATRIX A
C
```

```
      CALL FACTOR ( A , DUMMY , NF+1 , NDIM )
      CALL INVERT ( A , DUMMY , NF+1 , NDIM , AI )
C
C     COMPUTE THE VALUES OF THE ABSORPTION COEFFICIENTS (B) (B=AI*Y)
C
      DO 13 I=1,NFZ
      DO 13 J=1,NFZ
      SUM=0.0
      DO 14 K=1,NFZ
      SUM= SUM + AI(I,K)*Y(K,J)
   14 CONTINUE
      B(I,J)=SUM
   13 CONTINUE
      RETURN
      END
```

```
$IBFTC QDOT     DECK

      SUBROUTINE QDOT
C
C     THIS SUBROUTINE DETERMINES THE HEAT TRANSFER TO M , M+1 , AND
C     SURROUNDING SURFACES
C
      DIMENSION ES(10) , ABSR(10) , REFS(10) , TS(10) , ARES(10)
      COMMON / EAS / AT , AH , QOA , T(20,10) , F13 , F14 , F23 , F24
      COMMON/NEW/ FSSHTT(6) , FSSTTH(6) , FSNHTT(20,6) , FSNTTH(20,6) ,
     1            FNNHTT(20,20,6) , FNNTTH(20,20,6) , AREA(20,7) ,
     2            FNSHTT(20,6) , FNSTTH(20,6) , R(20,7) , AREAT(7) ,
     3         FNHTSR(20,6) , FNTTSR(20,6) , FSRTNH(20,6) ,
     4            FSRTNT(20,6) , FSRSR(6)
      COMMON / BULL/ EMS(20,9,2) , AB(20,9,2) , REF(20,9,2)
      COMMON /T3/ QOA2 , QSUR , QOAS
      COMMON / T2 / B(41,41) , Q(41)
      COMMON C(1000)
      EQUIVALENCE
     1(C(1)  ,ABSR  ) , (C(11) ,ARES  ) , (C(21) ,D     ) ,
     2(C(31) ,ES    ) , (C(41) ,IVCOND) , (C(42) ,ICONDR) ,
     3(C(43) ,ITMAX ) , (C(51) ,NAH   ) , (C(71) ,NAT   ) ,
     4(C(91) ,NA    ) , (C(291),NEH   ) , (C(311),NET   ) ,
     5(C(331),NE    ) , (C(531),NCOND ) , (C(541),NCASE ) ,
     6(C(542),NELIPS) , (C(543),NRADS ) , (C(544),NRNGS ) ,
     7(C(545),NSHLDS) , (C(546),NCALCR) , (C(547),NVUFH ) ,
     7(C(545),NSHLDS) , (C(546),NSTEP ) , (C(547),NVUFH ) ,
     8(C(548),NVUFT ) , (C(549),PHI   ) , (C(550),PI    ) ,
     9(C(551),RS    ) , (C(561),RSH   ) , (C(562),RST   ) ,
     A(C(563),RH    ) , (C(564),RT    ) , (C(565),SOLAR ) ,
     B(C(566),SIGMA ) , (C(567),TOL   ) , (C(568),WI    ) ,
     C(C(571),SOLABS) , (C(591),STHICK) , (C(601),CVABS ) ,
     D(C(641),CVCOND) , (C(681),CVEMS ) , (C(721),TH    ) ,
     E(C(741),TS    ) , (C(751),TT    ) , (C(771),REFS  )
      M=NSHLDS+1
      IF ( M .NE. 1 .OR. SOLAR .EQ. 0.0 ) GO TO 9
C
C     CALCULATE THE HEAT TRANSFER DUE TO SOLAR FLUX.
C
      QSUM=0.0
      DO 8 N=1,NRNGS
      IF ( N .EQ. 1 ) Q(N)=PHI*PI*R(1,2)**2*SOLABS
      IF ( N .NE. 1 ) Q(N)=PHI*PI*(R(N,2)**2 - R(N-1,2)**2)*SOLABS
      Q(N)= Q(N)/SIGMA - EMS(N,2,1)*AREA(N,2)*T(N,2)**4
      QSUM=QSUM + Q(N)
    8 CONTINUE
      QOA=QSUM/AREAT(2)*SIGMA
      QOAS=0.0
      QSUR=0.0
      QOA2=0.0
      RETURN
    9 CALL COEF ( M , B )
```

```
      NS=NRNGS + 1
      NF=2*NRNGS
      NZ=NF+1
C
C     CALCULATE THE HEAT TRANSFER TO THE TANK. Q(J+NRNGS) IS THE HEAT
C     TRANSFERED TO THE J TH ELEMENT ON THE TANK
C
      QSUM=0.0
      DO 13 N=NS,NF
      SBE=0.0
      DO 14 NN=1,NF
      IF( NN .GT. NRNGS ) GO TO 15
      SBE= SBE + B(NN,N)*T(NN,M)**4*EMS(NN,M,2)*AREA(NN,M)
      GO TO 14
   15 N1=NN-NRNGS
      SBE = SBE + B(NN,N)*T(N1,M+1)**4*EMS(N1,M+1,1)*AREA(N1,M+1)
   14 CONTINUE
      SBE = SBE + B(NF+1,N)*TS(M)**4*ES(M)*ARES(M)
      N1=N-NRNGS
      Q(N) = SBE - T(N1,M+1)**4*EMS(N1,M+1,1)*AREA(N1,M+1)
      QSUM=QSUM+Q(N)
   13 CONTINUE
      QOA=QSUM/AREAT(M+1)*SIGMA
C
C     CALCULATE THE HEAT TRANSFER TO THE SURFACE ADJACENT TO THE TANK.
C
      QSUM=0.0
      NF=2*NRNGS
      DO 10 N=1,NRNGS
      SBE=0.0
      DO 11 NN=1,NF
      IF ( NN.GT. NRNGS ) GO TO 12
      SBE = SBE + B(NN,N)*T(NN,M)**4*EMS(NN,M,2)*AREA(NN,M)
      GO TO 11
   12 N1=NN-NRNGS
      SBE=SBE + B(NN,N)*T(N1,M+1)**4*EMS(N1,M+1,1)*AREA(N1,M+1)
   11 CONTINUE
      SBE=SBE + B(NF+1,N)*TS(M)**4*ES(M)*ARES(M)
      Q(N)= SBE -T(N,M)**4*EMS(N,M,2)*AREA(N,M)
      QSUM=QSUM + Q(N)
   10 CONTINUE
C
C     CALCULATE THE HEAT TRANSFER TO THE SURROUNDINGS.
C
      ADVD=AREAT(M)
      IF ( M .EQ. 1 .AND. SOLAR .NE. 0.0 ) ADVD=AREAT(M+1)
      QOA2=QSUM/ADVD*SIGMA
      QSUR=0.0
      DO 17 N=1,NF
      IF ( N .GT. NRNGS ) GO TO 16
      QSUR = QSUR + B(N,NF+1)*T(N,M)**4*EMS(N,M,2)*AREA(N,M)
      GO TO 17
   16 N1=N-NRNGS
      QSUR=QSUR+B(N,NF+1)*T(N1,M+1)**4*EMS(N1,M+1,1)*AREA(N1,M+1)
   17 CONTINUE
      QSUR = QSUR + ( B(NF+1,NF+1) - 1.0 )*TS(M)**4*ES(M)*ARES(M)
```

```
      QDOT          -   EFN    SOURCE STATEMENT  -   IFN(S)   -

      QSOR=QSOR*SIGMA
      QOAS=QSOR/AREAS(M)
      RETURN
      END
```

```
$IBFTC FACTOR  DECK

      SUBROUTINE FACTOR(A,ROW,ORDER,DIM)
C
C     FACTOR THE MATRIX A INTO TWO TRIANGULAR MATRICES ONE OF WHICH
C     HAS A UNITARY DIAGONAL.
C     A        THE MATRIX OF SIZE ORDER WHICH IS TO BE INVERTED.
C     D        THE INVERSE OF A. ( USED IN INVERT )
C     ORDER    THE LENGTH OF EACH SIDE OF THE MATRICES A AND D.
C     DIM      THE DIMENSION OF THE MATRICES A AND D AND THE VECTOR ROW
C              IN THE CALLING PROGRAM.
C     ROW      A DUMMY VARIABLE OF LENGTH DIM TRANSFERED FROM THE CALLING
C              PROGRAM.
C
      INTEGER ONE,TWO,ROW,ORDER,DIM
      DIMENSION A(DIM,DIM),ROW(DIM)
      DOUBLE PRECISION T,ZERO
      REAL MAX
      DATA ZERO/0.0D0/
      N=ORDER
      ASSIGN 150 TO ONE
      ASSIGN 160 TO TWO
      DO 95 I=1,N
      IP1=I+1
      IM1=I-1
      GO TO ONE,(10,150)
   10 DO 30 L=I,N
      T=ZERO
      DO 20 K=1,IM1
   20 T=T+A(K,I)*A(L,K)
   30 A(L,I)=A(L,I)-T
   40 MAX=0.0
      DO 50 L=I,N
      IF(ABS(A(L,I)).LE.ABS(MAX))GO TO 50
      NI=L
      MAX=A(L,I)
   50 CONTINUE
      IF(MAX.EQ.0.0)GO TO 140
      ROW(I)=NI
      IF(I.EQ.NI)GO TO 180
      DO 60 K=1,N
      S=A(I,K)
      A(I,K)=A(NI,K)
   60 A(NI,K)=S
   65 GO TO TWO,(70,160)
   70 DO 90 L=IP1,N
      T=ZERO
      DO 80 K=1,IM1
   80 T=T+A(I,K)*A(K,L)
   90 A(I,L)=(A(I,L)-T)/MAX
   95 CONTINUE
  140 ORDER=IM1
```

```
      WRITE(6,141)
  141 FORMAT(/ 53H SUBROUTINE FACTOR HAS ENCOUNTERED A SINGULAR MATRIX.)
      CALL EXIT
  150 ASSIGN 10 TO ONE
      GO TO 40
  160 DO 170 L=2,N
  170 A(1,L)=A(1,L)/MAX
      ASSIGN 70 TO TWO
      GO TO 95
  180 IF(I.EQ.N)RETURN
      GO TO 65
      END
```

ERROR MESSAGE NUMBER 1

ERROR MESSAGE NUMBER 2

ERROR MESSAGE NUMBER 3

```
$IBFTC INVERT  DECK

      SUBROUTINE INVERT(A,ROW,ORDER,DIM,D)
C
C     DETERMINE THE INVERSE OF A FROM THE TWO TRIANGULAR FACTORS OF A
C
      INTEGER ROW,ONE,DIM,ORDER
      DIMENSION A(DIM,DIM),ROW(DIM),D(DIM,DIM)
      DOUBLE PRECISION T,ZERO
      DATA ZERO/0.0D0/
      N=ORDER
      ASSIGN 60 TO ONE
      I=N
    5 IP1=I+1
      IM1=I-1
      DO 30 M=1,I
      L=IP1-M
      T=ZERO
      GO TO ONE,(10,60)
   10 LP1=L+1
      DO 20 K=LP1,N
   20 T=T+A(K,L)*D(I,K)
   30 D(I,L)=(FLOAT(L/I)-T)/A(L,L)
      IF(I.EQ.1)GO TO 70
      DO 50 M=1,IM1
      L=I-M
      T=ZERO
      LP1=L+1
       DO 40 K=LP1,N
   40 T=T+A(L,K)*D(K,I)
   50 D(L,I)=-T
      I=IM1
      GO TO 5
   60 ASSIGN 10 TO ONE
      GO TO 30
   70 I=N-1
   80 K=ROW(I)
      DO 90 L=1,N
      S=D(L,I)
      D(L,I)=D(L,K)
   90 D(L,K)=S
      IF(I.EQ.1)RETURN
       I=I-1
      GO TO 80
      END

ERROR MESSAGE NUMBER     1
```

LISTING OF INPUT

```
$OUTPUT
ICONDR=          1, ITMAX =        200, IVCOND=          1, NCALCR=          1, NCASE =          1,
NELIPS=          0, NRADS =          1, NRNGS =         20, NSHLDS=          2, NVUFH =          0,
NVUFT =          0, PHI   =  4.4200000E 02, RH    =  0.          , RSH   =  0.          , RST   =  0.          ,
RT    =  1.0000000F C0, SIGMA =  1.7130000E-C9, SOLABS=  4.9999999E-02, SOLAR =  1.0000000E 00, TOL   =  1.0000000E-02,
$ END
  TBABS1  0.2000E-01  0.          0.          0.          TBEMS1  0.2000E-01  0.          0.          0.
SHIELD RADIUS =  0.100CE 01  0.1000E 01
```

PROPERTIES OF SURROUNDINGS BETWEEN SURFACES

SPACING	DISTANCE	AREA	ABSORPTIVITY	EMISSIVITY	TEMPERATURE
2	0.100	1.000	1.000	1.000	0.
3	0.100	1.000	1.000	1.000	0.

```
NE1B =  1
NA1B =  1
NE1T =  1
NA1T =  1
NE2B =  1
NA2B =  1
NE2T =  1
NA2T =  1
 NET =  1
 NAT =  1
  TT =     37.000
```

LISTING OF OUTPUT

```
NO. ITERATIONS =   4       SOLAR = 1.          QOAT =  0.1188E 00          TOLX=0.01000
```

M	TEMP	R(N)	R(N)/RS
1	772.855	0.224	0.224
	772.292	0.316	0.316
	771.660	0.387	0.387
	771.002	0.447	0.447
	770.325	0.500	0.500
	769.630	0.548	0.548
	768.918	0.592	0.592
	768.188	0.632	0.632
	767.440	0.671	0.671
	766.672	0.707	0.707
	765.882	0.742	0.742
	765.069	0.775	0.775
	764.231	0.806	0.806
	763.363	0.837	0.837
	762.462	0.866	0.866
	761.525	0.894	0.894
	760.548	0.922	0.922
	759.530	0.949	0.949
	758.486	0.975	0.975
	757.460	1.000	1.000

M	TEMP	R(N)	R(N)/RS
2	443.449	0.224	0.224
	440.095	0.316	0.316
	436.257	0.387	0.387
	432.164	0.447	0.447
	427.846	0.500	0.500
	423.298	0.548	0.548
	418.505	0.592	0.592
	413.443	0.632	0.632
	408.081	0.671	0.671
	402.378	0.707	0.707
	396.284	0.742	0.742
	389.737	0.775	0.775
	382.650	0.806	0.806
	374.913	0.837	0.837
	366.367	0.866	0.866
	356.787	0.894	0.894
	345.835	0.922	0.922
	333.038	0.949	0.949
	317.852	0.975	0.975
	300.015	1.000	1.000

NO. ITERATIONS = 2 SOLAR = 1. COAT = 0.1188E 00 TOLX=0.00500

M	TEMP	R(N)	R(N)/RS
1	772.855	0.224	0.224
	772.292	0.316	0.316
	771.660	0.387	0.387
	771.002	0.447	0.447
	770.325	0.500	0.500
	769.630	0.548	0.548
	768.918	0.592	0.592
	768.188	0.632	0.632
	767.440	0.671	0.671
	766.672	0.707	0.707
	765.882	0.742	0.742
	765.069	0.775	0.775
	764.231	0.806	0.806
	763.363	0.837	0.837
	762.462	0.866	0.866
	761.525	0.894	0.894
	760.548	0.922	0.922
	759.530	0.949	0.949
	758.486	0.975	0.975
	757.460	1.000	1.000

M	TEMP	R(N)	R(N)/RS
2	443.449	0.224	0.224
	440.095	0.316	0.316
	436.257	0.387	0.387
	432.164	0.447	0.447
	427.846	0.500	0.500
	423.298	0.548	0.548
	418.505	0.592	0.592
	413.443	0.632	0.632
	408.081	0.671	0.671
	402.378	0.707	0.707
	396.284	0.742	0.742
	389.737	0.775	0.775
	382.650	0.806	0.806
	374.913	0.837	0.837
	366.367	0.866	0.866
	356.787	0.894	0.894
	345.835	0.922	0.922
	333.038	0.949	0.949
	317.852	0.975	0.975
	300.015	1.000	1.000

REFERENCES

1. Smolak, George R.; Knoll, Richard H.; and Wallner, Lewis E.: Analysis of Thermal-Protection Systems for Space-Vehicle Cryogenic-Propellant Tanks. NASA TR R-130, 1962.

2. Jones, L. R.; and Barry, D. G.: Lightweight Inflatable Shadow Shields for Cryogenic Space Vehicles. J. Spacecraft Rockets, vol. 3, no. 5, May 1966, pp. 722-728.

3. Nichols, Lester D.: Effect of Shield Position and Absorptivity on Temperature Distribution of a Body Shielded from Solar Radiation in Space. NASA TN D-578, 1961.

4. Nothwang, George J.; Arvesen, John C.; and Hamaker, Frank M.: Analysis of Solar-Radiation Shields for Temperature Control of Space Vehicles Subjected to Large Changes in Solar Energy. NASA TN D-1209, 1962.

5. Arvesen, John C.; and Hamaker, Frank M.: Effectiveness of Radiation Shields for Thermal Control of Vehicles on the Sunlit Side of the Moon. NASA TN D-2130, 1964.

6. Sparrow, E. M.; and Gregg, J. L.: Radiant Interchange Between Circular Disks Having Arbitrarily Different Temperatures. J. Heat Transfer, vol. 83, no. 4, Nov. 1961, pp. 494-502.

7. Knoll, R. H.; Bartoo, E. R.; and Boyle, R. J.: Shadow Shield Experimental Studies. Presented at the Conference on Long-Term Cryo-Propellant Storage in Space, George C. Marshall Space Flight Center, Oct. 12-13, 1966.

8. Bonneville, Jacques M.: Design and Optimization of Space Thermal Protection for Cryogens-Analytic Techniques and Results. Rep. ADL-65958-02-01, Arthur D. Little, Inc., (NASA CR-54190), Dec. 18, 1964.

9. Perlmutter, M.; and Siegel, R.: Effect of Specularly Reflecting Gray Surface on Thermal Radiation Through a Tube and From Its Heated Wall. J. Heat Transfer, vol. 85, no. 1, Feb. 1963, pp. 55-62.

10. Gebhart, B.: Unified Treatment for Thermal Radiation Transfer Processes-Gray, Diffuse Radiators and Absorbers. Paper No. 57-A-34, ASME, 1957.

11. Sparrow, E. M.; Eckert, E. R. G.; and Jonsson, V. K.: An Enclosure Theory for Radiative Exchange Between Specularly and Diffusely Reflecting Surfaces. J. Heat Transfer, vol. 84, no. 4, Nov. 1962, pp. 294-300.

12. Anon.: IBM 7090/7094 IBSYS Operating System Version 13, Fortran IV Language. Form C28 6390-2, IBM Data Processing Division.

13. Dummer, R. S.; and Breckenridge, Jr., W. T.: Radiation Configuration Factors Program. Rep. ERR AN-224, General Dynamics/Astronautics, Feb. 1963.

14. Faddeeva, V. N. (Curtis D. Benster, trans.): Computational Methods in Linear Algebra. Dover Publications, 1959.

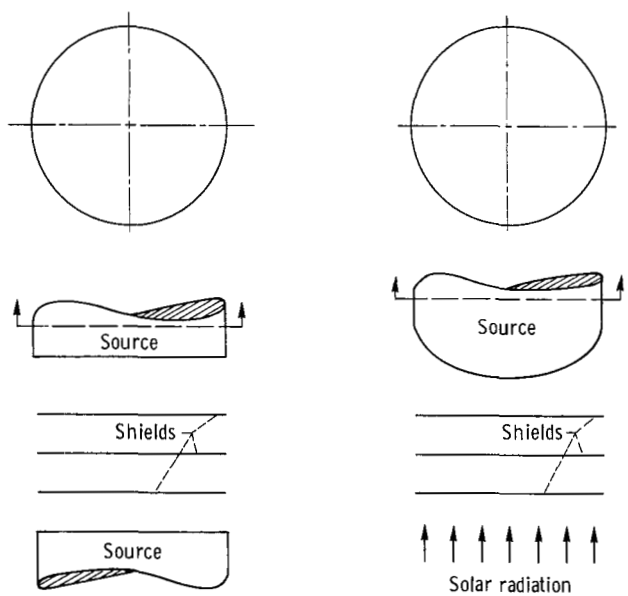

Figure 1. - Schematic drawing of two possible shadow shield configurations.

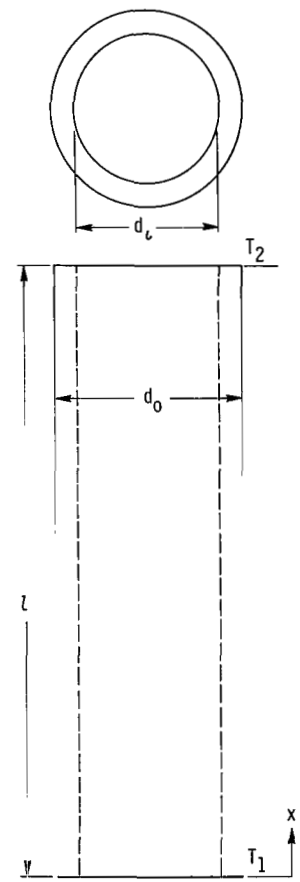

Figure 2. - Representation of hollow structural member. Inside surface diameter of strut, d_i; outside surface diameter of strut, d_o; strut length, l; temperatures at ends of strut, T_1 and T_2; distance along strut, x.

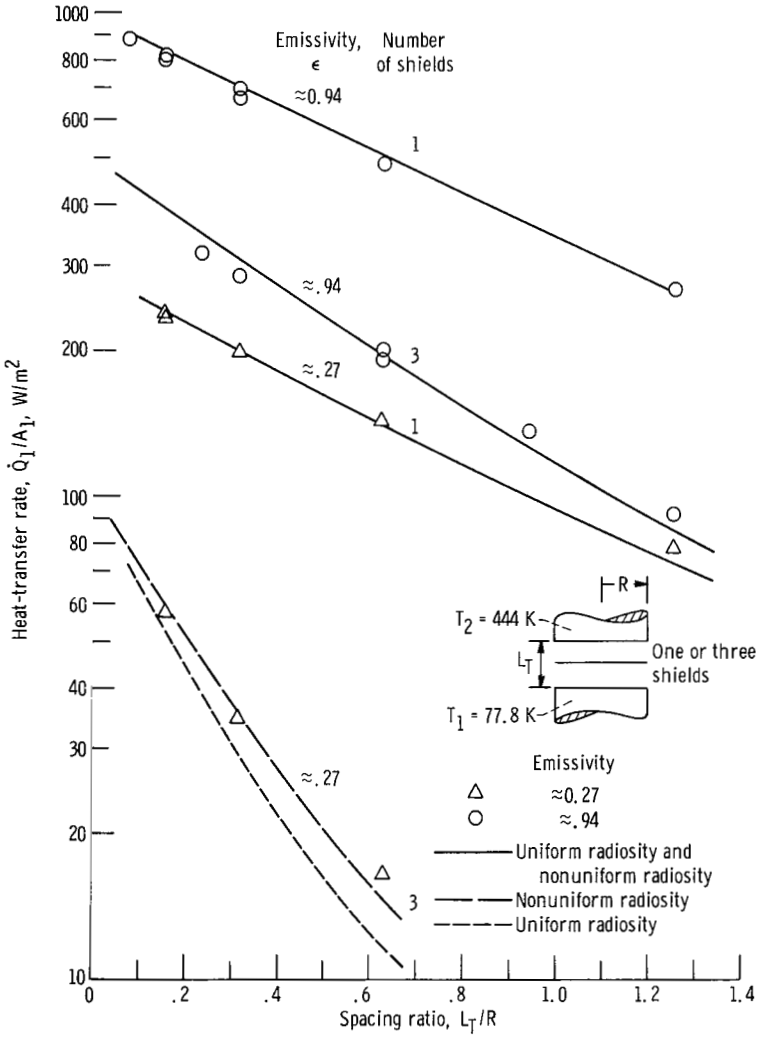

Figure 3. - Comparison of analytic and experimental heat-transfer rates.

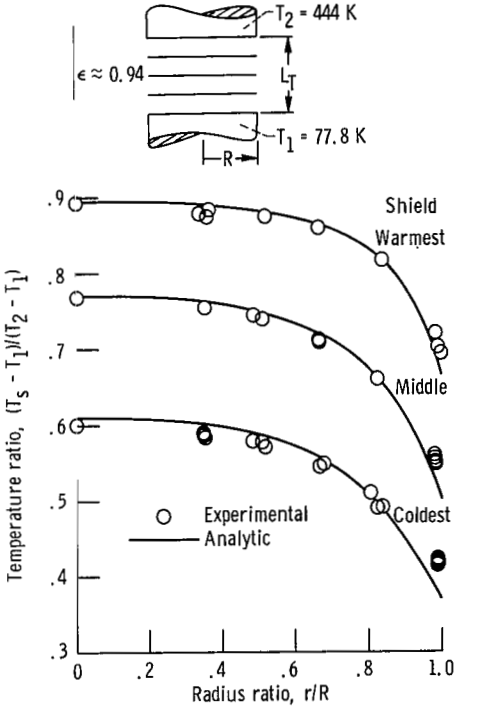

Figure 4. - Comparison of analytic and experimental temperature distributions for three blackened Mylar shields. Spacing ratio, L_T/R = 0.628.

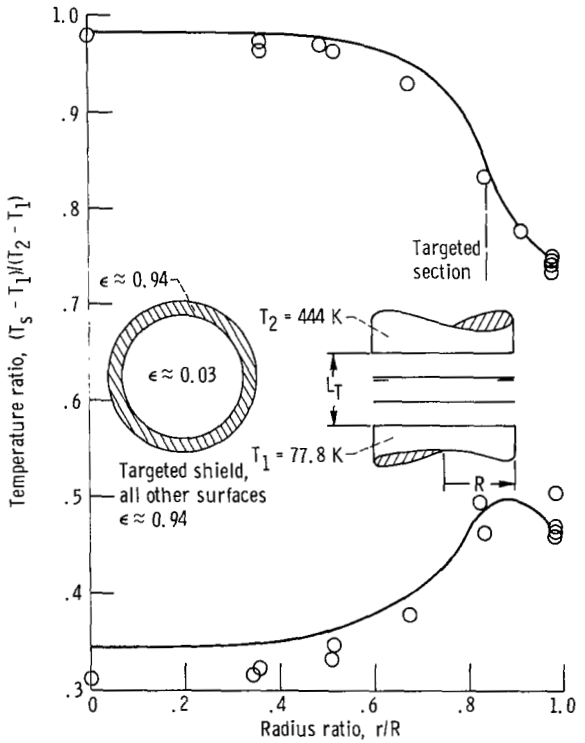

Figure 5. - Comparison of analytic and experimental temperature distributions for targeted shield system. Spacing ratio, $L_T/R = 0.47$; two shields.

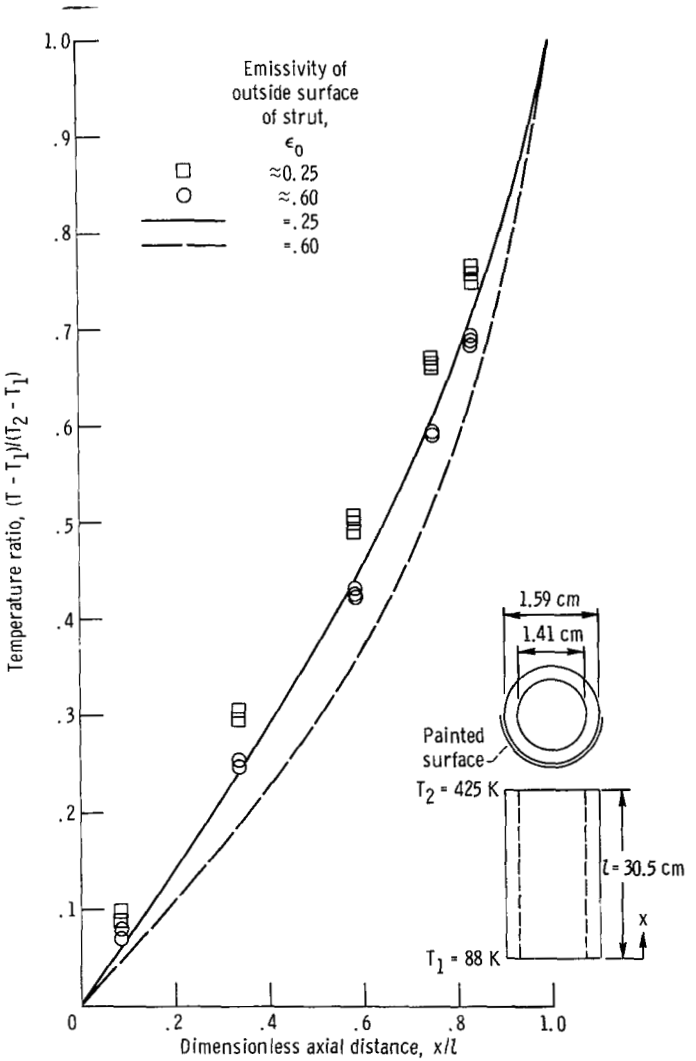

Figure 6. - Comparison of analytic and experimental strut temperature distributions.

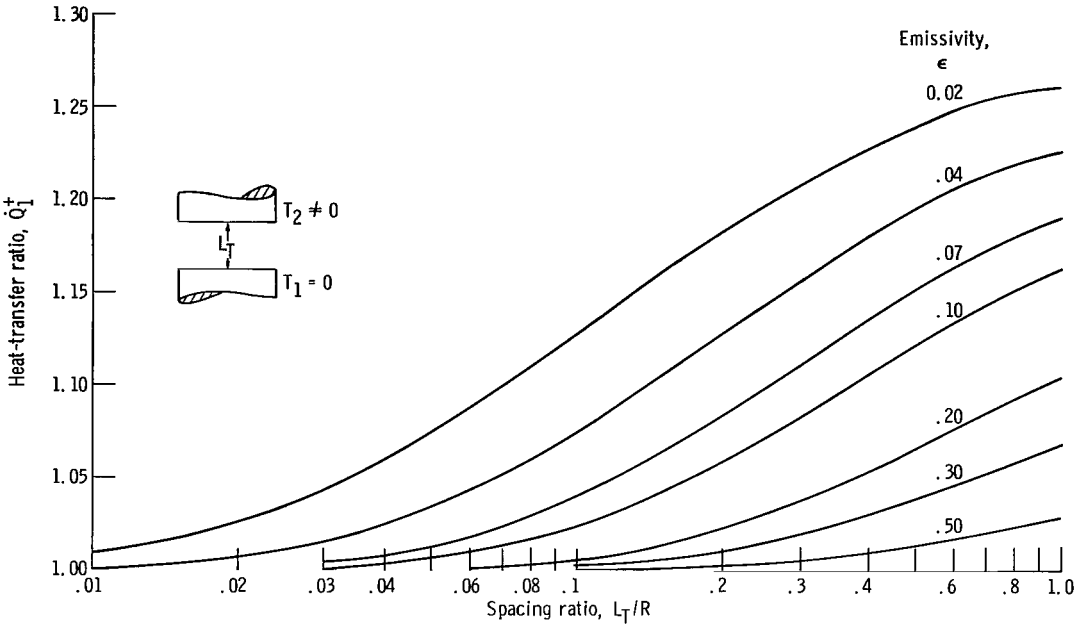

Figure 7. - Ratio of specular heat-transfer rate to diffuse heat-transfer rate as function of spacing ratio and emissivity. No shields; uniform radiosity.

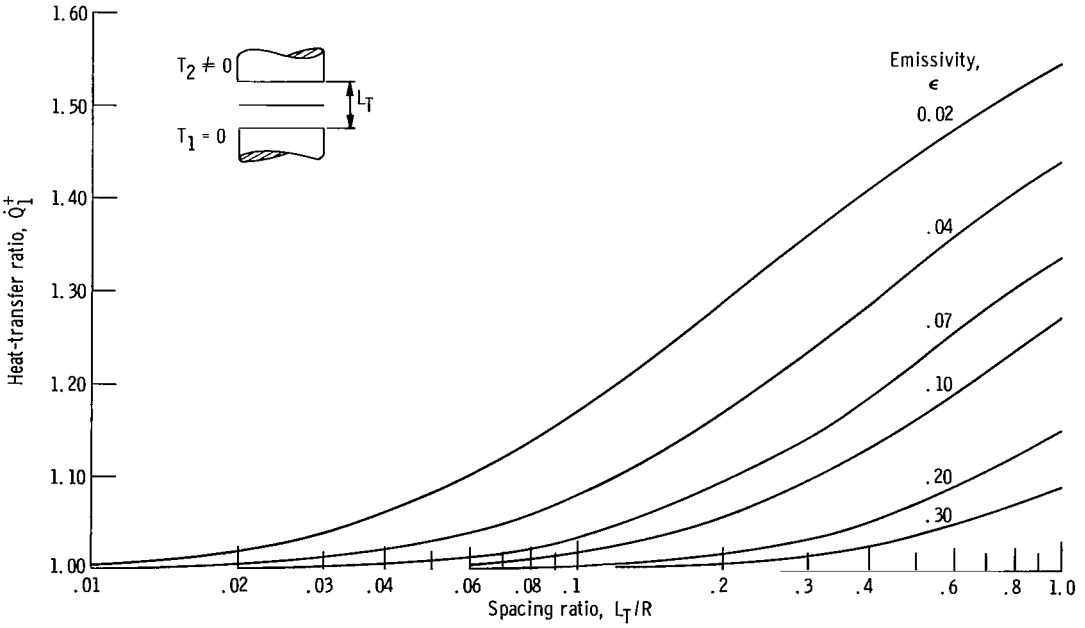

Figure 8. - Ratio of specular heat-transfer rate to diffuse heat-transfer rate as function of spacing ratio and emissivity. One shield; uniform radiosity.

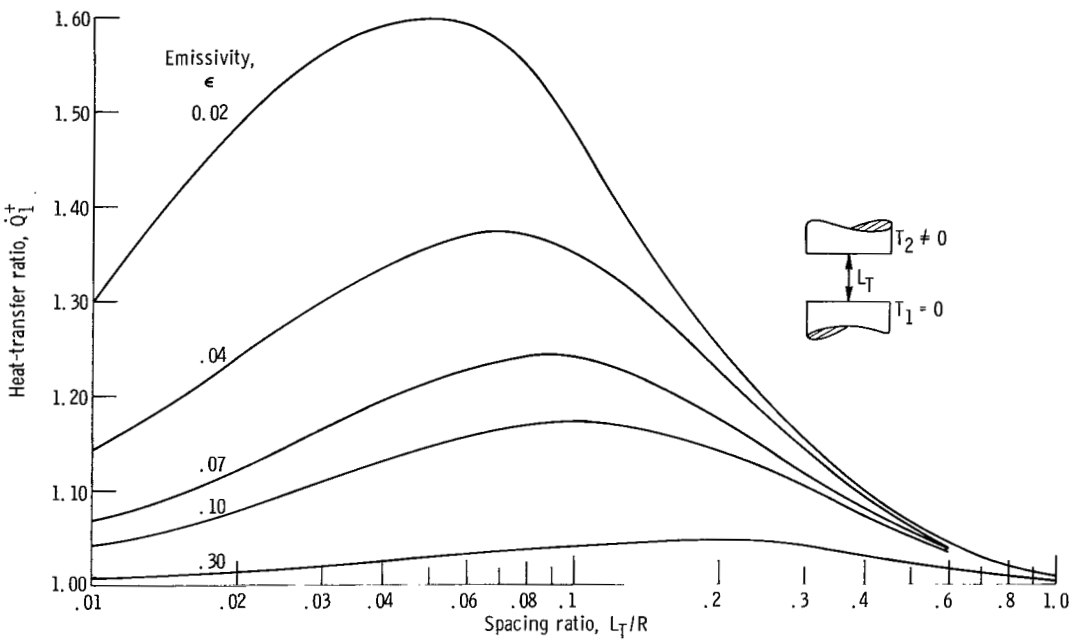

Figure 9. - Ratio of nonuniform radiosity heat-transfer rate to uniform radiosity heat-transfer rate as function of spacing ratio and emissivity. No shields.

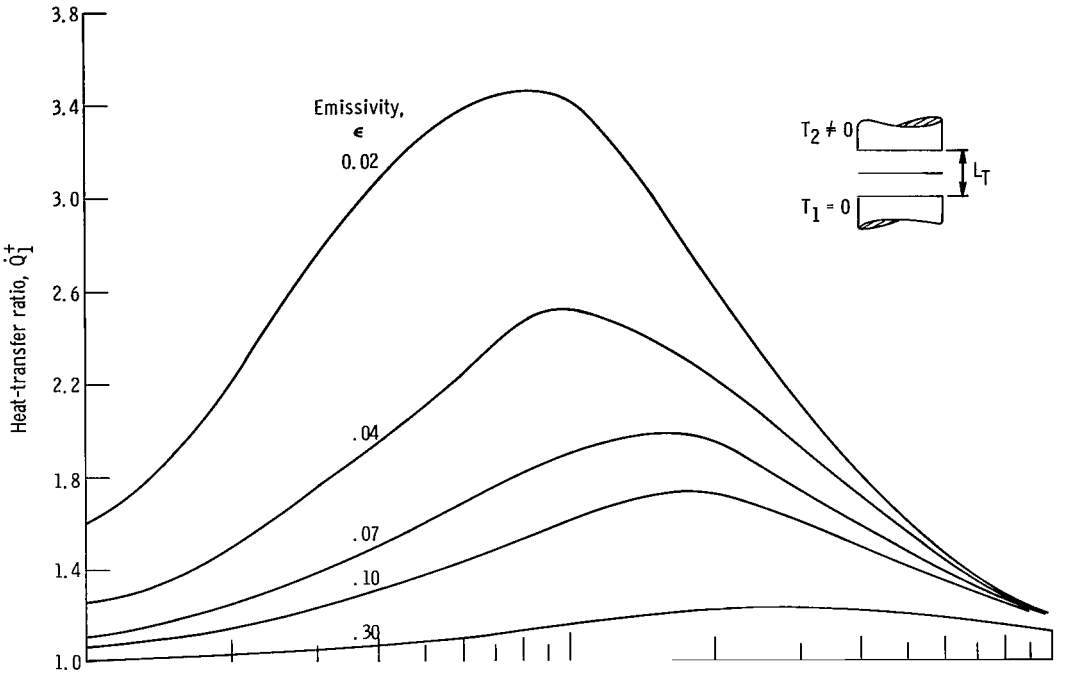

(a) Nonconducting shield.

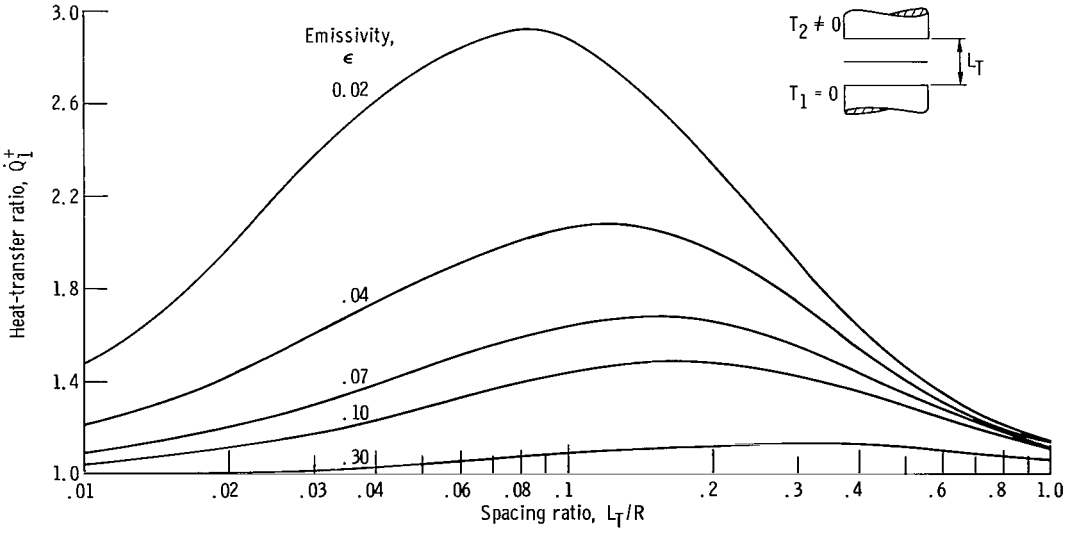

(b) Uniform temperature shield.

Figure 10. - Ratio of nonuniform radiosity heat-transfer rate to uniform radiosity heat-transfer rate as function of spacing ratio and emissivity. One shield.

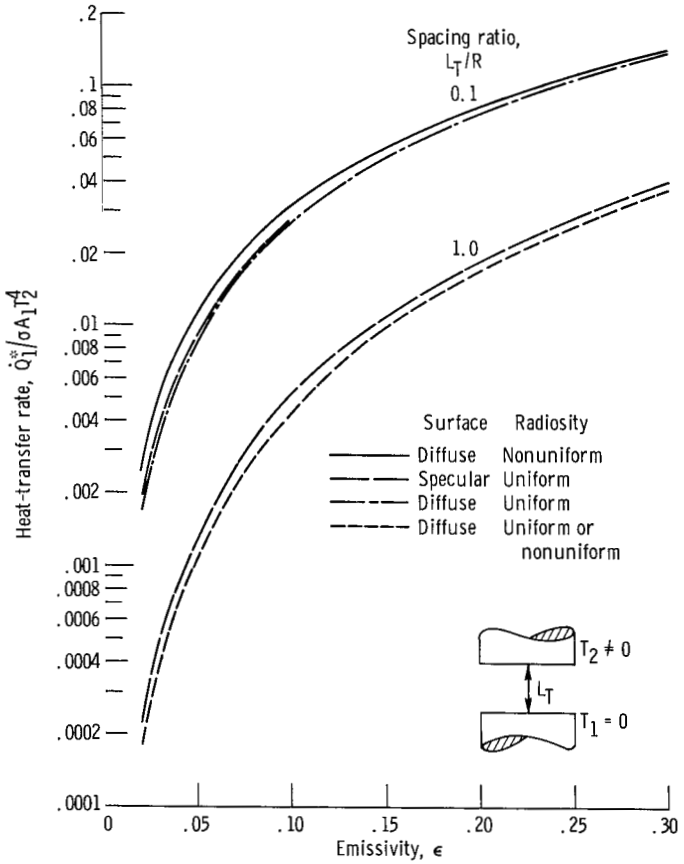

Figure 11. - Heat-transfer rate as function of emissivity for different surface assumptions. No shields.

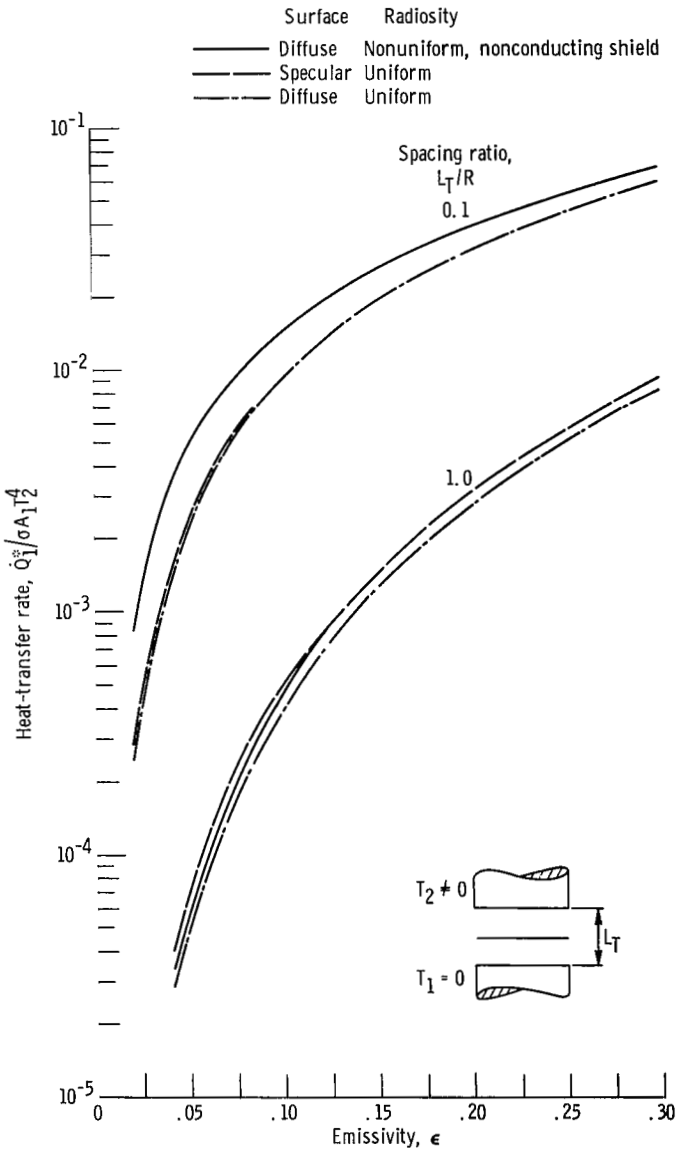

Figure 12. - Heat-transfer rate as function of emissivity for different surface assumptions. One shield.

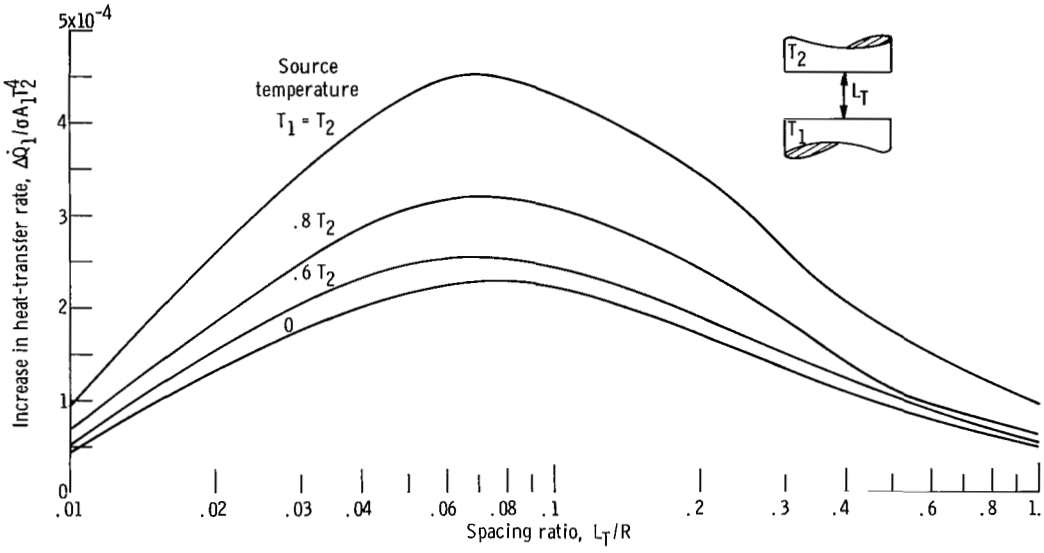

Figure 13. - Increase in heat-transfer rate due to specular surfaces as function of spacing ratio and source temperature ratio. Emissivity, 0.02; no shields.

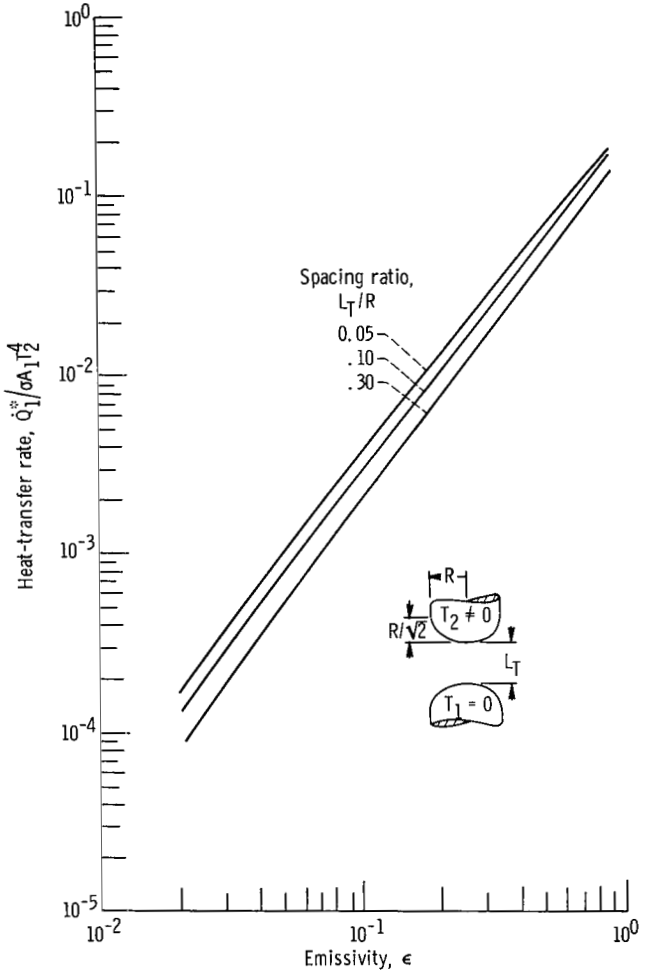

Figure 14. - Heat-transfer rate as function of emissivity and spacing ratio for two oblate spheroids. No shields.

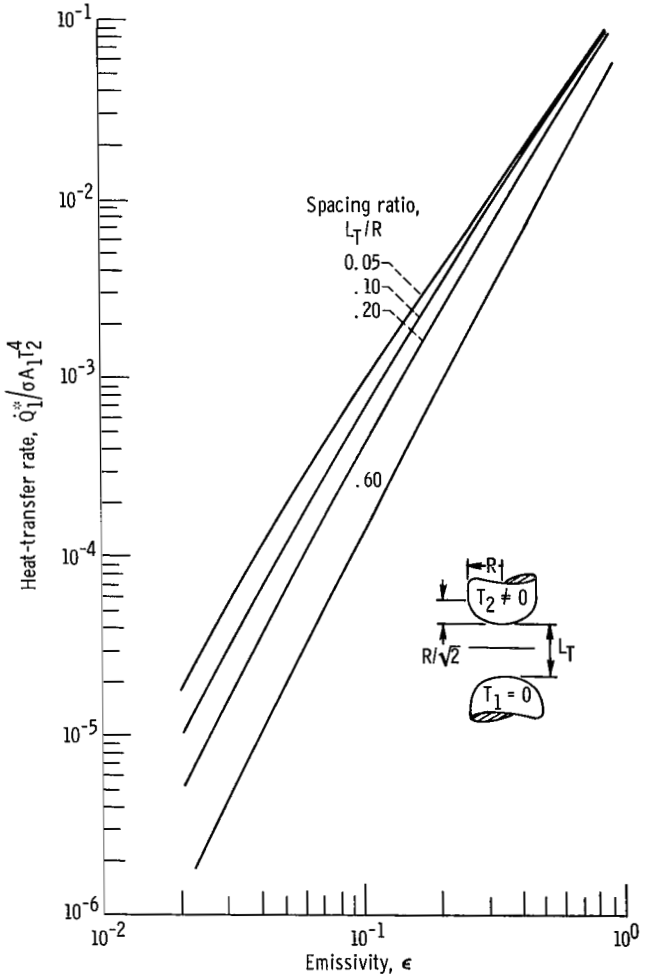

Figure 15. - Heat-transfer rate as function of emissivity and spacing ratio for two oblate spheroids. One shield.

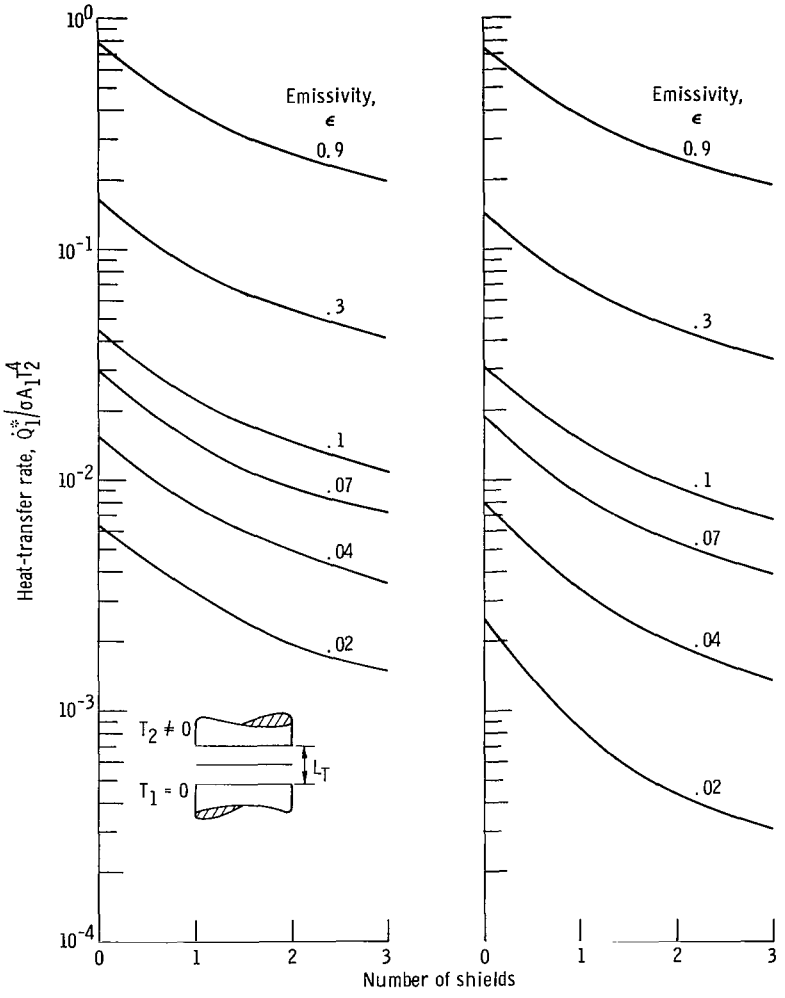

(a) Spacing ratio, 0.03.

(b) Spacing ratio, 0.1.

Figure 16. - Effect of number of shields on heat-transfer rate to a plane source at zero temperature.

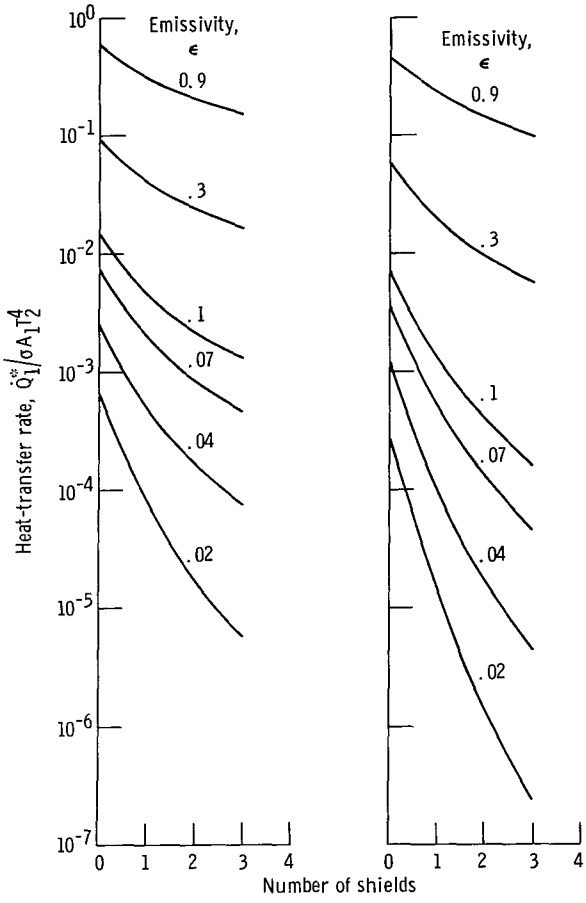

(c) Spacing ratio, 0.3. (d) Spacing ratio, 0.6.

Figure 16. - Concluded.

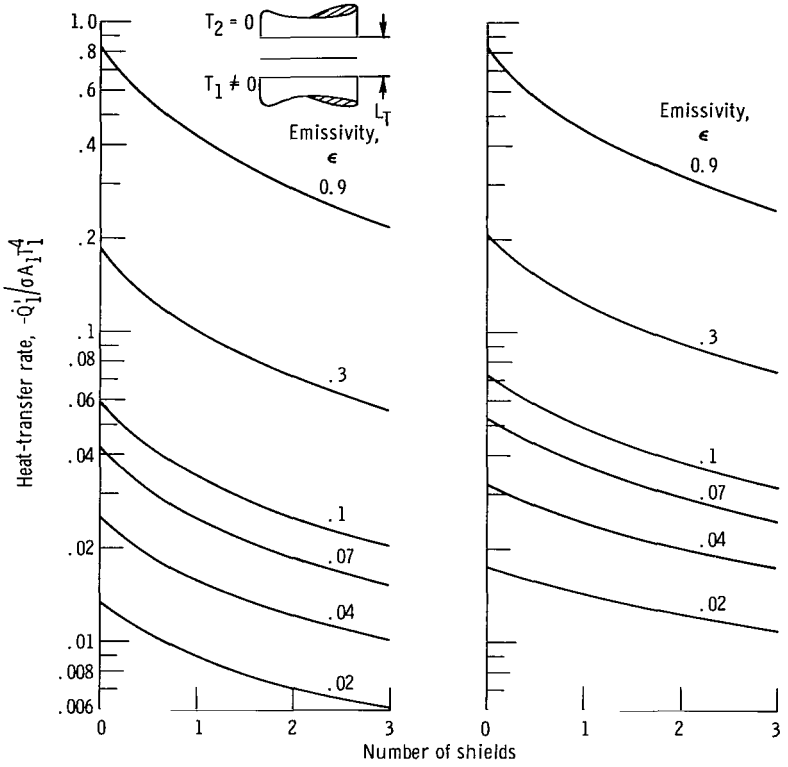

(a) Spacing ratio, 0.03.

(b) Spacing ratio, 0.1.

Figure 17. - Effect of number of shields on heat-transfer rate to plane source at nonzero temperature.

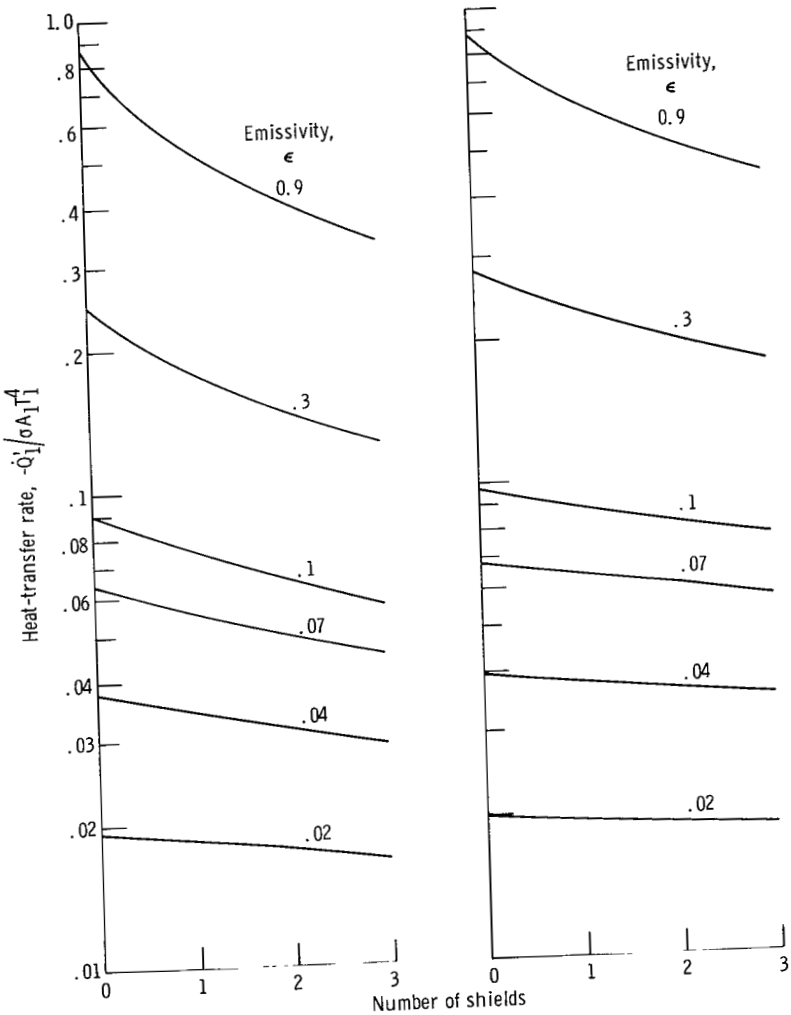

(c) Spacing ratio, 0.3.

(d) Spacing ratio, 0.6.

Figure 17. - Concluded.

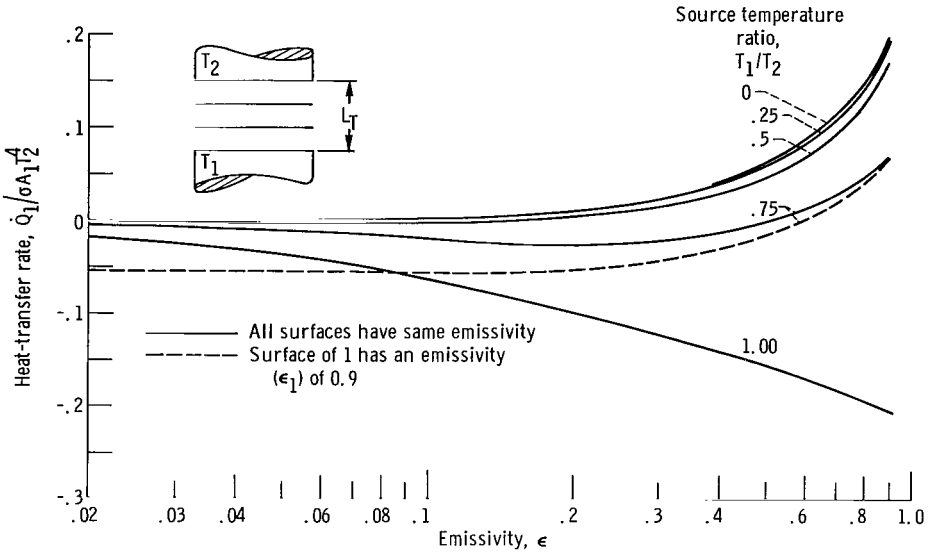

Figure 18. - Effect of emissivity and source temperature ratio on heat-transfer rate. Spacing ratio, 0.3; two shields.

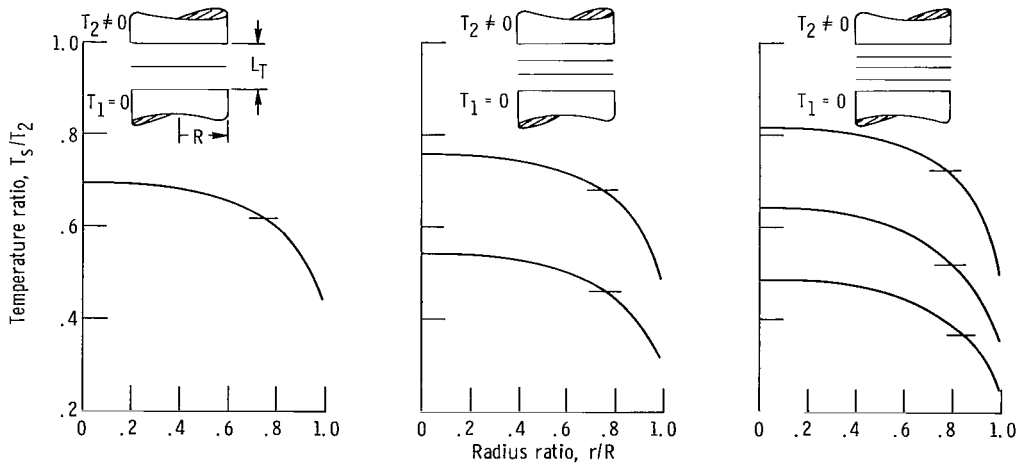

(a) One shield. (b) Two shields. (c) Three shields.

Figure 19. - Radial temperature distributions for one, two, and three shields. Spacing ratio, 0.1; emissivity, 0.02.

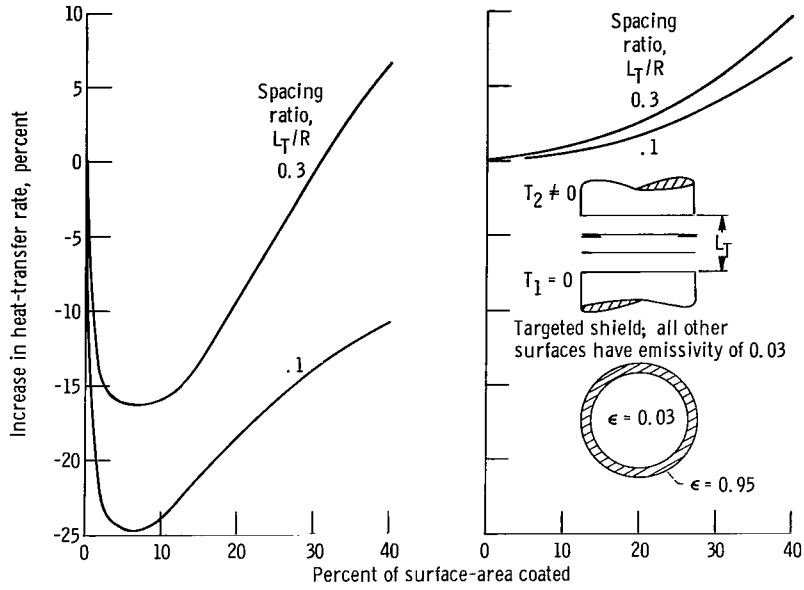

(a) Uniform temperature shields.

(b) Nonconducting shields.

Figure 20. - Effect of targeting on heat-transfer rate for uniform temperature and nonconducting shields.

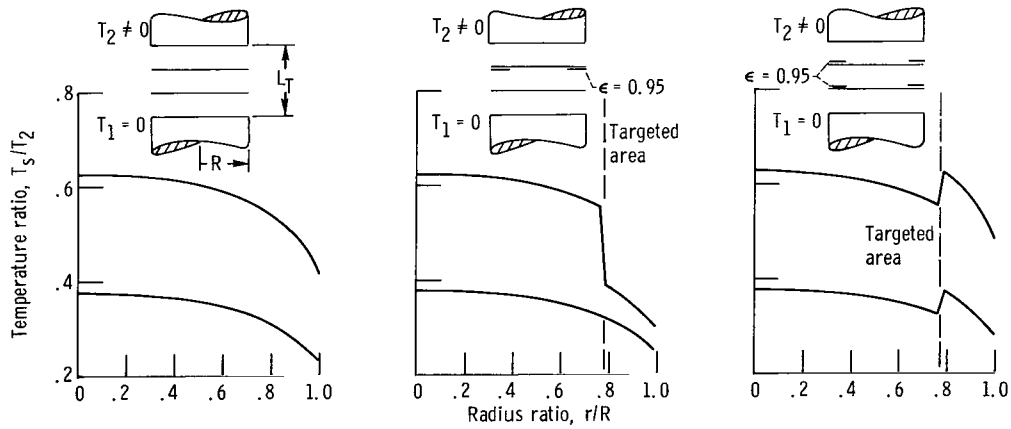

(a) No shields targeted; heat-transfer rate, $\dot{Q}_1^*/\sigma A_1 T_2^4$, 0.64×10^{-4}.

(b) One shield targeted; heat-transfer rate, $\dot{Q}_1^*/\sigma A_1 T_2^4$, 0.70×10^{-4}.

(c) Two shields targeted; heat-transfer rate, $\dot{Q}_1^*/\sigma A_1 T_2^4$, 0.78×10^{-4}.

Figure 21. - Effect of targeting on radial temperature distributions for nonconducting shields. Spacing ratio, 0.3; emissivity of nontargeted surfaces, 0.03.

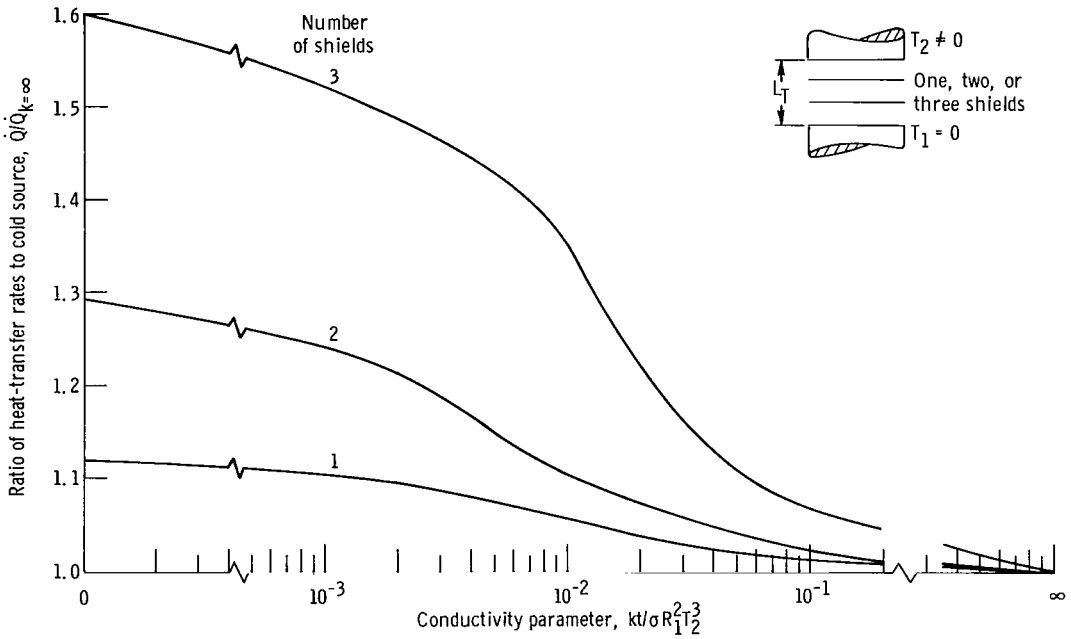

Figure 22. - Effect of shield conductivity on heat-transfer rate for one, two, and three shields. Spacing ratio, 0.1; emissivity, 0.1.

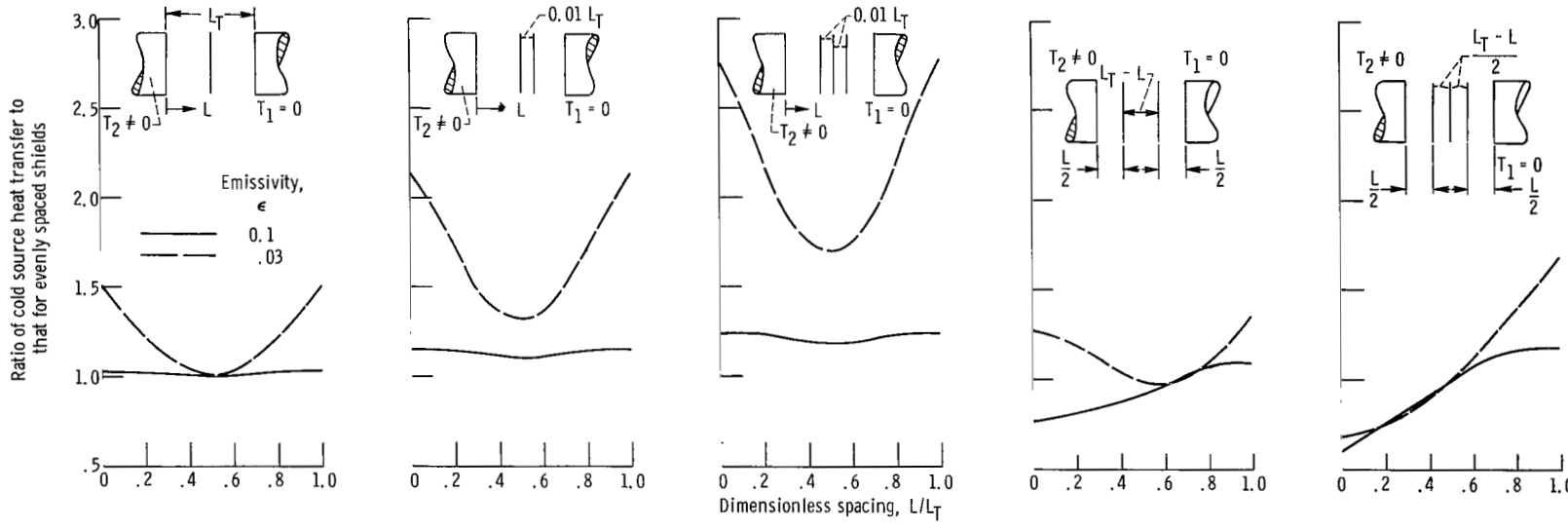

(a) One shield.

(b) Two shields.

(c) Three shields.

(d) Two shields; variable spacing.

(e) Three shields; variable spacing.

Figure 23. - Effect of variation in shield position on heat-transfer rate. Spacing ratio, 0.2.

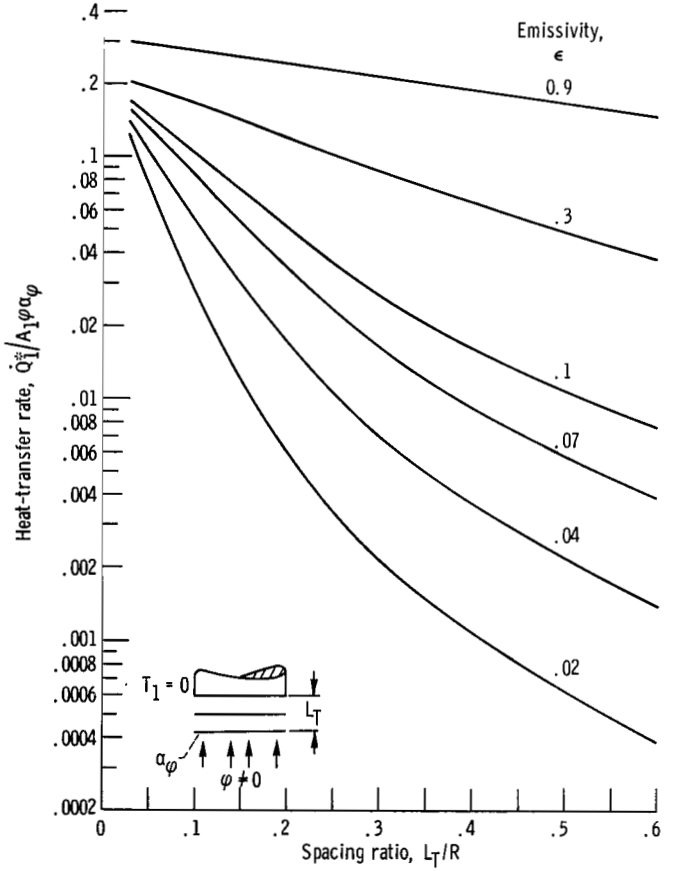

Figure 24. - Heat-transfer rate due to solar flux as function of spacing ratio and emissivity. Two shields.

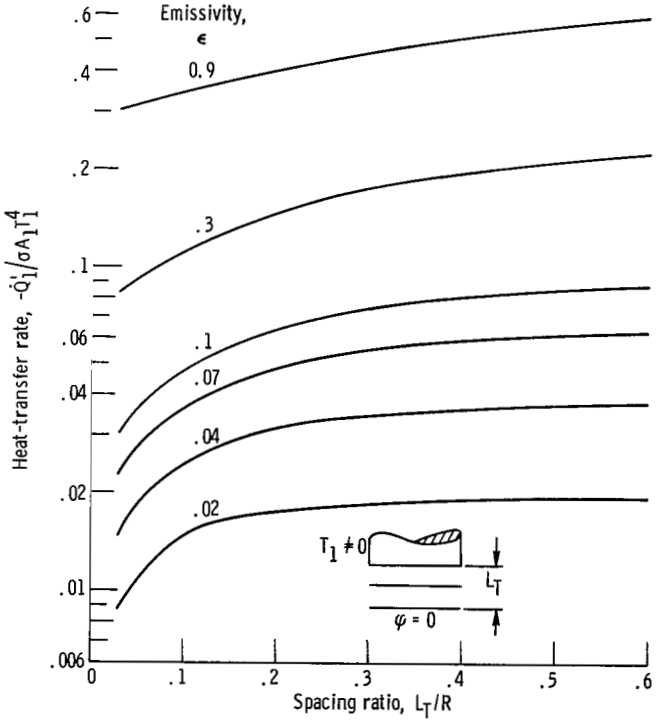

Figure 25. - Heat-transfer rate to source in absence of solar flux as function of spacing ratio and emissivity. Two shields.

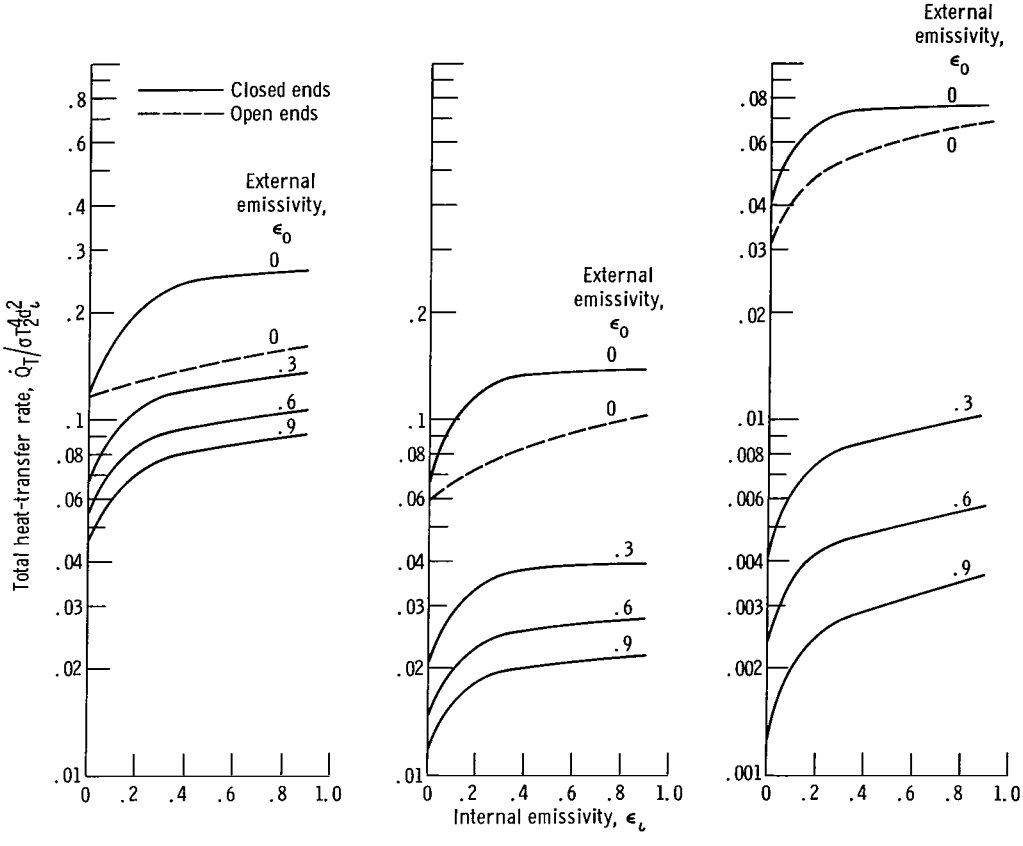

(a) Ratio of strut length to diameter, 5; radiation to conduction parameter, 125.

(b) Ratio of strut length to diameter, 10; radiation to conduction parameter, 500.

(c) Ratio of strut length to diameter, 20; radiation to conduction parameter, 2000.

Figure 26. - Total heat-transfer rate through strut as function of internal and external emissivity.

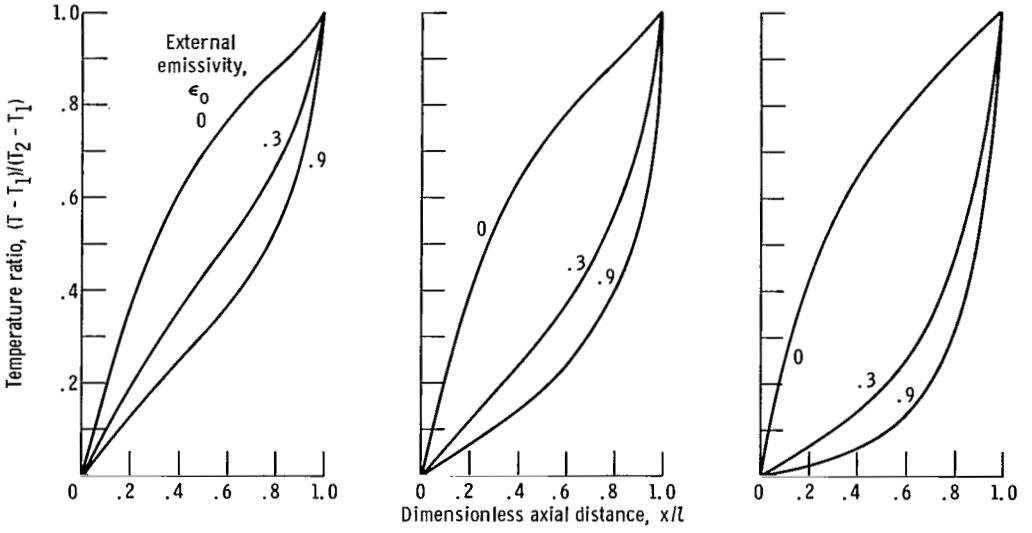

(a) Ratio of strut length to diameter, 5; radiation to conduction parameter, 125.

(b) Ratio of strut length to diameter, 10; radiation to conduction parameter, 500.

(c) Ratio of strut length to diameter, 20; radiation to conduction parameter, 2000.

Figure 27. - Effect of external emissivity and length to diameter ratio on strut temperature distribution. End temperature ratio, 10; internal emissivity, 0.6.

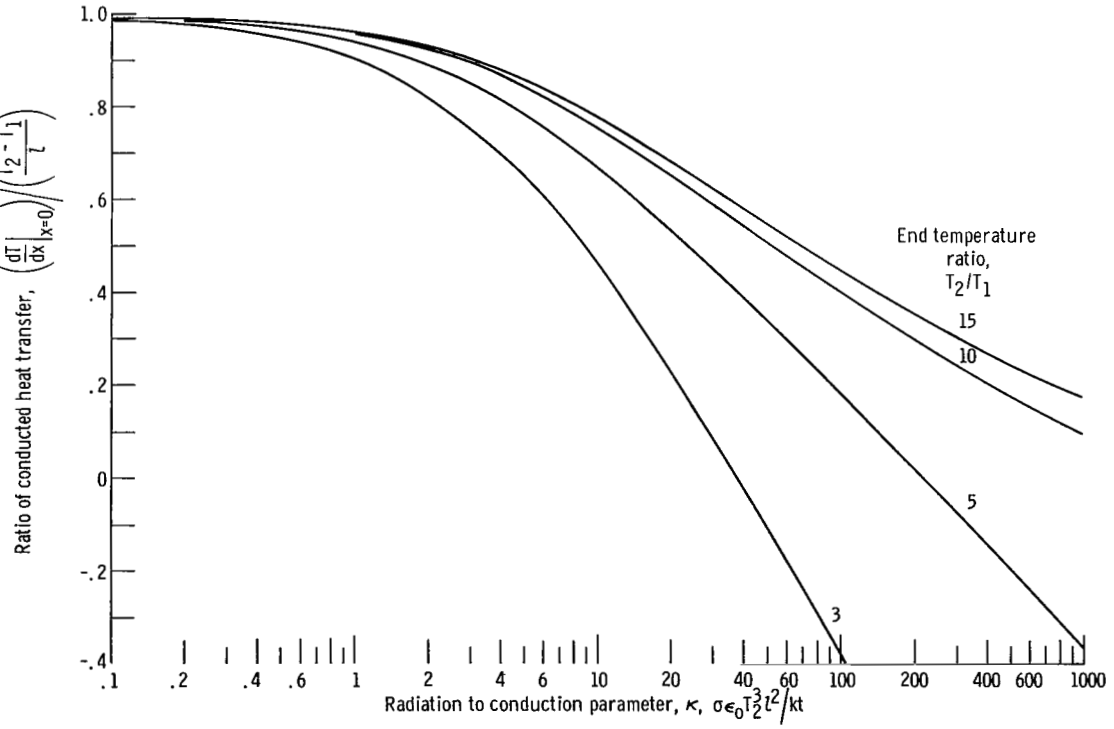

Figure 28. - Effect of radiation to conduction parameter on conducted heat-transfer rate for constant end temperature ratios. Internal emissivity, 0.

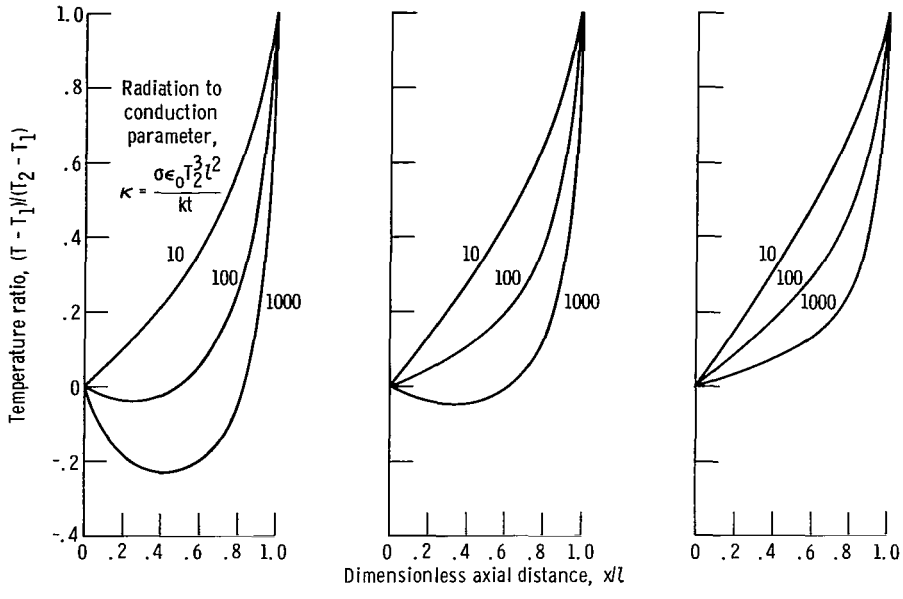

(a) End temperature ratio, 3.

(b) End temperature ratio, 5.

(c) End temperature ratio, 15.

Figure 29. - Temperature distributions for constant values of radiation to conduction parameter and end temperature ratios. Internal emissivity, 0.

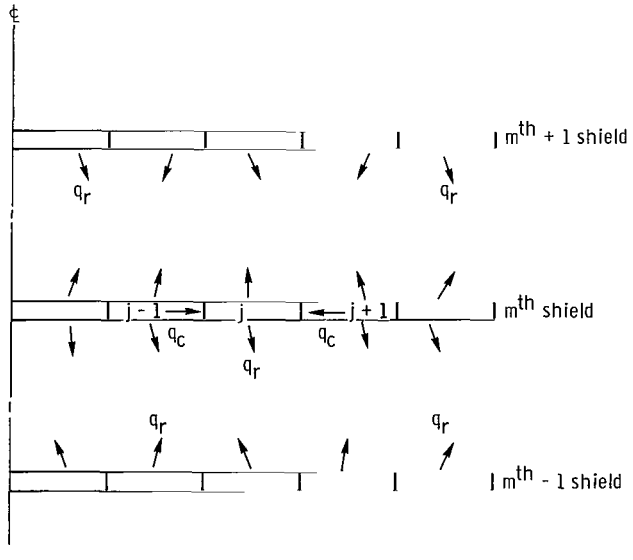

Figure 30. - Schematic drawing of heat balance for element of shield. Surface being considered, j; conducted heat transfer rate, q_c; radiant heat transfer rate, q_r.

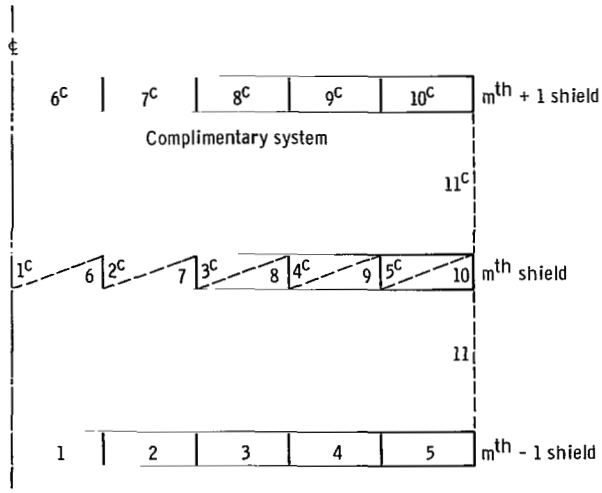

Figure 31. - Schematic drawing of element numbering used in heat balances. Number of elements on each surface of each system, n, 5; total number of elements in system, k, 2n + 1.

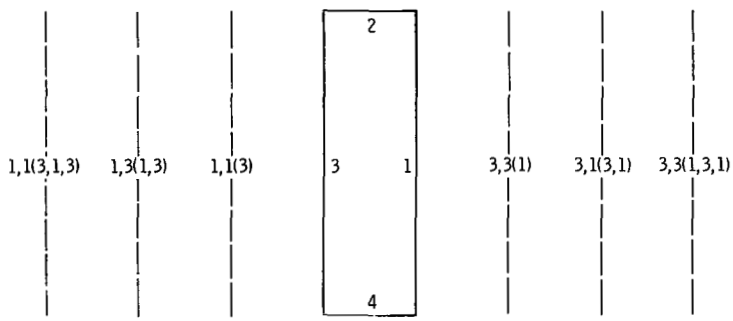

Figure 32. - Apparent spacing between surfaces due to specular reflectivity. Surfaces 1 and 3 are specularly reflecting and 2 and 4 are windows.

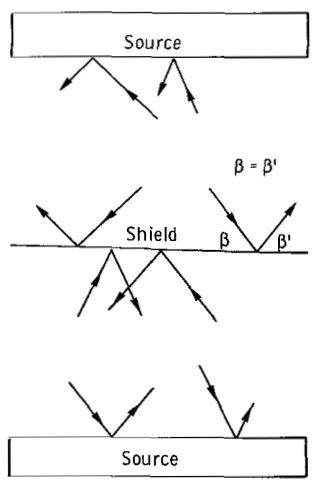

Figure 33. - Schematic drawing of reflected energy for specular surfaces.

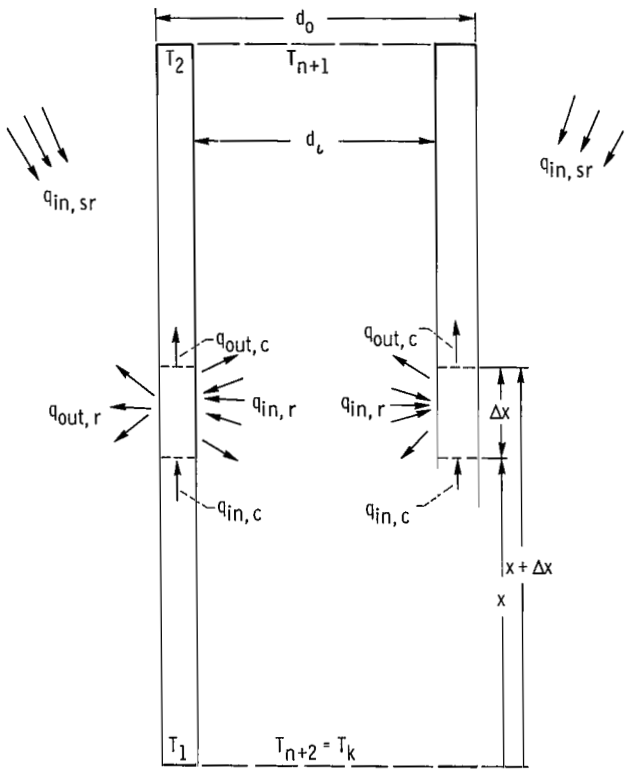

Figure 34. - Sources of heat transfer to element of strut. Inside diameter of strut, d_i; outside diameter of strut, d_o; conducted heat-transfer rate toward element, $q_{in,c}$; radiant heat-transfer rate toward surface, $q_{in,r}$; heat-transfer rate from surroundings, $q_{in,sr}$; conducted heat-transfer rate away from element, $q_{out,c}$; radiant heat-transfer rate away from surface, $q_{out,r}$; temperature at ends of strut, T_1 and T_2; temperature of end disks, T_{n+1} and T_{n+2}; distance along strut, x.

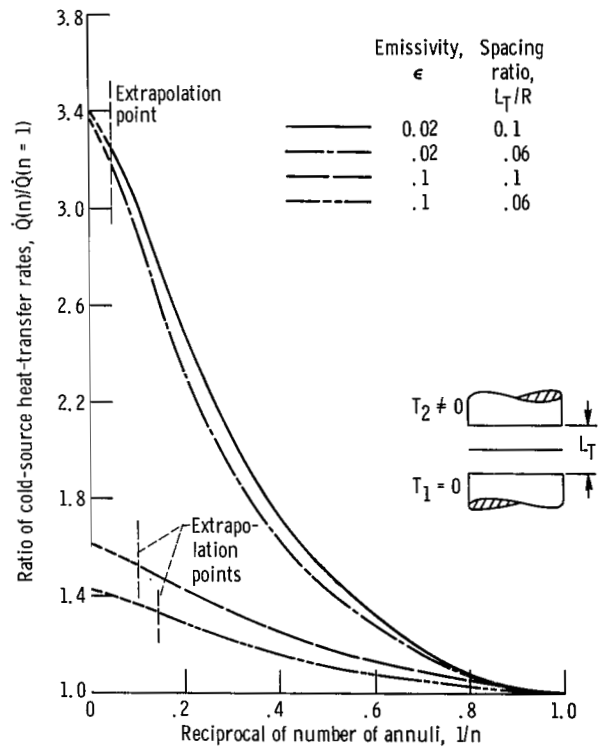

Figure 35. - Ratio of heat-transfer rate to that for single annulus as function of reciprocal of number of annuli. One shield.

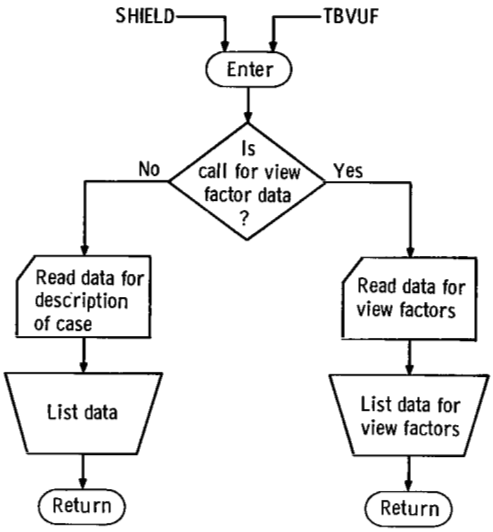

Figure 36. - Flow chart of subroutine INPUT.

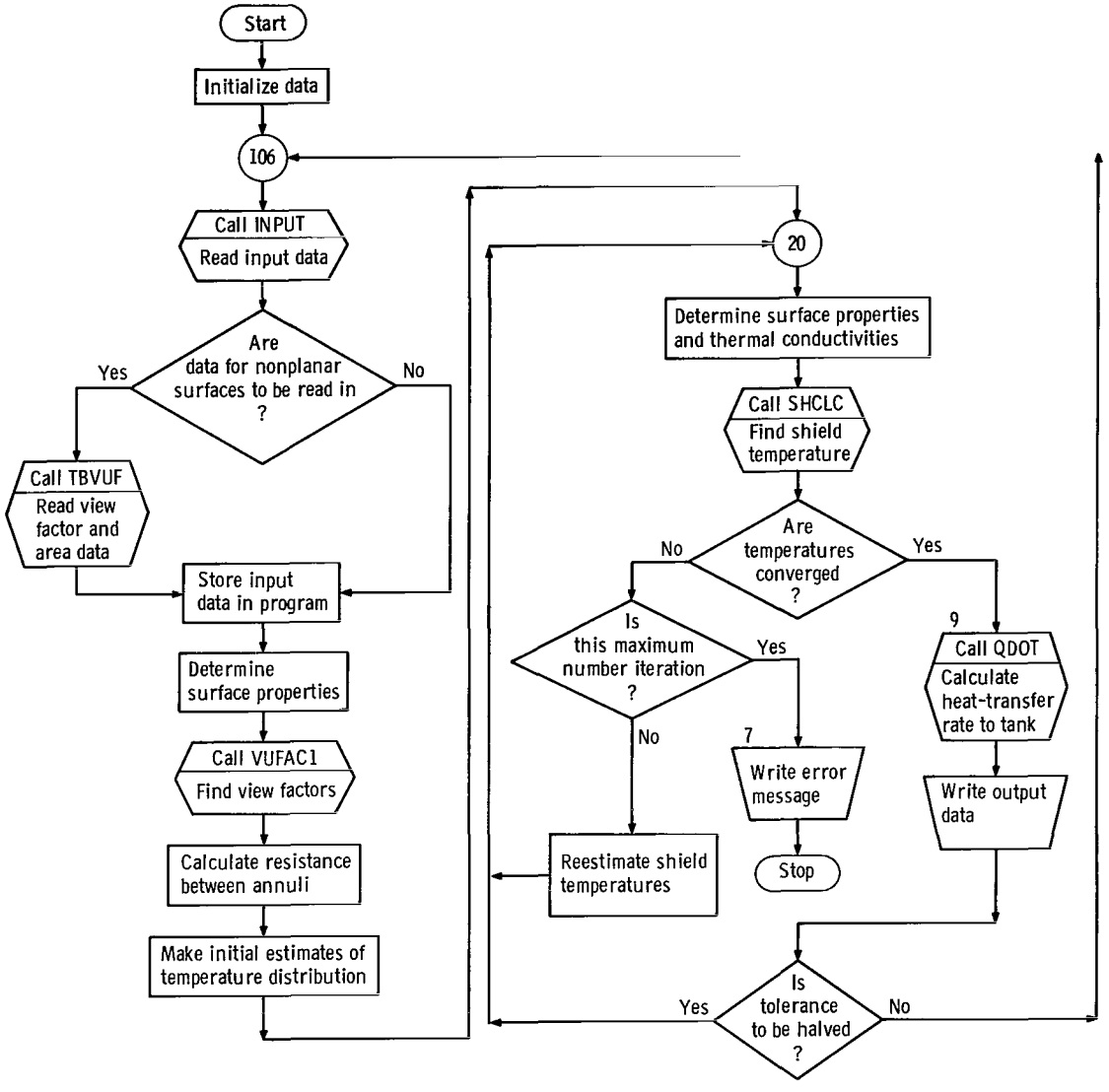

Figure 37. - Flow chart of routine SHIELD.

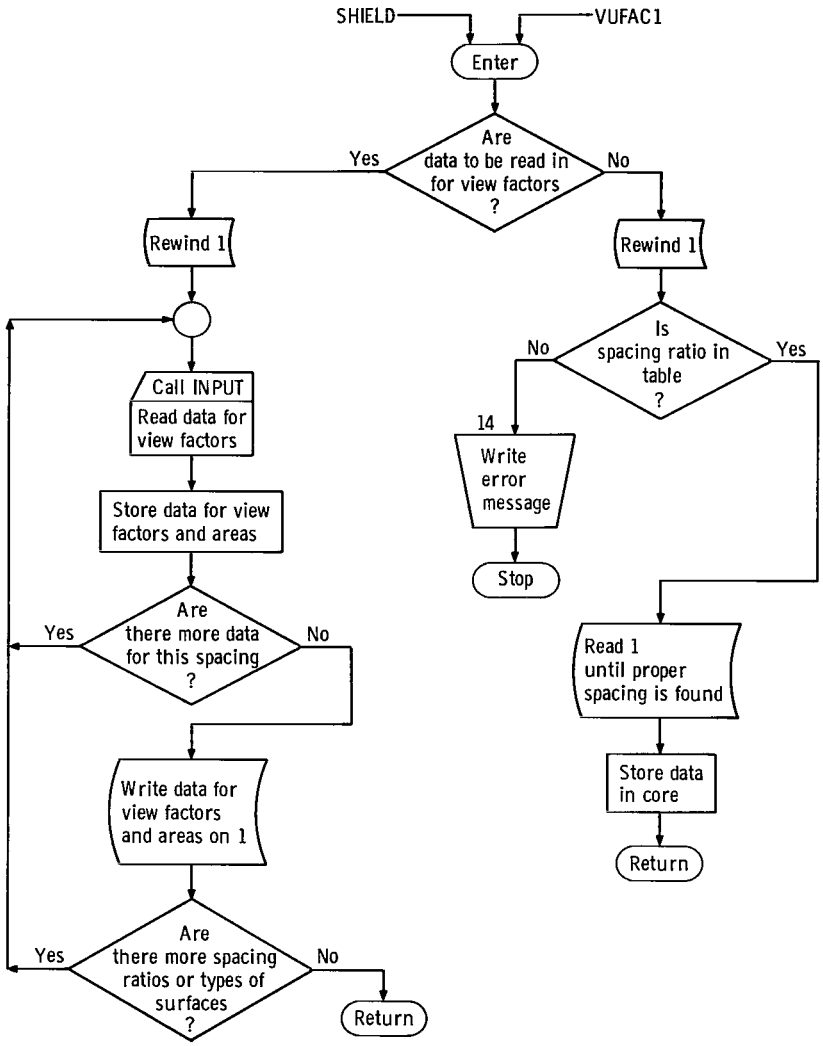

Figure 38. - Flow chart of subroutine TBVUF.

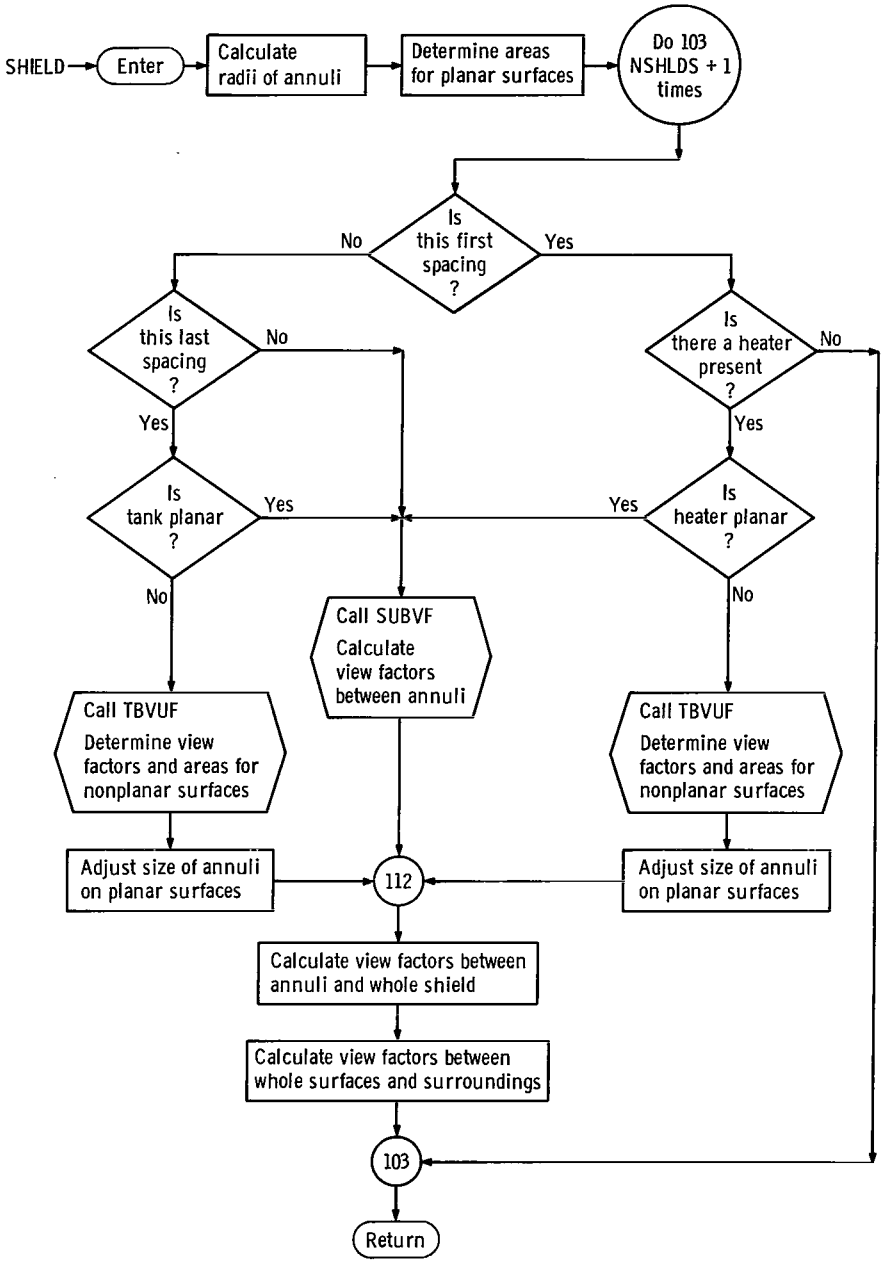

Figure 39. - Flow chart of subroutine VUFAC1.

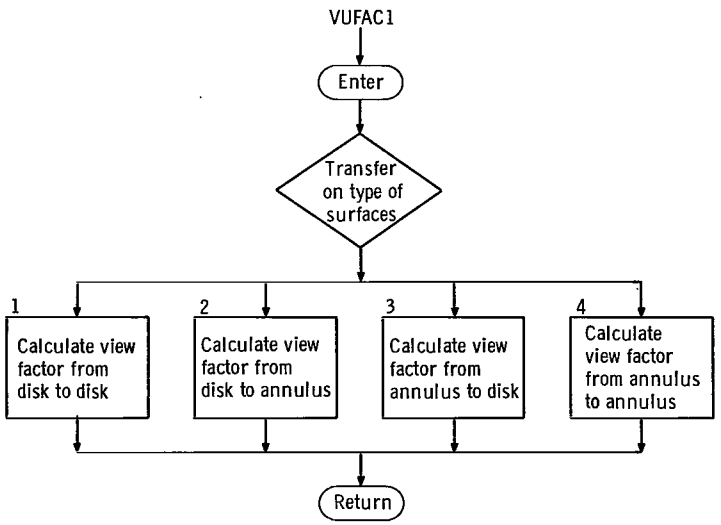

Figure 40. - Flow chart of subroutine SUBVF.

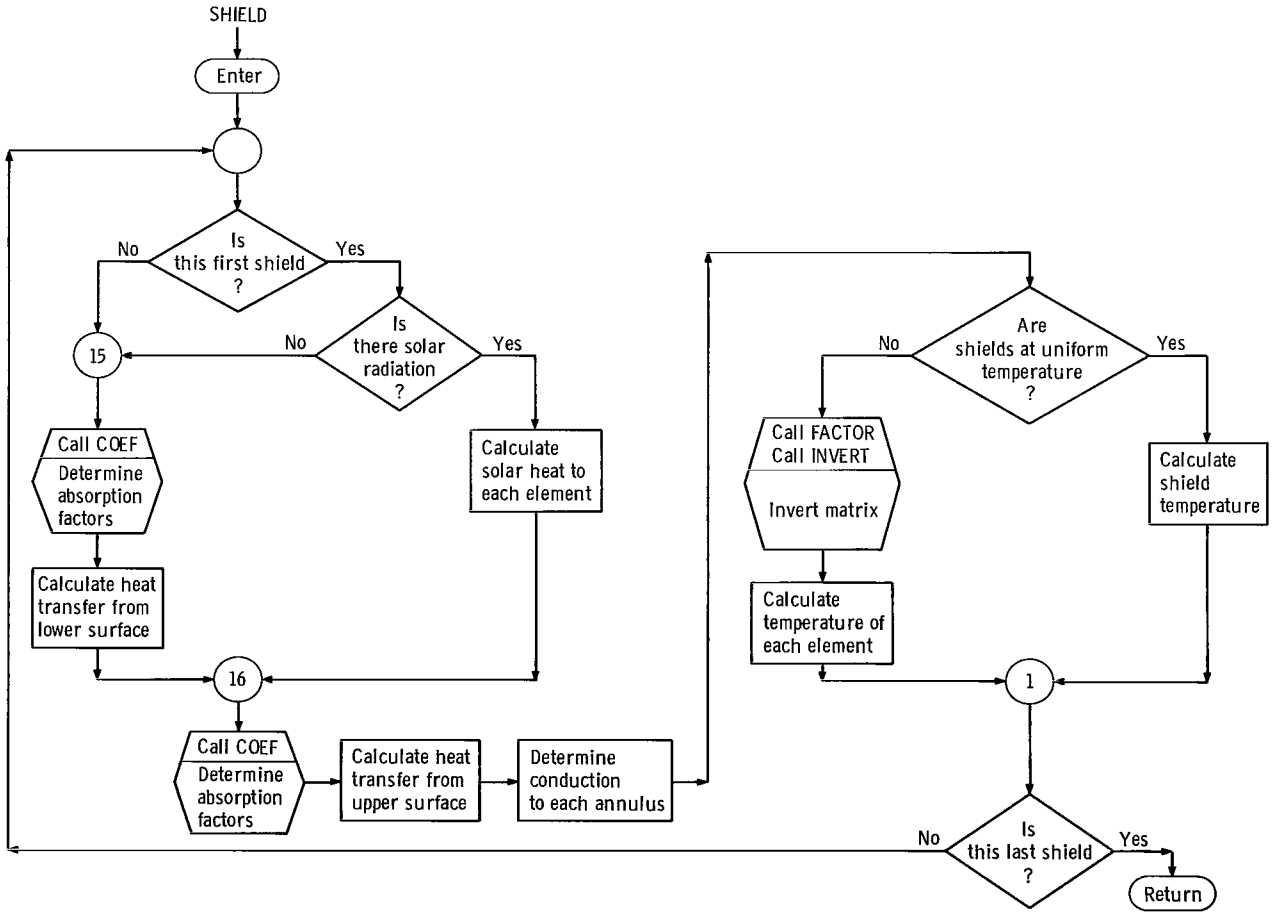

Figure 41. - Flow chart of subroutine SHCLC.

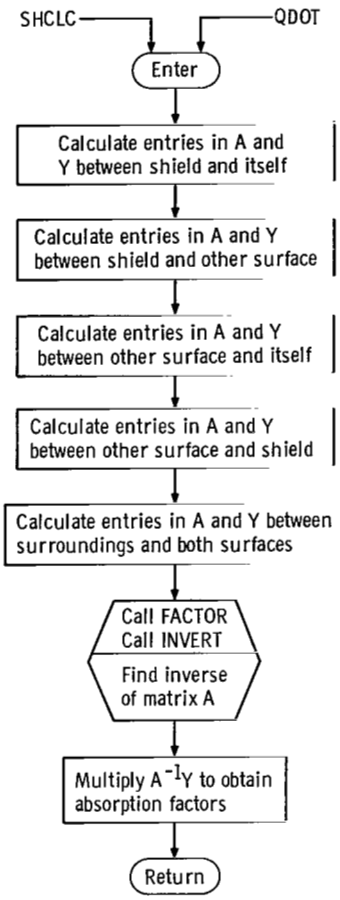

Figure 42. - Flow chart of subroutine COEF.

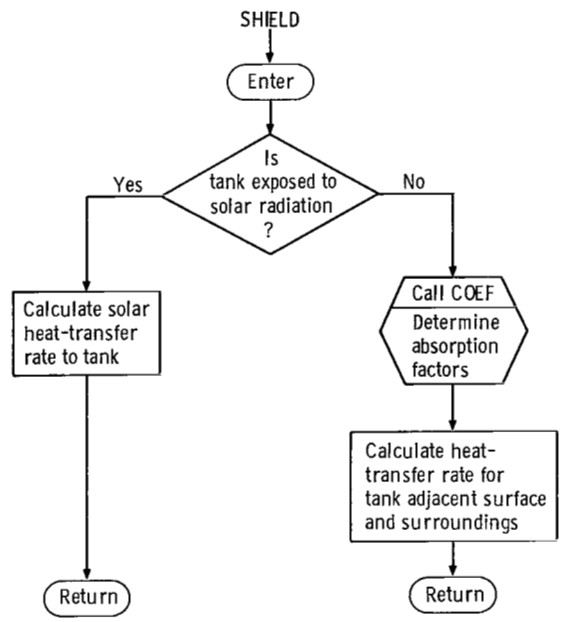

Figure 43. - Flow chart of subroutine QDOT.

"The aeronautical and space activities of the United States shall be conducted so as to contribute . . . to the expansion of human knowledge of phenomena in the atmosphere and space. The Administration shall provide for the widest practicable and appropriate dissemination of information concerning its activities and the results thereof."

—NATIONAL AERONAUTICS AND SPACE ACT OF 1958

NASA SCIENTIFIC AND TECHNICAL PUBLICATIONS

TECHNICAL REPORTS: Scientific and technical information considered important, complete, and a lasting contribution to existing knowledge.

TECHNICAL NOTES: Information less broad in scope but nevertheless of importance as a contribution to existing knowledge.

TECHNICAL MEMORANDUMS: Information receiving limited distribution because of preliminary data, security classification, or other reasons.

CONTRACTOR REPORTS: Scientific and technical information generated under a NASA contract or grant and considered an important contribution to existing knowledge.

TECHNICAL TRANSLATIONS: Information published in a foreign language considered to merit NASA distribution in English.

SPECIAL PUBLICATIONS: Information derived from or of value to NASA activities. Publications include conference proceedings, monographs, data compilations, handbooks, sourcebooks, and special bibliographies.

TECHNOLOGY UTILIZATION PUBLICATIONS: Information on technology used by NASA that may be of particular interest in commercial and other non-aerospace applications. Publications include Tech Briefs, Technology Utilization Reports and Notes, and Technology Surveys.

Details on the availability of these publications may be obtained from:

SCIENTIFIC AND TECHNICAL INFORMATION DIVISION

NATIONAL AERONAUTICS AND SPACE ADMINISTRATION

Washington, D.C. 20546